AD A061428

AFML-TR-78-102

A FEASIBILITY STUDY FOR DEVELOPMENT OF
STRUCTURAL ALUMINUM ALLOYS FROM RAPIDLY
SOLIDIFIED POWDERS FOR
AEROSPACE STRUCTURAL APPLICATIONS

*R. E. LEWIS*
*D. WEBSTER*
*I. G. PALMER*
*LOCKHEED PALO ALTO RESEARCH LABORATORY*
*3251 HANOVER STREET*
*PALO ALTO, CALIFORNIA 94304*

JULY 1978

TECHNICAL REPORT AFML-TR-78-102
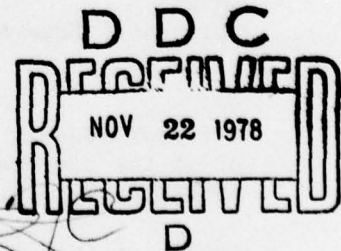Final Report for Period June 1977 — May 1978

Approved for public release; distribution unlimited.

DDC
RECEIVED
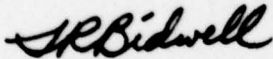NOV 22 1978
D

DDC FILE COPY

78 11 14 026

# NOTICE

When Government drawings, specifications, or other data are used for any purpose other than in connection with a definitely related Government procurement operation, the United States Government thereby incurs no responsibility nor any obligation whatsoever; and the fact that the government may have formulated, furnished, or in any way supplied the said drawings, specifications, or other data, is not to be regarded by implication or otherwise as in any manner licensing the holder or any other person or corporation, or conveying any rights or permission to manufacture, use, or sell any patented invention that may in any way be related thereto.

This report has been reviewed by the Information Office (IO) and is releasable to the National Technical Information Service (NTIS). At NTIS, it will be available to the general public, including foreign nations.
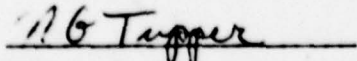
The views and conclusions contained in this document are those of the authors and should not be interpreted as representing the official policies, either expressed or implied, of the Defense Advanced Research Projects Agency or the U.S. Government.

This technical report has been reviewed and is approved for publication.

*SR Bidwell*

Lawrence R. Bidwell
Program Manager

FOR THE COMMANDER

*N G Tupper*

Nathan G. Tupper
Chief
Structural Metals Branch

# REPORT DOCUMENTATION PAGE

**READ INSTRUCTIONS BEFORE COMPLETING FORM**

| 1. REPORT NUMBER | 2. GOVT ACCESSION NO. | 3. RECIPIENT'S CATALOG NUMBER |
|---|---|---|
| AFML-TR-78-102 | | |

| 4. TITLE (and Subtitle) | 5. TYPE OF REPORT & PERIOD COVERED |
|---|---|
| A FEASIBILITY STUDY FOR DEVELOPMENT OF STRUCTURAL ALUMINUM ALLOYS FROM RAPIDLY SOLIDIFIED POWDERS FOR AEROSPACE STRUCTURAL APPLICATIONS. | Technical Report, for Period 1 June 1977 - 31 May 1978 |
| | 6. PERFORMING ORG. REPORT NUMBER |

| 7. AUTHOR(s) | 8. CONTRACT OR GRANT NUMBER(s) |
|---|---|
| Richard E. Lewis, Donald Webster, Ian G. Palmer | ARPA Order No. 3417 F33615-77-C-5186 |

| 9. PERFORMING ORGANIZATION NAME AND ADDRESS | 10. PROGRAM ELEMENT, PROJECT, TASK AREA & WORK UNIT NUMBERS |
|---|---|
| Lockheed Palo Alto Research Laboratory Lockheed Missiles and Space Co., Inc. 3251 Hanover St., Palo Alto, Ca. 94304 | Project 3417 |

| 11. CONTROLLING OFFICE NAME AND ADDRESS | 12. REPORT DATE |
|---|---|
| Defense Advanced Research Projects Agency (DoD) Wilson Boulevard Arlington, Va. 22209 | July 1978 |
| | 13. NUMBER OF PAGES |
| | 162 |

| 14. MONITORING AGENCY NAME & ADDRESS(if different from Controlling Office) | 15. SECURITY CLASS. (of this report) |
|---|---|
| Air Force Materials Laboratory Air Force Systems Command Wright-Patterson Air Force Base, Ohio 45433 | UNCLASSIFIED |
| | 15a. DECLASSIFICATION/DOWNGRADING SCHEDULE |

16. DISTRIBUTION STATEMENT (of this Report)

Approved for public release; distribution unlimited

17. DISTRIBUTION STATEMENT (of the abstract entered in Block 20, if different from Report)

18. SUPPLEMENTARY NOTES

19. KEY WORDS (Continue on reverse side if necessary and identify by block number)

| | | |
|---|---|---|
| aerospace structures | Al-Mg | atomization |
| rapidly solidified powders | design trade-off studies | fracture mode |
| aluminum alloy | mechanical properties | vacuum hot pressing |
| Al-Ca | microstructures | extrusion |
| Al-B | melt-spinning | Al 7075 |

20. ABSTRACT (Continue on reverse side if necessary and identify by block number)

A study was conducted to determine the feasibility of developing aluminum alloys from rapidly solidified powders having significant improvements in properties for aerospace structural applications. This study was comprised of four tasks: (1) survey of current technology for rapid solidification of aluminum alloy powders, (2) metallurgical and property evaluation of unusual composition aluminum alloys having some promise for advanced structural applications, (3) a series of design tradeoff studies of selected space, missile, and aircraft structures to assess the effect of assumed property improvements

DD FORM 1473 EDITION OF 1 NOV 65 IS OBSOLETE
1 JAN 73

on weight savings and, where possible, performance, and (4) formulation of a plan to exploit advanced aluminum alloys for application to new weapons systems where significant improvements in systems effectiveness would result.

The survey of current technology identifies promising alloy systems and methods of producing rapidly solidified powders. The most interesting property combination appears to be achieved by alloys of aluminum containing up to 3 weight percent lithium.

The novel composition aluminum alloys evaluated included separately 2 weight percent calcium, 20 weight percent magnesium and 1 weight percent boron. Additionally, 7075 commercial alloy was included, for comparison purposes. The alloys were made by induction melting small ingots, remelting and rapidly solidifying into small particulate using melt-spinning or centrifugal atomization, and helium gas quenching. The powders were vacuum hot pressed and extruded at a 10:1 reduction ratio to make a rectangular bar from which tensile and fracture toughness specimens were obtained. Microstructure of the as-solidified particulate and extruded product were obtained. The most significant result was a 12 percent increase in elastic modulus in the Al-2Ca alloy, with no significant change in density. In the Al-20Mg alloy, a 13 percent decrease in density was obtained; however, the elastic modulus also decreased 27 percent.

The tradeoff studies indicate a number of areas where significant weight savings would obtain by application of new aluminum alloys exhibiting 15 percent or more increased modulus coupled with 11 percent or more decreased density. Strength-critical aerospace components would similarly benefit by increased strength combined with decreased density.

Recommendations for the development of advanced aluminum alloys from rapidly solidified powders was formulated. The goal established for alloy development is a 30 percent increased specific stiffness (elastic modulus-to-density ratio). Applications for significant improvement in weight savings and concomitant performance are the Advanced Tactical Fighter aircraft (AF), Subsonic V/STOL aircraft (NAVY), and Advanced TRIDENT-D5 FBM (NAVY), all of which are to be developed in the next decade.

FOREWORD

The report is the result of a feasibility study for the development of structural aluminum alloys from rapidly solidified powders for aerospace structural applications. The authors of this report are R. E. Lewis, D. Webster, and I. G. Palmer, of LMSC, Inc. The work was performed by the following LMSC, Inc. personnel.

| | |
|---|---|
| Principal Investigators | - R. E. Lewis and D. Webster |
| Summary of Current Technology | - I. G. Palmer |
| Materials Processing | - D. D. Crooks |
| Properties Evaluation | - D. D. Crooks, R. L. Boorn |
| Optical Microscopy | - A. Hansen |
| Transmission Electron Microscopy | - H. Kawayoshi, V. Phillips |
| Scanning Electron Microscopy | - A. Gleason |
| Space Systems Design Trade-Off Studies | - E. Loss |
| Missile Systems Design Trade-Off Studies | - W. M. Brown and J. E. Butler |

In addition, G. Wald, F. Strunk and R. Mejares of the Lockheed-California Co. performed the design trade-off studies of air vehicle (airplane) structures.

78 11 14 026

CONTENTS

CONTENTS (Cont'd)

TABLES

TABLES (Cont'd)

ILLUSTRATIONS

ILLUSTRATIONS (Cont'd)

ILLUSTRATIONS (Cont'd)

ILLUSTRATIONS (Cont'd)

## Section 1
## INTRODUCTION

Three major new aerospace systems are to be developed in the next decade which will have significantly advanced military capabilities. They are an Advanced Tactical Fighter (Air Force), Vertical/Short Takeoff and Landing Reconnaissance Airplane (Navy), and Advanced Fleet Ballistic Missile (Navy). In each of these, improved structural materials properties are needed to significantly improve range, payload, and service life over that which would result from current technology.

The most common presently used structural materials in aerospace systems are alloys of aluminum. Selective use is made of other metals and alloys such as high strength steel and titanium, magnesium, and various composite materials. In order to significantly improve operational effectiveness of new aerospace weapons systems, any new materials developed must be stronger or stiffer than materials currently available. In order to identify those property goals which would have a maximum payoff in these new systems, design trade-off studies have been and are being performed. These studies include advanced aluminum alloys, titanium alloys and composites. Two important considerations in these studies are pertinent to the present work:

(1) Improved aluminum alloys are of major interest to aerospace manu-
facturers because of the extensive existing manufacturing technology
and capability directly suitable for this class of alloys.

(2) The development of improved aluminum alloys which exhibit significantly
higher stiffness and/or strength properties is technically feasible.

## 1.1 Objective

The major objective of this program is to determine the feasibility of developing aluminum alloys from rapidly solidified powders having significant improvements in mechanical properties for aerospace structural applications. Specific objectives include (1) the determination of properties of unique aluminum alloys prepared from rapidly solidified powders, and the determination of the degree to which these properties are superior to commercially available alloys, (2) the prediction of benefits of weight, payload, and service life of the unique alloys for typical aircraft, missile, and space systems, (3) the identification of promising alloys for further development, and (4) recommendation of plans for major development of new aluminum alloys and structural forms pertinent to the aerospace industry.

## 1.2 Problem

Improvement in currently available materials is seriously limited by basic physical and mechanical metallurgy. Alloying of aluminum to significantly increase strength above that exhibited by 7075-T6 results in a serious loss in fracture toughness and stress corrosion resistance. For these reasons, 7079 and 7178 alloys, for example, have not been of practical use to aerospace designers even though they exhibit a 30 to 40 percent increase in strength over commonly used alloys. Ultra high specific strength or stiffness metals such as beryllium, steels and titanium alloys are either too expensive or too low in toughness to replace aluminum alloys in current applications. Development of graphite-aluminum metal matrix composites promises to contribute significant structural efficiency where uniaxial or biaxial properties suffice and where its low bearing strength is not a penalizing deficiency. However, graphite-aluminum composites are not useful where triaxial tensile, in-plane shear, or bearing loads are major factors of the structural design due to low fiber-matrix interfacial bond strength.

Thus, major advances in the usefulness of new aerospace systems are expected from development of unique monolithic aluminum alloys exhibiting higher strength, stiffness, toughness, and fatigue behavior and lower density and susceptibility to stress corrosion cracking.

## 1.3 Approach

An important degree of freedom in developing new alloys exhibiting improved properties is obtained by rapid solidification from the melt. Compositions and grain sizes not possible by conventional casting can be obtained by solidification rates of at least $10^5$ $^{\circ}$K/sec. This has been demonstrated by quenching a thin stream or small droplets of liquid metal in gas, liquid or impingement on a chilled solid surface. Small lots of a variety of metals and alloys have been produced under laboratory conditions then consolidated by hot pressing and extrusion, and unique microstructures and properties appear to be achieved. However, for aluminum alloys, no systematic study had been undertaken to evaluate the feasibility of this approach or to predict the impact on weapon development or nature of warfare, presuming significant improvement in properties is obtained in a scale suitable for full-size structures applications. The work reported herein is a study of *the feasibility of developing aluminum alloys from rapidly solidified powders* having significantly improved properties.

This study consists of four tasks. Task I involves a survey of current technology in rapidly-quenched aluminum powders. Task II is an evaluation of unique, promising alloy compositions. Task III is a series of design tradeoff studies to predict potential gains in selected aerospace structural applications of new alloys achieving pertinent property improvements. Task IV includes an analysis of the results of the first three tasks and the development of a detailed plan to exploit new aluminum alloys produced from rapidly-quenched powders.

3

## Section 2
## SURVEY OF CURRENT TECHNOLOGY

### 2.1 Rapid Solidification

In recent years a considerable background of information has been published
on the improved structures and properties obtained by the rapid quenching of
alloys from the melt.  A summary of recent information is given in the
Proceedings of the Second International Conference on Rapid Quenching held
in November 1975 at M.I.T. (1,2).  Rapid quenching can be achieved by a
variety of methods ranging from gas or water atomization to metallic substrate
(splat) quenching.  The cooling rates obtained during solidification, esti-
mated for example by measurement of dendrite arm spacings (3,4), range from
$10^0$-$10^3$ K/sec. for gas atomization, to $10^6$-$10^9$ K/sec. for various splat
methods.  The quenching rates of interest in the present study are those
which produce microcrystalline structures showing improved mechanical
properties, and in rapidly quenched aluminum alloys they range from $10^3$-$10^6$
K/sec.  The most significant benefits achievable from these microcrystalline
structures are as follows.

o  Decreased Grain Size

   There is a progressive decrease in grain size with increasing cooling
   rate, and grain sizes of $\leq 1\mu$m can be obtained.  The decrease in
   grain size increases both strength and toughness.

o  Increased Solid Solubility

   Quenching from the melt increases solid solubility, often by orders
   of magnitude compared to equilibrium conditions.  These increases
   can produce unique alloy structures, new precipitated phases and
   large increases in volume fraction of precipitate during aging.

4

o Elimination of Segregated Phases

Rapid quenching can either eliminate the complex intermetallic
particles which form in conventionally cast aluminum alloys (e.g.
AlCuMnFe intermetallics), or reduce the size of the particles which
form to give a fine dispersion of sub-micron sized particles and an
improvement in properties, particularly toughness.

## 2.2 Rapidly Solidified Aluminum Alloys

Studies on rapidly solidified aluminum alloys can be divided into two groups.
The first group includes studies of the rapidly solidified powder particles,
both as-solidified and after various thermal treatments; these studies include
chemical analysis, microstructure (both optical and TEM), microhardness and
lattice parameter. Of particular interest has been the identification of the
various precipitation processes by which the supersaturated solid solutions
obtained by the rapid solidification decompose into the equilibrium phases,
and correlation of the changes in microstructure with observed changes in
lattice parameter, microhardness, etc. The second group of studies has been
concerned mainly with consolidation of the rapidly solidified powders, using
such methods as cold compaction, vacuum hot pressing, hot extrusion and cold
swaging. The resulting microstructures and physical and mechanical properties
of the bulk material have been correlated with the consolidation parameters
and heat treatments used. The aim has been to develop the consolidation
processes which provide the optimum combination of the desired mechanical
properties. In the following review of published work on rapidly solidified
aluminum alloys only the most recent or relevant papers are described and
only those which deal with alloy systems having potentially useful mechanical
properties at ambient or elevated temperature.

## 2.2.1 Microstructural Studies on Rapidly Solidified Powders

A summary of the papers reviewed in this section is given in Table 1.

**TABLE 1**

**MICROSTRUCTURAL STUDIES ON RAPIDLY SOLIDIFIED ALLOYS**

| ALLOY SYSTEM | QUENCHING METHOD | COOLING RATE K/sec. | PROPERTIES EVALUATED* | | | | REFERENCE |
|---|---|---|---|---|---|---|---|
| | | | 1 | 2 | 3 | 4 | |
| Al-Cr | Gun | $10^6$ | √ | √ | | √ | 5,6 |
| Al-Cr,Al-Mn,Al-Cu Al-Fe,Al-Co,Al-Ni | Gun | $>10^6$ | √ | √ | | | 7 |
| Al-Cu | Gun | $>10^6$ | √ | √ | √ | | 8,9,10 |
| Al-Cu | Plasma Sprayed | | √ | √ | | | 11 |
| Al-Fe | Gun | | √ | √ | | √ | 12 |
| Al-Fe,Al-Fe-Mn Al-Fe-Zr | Gun | | √ | √ | | | 13 |
| Al-Fe,Al-Ni Al-Cr,Al-Mn | Electron Beam | | √ | √ | | | 14 |
| Al-Mg-Si | | | √ | √ | | √ | 15 |
| Al-Mg,Al-Si, Al-Mg-Zr,Al-Mg-Mn | Arc Sprayed | $10^4$-$10^5$ | √ | √ | | √ | 16 |
| Al-Mn | | | √ | √ | √ | √ | 17 |
| Al-Mn | Gun | | √ | | | √ | 18 |
| Al-Ni | Gun | | √ | | | √ | 19 |
| Al-Zr | | | √ | √ | | | 20,21 |
| Al-Hf | | | √ | | | | 22 |

* 1. Microstructure
  2. Microhardness
  3. Microanalysis
  4. Lattice Parameter

6

## Al-Cr Alloys

Rapidly quenched Al-Cr alloys have been studied by Furrer and Warlimont (5,6). They used a gun technique to obtain cooling rates of $10^6$ K/sec. and studied the microstructure and phase composition of alloys containing up to 7 at % Cr. Six different decomposition mechanisms of the supersaturated solid solutions were identified. Fontaine (7) also studied Al-Cr and other Al-transition metal alloys up to 3 at %, and concluded that Cr, Mn and Cu substitute at random for Al atoms, whereas Fe, Co and Ni form clusters responsible for the high hardness values observed in these systems.

## Al-Cu Alloys

Williams and Edington (8,9) studied the microstructural characteristics of rapidly quenched Al-Cu alloys. They splat quenched seven alloys with copper additions up to the eutectic (17.3 at % Cu) composition using a gun system to obtain cooling rates of $> 10^6$ K/sec. They examined the microstructures of as-quenched powders in the TEM and also performed high resolution microanalysis in the TEM. Davies and Hull (10) also used a gun technique in an inert atmosphere to study the microstructure of the Al-17.3 at % Cu eutectic composition. This study showed the importance of a low-oxygen quenching atmosphere in promoting efficient spreading of liquid particles and good thermal contact with the quenching surface. Their quenching method was sufficiently fast to cause the formation of amorphous phases. Krishnanand and Cahn (11) studied the properties of plasma sprayed Al-6 at % Cu and Al-12 at % Cu. The aim was to assess the usefulness of plasma spraying as a single stage process for splat quenching and compacting on a substrate. Very high hardness values (300 DPN) were obtained in the as-sprayed layers. They studied the hardness as a function of aging time and temperature and found strong secondary hardening effects.

## Al-Fe Alloys

Jones (12) studied the microhardness as a function of alloy composition for splat-cooled Al-Fe alloys with compositions in the range 0.5 - 13 at % Fe, and showed that the hardness increased continuously with increased alloy

7

content. The splats showed two different structures and the supersaturated regions of a splat were found to be twice as hard as the other regions. These regions in turn were twice as hard as conventionally cast material. Jacobs and coworkers (13) examined a splat-quenched Al-8 wt. % Fe alloy, and confirmed the presence of two different structures in as-quenched splats. They characterized each in terms of the dispersions and types of phases present, and investigated their decomposition behavior on annealing between 573 and 873 K. The effect on the microstructures of adding 3% Mn or 1% Zr to the alloy was also examined. The observed microstructures and phase transformations were correlated with microhardness measurements.

Gruhl and coworkers (14) produced rapidly quenched Al-Fe alloys (and also Al-Ni, Al-Cr and Al-Mn alloys) by local electron beam melting followed by rapid cooling. The Al-6% Fe alloy showed the most promising properties especially at temperatures above 200°C.

## Al-Mg Alloys

Bose and Kumar (15) studied rapidly solidified Al-Mg-Si alloys, with compositions chosen to give $Mg_2Si$ in the range 1-10% with excess Si up to 4-5%. Lattice parameter, microhardness and microstructure were studied as a function of $Mg_2Si$ content and annealing temperature.

Warlimont and Kunzman (16) studied Al-Mg, Al-Si, Al-Mg-Zr, Al-Mg-Mn commercial filler wire alloys, in the form of arc sprayed coatings, produced with a cooling rate of $10^4$-$10^5$ K/sec. Lattice parameter, hardness, microstructure and stress deflection measurements were made on the coated samples.

## Al-Mn Alloys

Ikeda and Nishi (17) studied precipitation processes in a supersaturated Al-3% Mn alloy obtained by rapid solidification. They measured hardness and lattice parameter and made x-ray diffraction and microanalysis measurements. The precipitation process was very complex and four different decomposition phases were identified. They also found that iron and silicon impurity elements had a significant effect on the precipitation process.

8

Bhat and coworkers (18) used a gun technique to produce rapidly quenched Al-Mn alloys, and extended the solid solubility by a factor of four. The supersaturated solid solutions were retained up to 523 K without significant decomposition. When decomposition occurred the equilibrium $Al_6Mn$ phase was precipitated.

## Al-Ni Alloys

Chattopadhyay and coworkers (19) used a gun technique to splat cool an Al-7 at % Ni alloy, and used TEM to study the metastable phase formed. This phase was unstable with respect to plastic deformation at room temperature, and also decomposed in 10 min. at 573 K.

## Al-Zr Alloys

Nes and Billdal (20) examined the transformation products formed during rapid solidification of Al-0.8 wt. % Zr and Al-1.5 wt. % Zr. They identified three different phases; the equilibrium $Al_3Zr$, a metastable cubic $Al_3Zr$ and a supersaturated Al-Zr solid solution. Dahl and coworkers (21) examined Al-1.2 % Zr alloys which were rapidly solidified in a water cooled mold. Aging at 573-673 K caused precipitation of spherical coherent particles of metastable cubic $Al_3Zr$, and distinct age hardening. At higher temperatures the equilibrium $Al_3Zr$ phase appeared. Repeated precipitation hardening was found to be not possible.

## Al-Hf Alloys

Ryum (22) performed a metallographic study of an Al-1.78 wt. % Hf alloy after rapid solidification, and high temperature annealing. Rapid solidification produced a supersaturated solid solution. On annealing, the intermediate $Al_3Hf$ phase precipitated as coherent spheres and dendrites. On continued annealing the equilibrium $Al_3Hf$ phase precipitated as a laminated structure with the intermediate phase.

9

### 2.2.2 Microstructure and Mechanical Property Measurements on Consolidated Material

A summary of the papers reviewed in this section is given in Table 2.

### Al-Cu-Mg Alloys

Lebo and Grant (23) studied the structure and properties of rapidly solidified 2024 Al alloy (Al-4.5% Cu-1.4% Mg-0.6% Mn). They used a splat method and estimated cooling rates of up to $10^6$ K/sec., based upon measurement of dendrite arm spacings. The flakes were screened and then consolidated by cold compaction, vacuum annealing and hot extrusion, using a reduction ratio of 20 to 1. The extruded material was cold swaged, solution treated, quenched and naturally aged. The splat cooled alloy had constituent particles of $1\mu$m or finer, compared to 5-20$\mu$m for the commercial material, and one of the constituent phases (AlCuFeMn) was virtually eliminated by the rapid quench. Very little coarsening of the dispersion of constituent particles occurred during the high temperature extrusion and solution treatment stages, although the grain size did coarsen significantly. Compared to the commercial alloy, the splat quenched material showed 15 to 29% improvement in yield and ultimate strength with no loss of ductility, a seven-fold increase in fatigue life at 207 MPa (30,000 psi), and a large improvement in the 423 K stress rupture life. The fracture characteristics were inhomogeneous due to the presence of finely dispersed oxide films.

### Al-Zn-Mg Alloys

Durand, Pelloux and Grant (24) studied the structure and properties of splat quenched 7075-Al type alloys (Al-6% Zn-1.3% Cu-2.3% Mg-0.2% Cr), in which modifications to the basic alloy included increases in Zn, Mg and Cu, and in one alloy, additions of Ni and Fe. Foils were produced by splat quenching using a copper roll method. The cooling rate was estimated to be $10^5$-$10^6$ K/sec. by measurement of dendrite arm spacings. Some degree of supersaturation occurred and resulted in rapid aging of the foils at room temperature and below. The structure was highly refined and coarse intermetallic particles were not formed. No Cr-rich phase could be identified and very few

TABLE 2

MICROSTRUCTURE AND MECHANICAL PROPERTY MEASUREMENTS ON
CONSOLIDATED MATERIAL

| ALLOY SYSTEM | QUENCHING METHOD | COOLING RATE K/sec. | CONSOLIDATION METHOD | PROPERTIES EVALUATED* | | | | | | REFERENCE |
|---|---|---|---|---|---|---|---|---|---|---|
| | | | | 1 | 2 | 3 | 4 | 5 | 6 | |
| Al-Cu-Mg (2024) | Splat | $10^6$ | Cold compaction, vac. annealing, hot extrusion | √ | √ | √ | √ | √ | | 23 |
| Al-Zn-Mg (7075) | Splat | $10^5$-$10^6$ | Vac. annealing, hot extrusion | √ | √ | | | | | 24 |
| Al-Zn-Mg (7075) | Melt Spinning | $10^5$-$10^6$ | Cold compaction, vac. annealing, hot pressing, hot extrusion | √ | √ | √ | | | | 25 |
| Al-Fe | Splat | $10^6$ | Cold compaction, annealing, hot extrusion | √ | √ | √ | | | √ | 26 |
| Al-Fe Al-Fe-Zr,Al-Fe-Mn | Gun | $>10^5$ | Cold compaction, hot extrusion | √ | √ | √ | | √ | √ | 27 |
| Al-Mn-Cu Al-Mn-Cr-Mg-Zn | Atomization | | | √ | √ | | | | √ | 29 |
| Al-Mn | Atomization | | Extrusion | √ | √ | | | | | 30 |
| Al-Cu-Mg-Li (2024 + Li) | Melt Spinning | $10^4$ | Cold compaction, vac. hot pressing, hot extrusion | √ | √ | | √ | | √ | 47 |
| Al-Cu-Mg-Li (2024 + Li) | Splat | $10^4$ | Cold compaction, hot extrusion | √ | √ | | √ | √ | √ | 48 |
| Al-Zn-Mg-Cu-Co (MA67,MA87) | Atomization | $10^3$-$10^5$ | Cold compaction, vac. annealing,hot pressing, hot extrusion | √ | √ | | √ | √ | √ | 60,61 |

* 1. Microstructure   3. Elevated Temperature Tensile   5. Creep
  2. Tensile   4. Fatigue   6. Corrosion/Stress Corrosion

11

Fe and Si rich particles were found. Foils were solution heat treated, quenched and aged. Resultant grain sizes were in the range 10-35μm, and all inclusions were found as a fine dispersion of particle size less than 0.5μm.

Foils were consolidated by vacuum annealing followed by hot extrusion using a ratio of 20 to 1. Some alloys were cold swaged after extrusion. Consolidated material was solution treated, quenched and aged. Tensile properties were compared with values for commercial (ingot) bar 7075-T6 and 7075 produced from air atomized powders with a quench rate of about $10^3$ K/sec. The alloys with modifications of the 7075 composition had excellent tensile properties, and were significantly stronger than 7075. The improved properties were attributed to a finer substructure and a finer dispersion of $FeAl_3$ type intermetallic particles.

Mobley, Clauer and Wilcox (25) studied the properties of 7075 Al compacted from rapidly solidified melt-spun ribbon; the cooling rate was estimated to be $10^5$-$10^6$ K/sec. Material was consolidated by cold pressing, vacuum annealing, hot pressing and hot extrusion with a 36:1 reduction ratio. Extruded material was heat treated to the T-6 condition, which resulted in a very fine equiaxed grain size (1-10μm). The mechanical properties were compared with those of commercial material. The room temperature yield strength and ductility were about 10% higher than the commercial material. The strength level remained greater up to about 573 K. At about 673 K the alloy exhibited superplastic tendencies ($\varepsilon \sim 200\%$), attributed to the fine grain size.

## Al-Fe Alloys

Faninger, Merz and Winter (26) studied the elevated temperature strength, and the corrosion resistance of Al-6% Fe and Al-8% Fe containing small additions of Mg, Mn and Cr. Powders were produced by a splat process giving a cooling rate of $10^6$ K/sec. The powders were cold compacted, annealed at 673 K, and extruded using a reduction ratio in the range 25:1 to 38:1   The consolidated

12

materials showed good elevated temperature strength up to 573 K which was attributed to dispersion hardening, and good corrosion resistance; the small additions of Cr and Mn had beneficial effects on these properties. Thursfield and Stowell (27) examined the properties of a splat quenched binary Al-8 wt. % Fe alloy, and ternary alloys containing additions of Zr and Mn. The alloys were quenched by means of a gun technique, giving cooling rates in excess of $10^5$ K/sec. The microstructures of the same alloys were examined by TEM by Jacobs, Doggett and Stowell (13). The alloys were consolidated by cold compaction followed by hot extrusion. The alloys had exceptional high temperature tensile properties, and room temperature properties equivalent to those of the strongest Al alloys available. The microstructure and room temperature strength of the Al-8 wt. % Fe alloy were stable up to 613 K. The strength of the splat cooled alloy was substantially superior to that of an Al-8 wt. % Fe alloy studied by Towner (28) and made by gas atomization (with a cooling rate of $10^3$ K/sec.), at all temperatures up to 673 K. These results were attributed directly to the difference in cooling rate employed in the two techniques. The elastic modulus of the alloys was also measured as a function of temperature from 293 K to 673 K. At 293 K the modulus was 81GPa (11.8 x $10^6$ psi) and at 373 K 72GPa (10.4 x $10^6$ psi). Additions of 1 wt. % Zr to the Al-8 wt. % Fe alloy resulted in improved strength at all temperatures and particularly between 573 K and 723 K. Additions of Mn to the alloy improved the strength at temperatures between 373 K and 523 K.

## Al-Mn Alloys

Rostoker et al (29) studied the properties of Al-Mn-Cu and Al-Mn-Cr-Mg-Zn alloys produced from consolidated powder which had been made by atomization. The alloys showed high yield strengths and hardnesses which resisted softening at temperatures as high as 623 K. Some alloys showed good high temperature yield strength. Preliminary tests showed that the alloys were not susceptible to stress corrosion cracking at stresses of yield strength magnitude.

Sheppard (30) studied the properties of Al-Mn alloys produced by extrusion of atomized powders. The structure and substructure of the alloys was

investigated, and the properties compared with those of other alloys produced by powder metallurgy.

## 2.3 Physical Metallurgy of Aluminum Alloys and Effects of Rapid Solidification

The physical metallurgy of aluminum alloys has been recently reviewed in a number of articles (see for example the Symposium on Advances in the Physical Metallurgy of Aluminum Alloys 1975 (31), Staley (32), Starke (33)).

The parameters of importance which determine the mechanical properties of high strength aluminum alloys will be reviewed here, and the extent to which these can be significantly changed by rapid solidification in order to improve the mechanical properties will be discussed.

The most significant metallurgical factor which influences mechanical properties is the type and distribution of second phase particles. In commercial alloys these have been classified into three types:

(1)  Constituent particles. These are Fe, Si and Cu rich inclusions 0.1 to 10μm in dia., formed during casting. Fe and Si are usually impurities, whereas Cu is a deliberate alloying addition.

(2)  Intermediate particles or dispersoids, rich in Cr, Mn or Zr, 0.05 to 0.5μm in size, which are used to control recrystallization and grain growth.

(3)  Precipitate particles, rich in Cu, Mg, Zn, etc., which have dimensions from 0.01 to 0.5μm, and are used to strengthen the matrix.

The role of these different particle dispersions, together with other important parameters such as grain size, will be discussed more fully below.

## High Modulus Aluminum Alloys

Significant increases in the modulus of aluminum alloys can be achieved by the presence of a large volume fraction of a fine dispersion of second phase

14

particles of high elastic modulus. Solid solution alloying or texture modifications can also increase the modulus, but in general to a lesser extent. The dispersion of second phase particles can be achieved in two ways, either as precipitates during conventional age hardening of solution treated and quenched material, or as a relatively insoluble dispersoid which precipitates during cooling or subsequent processing. The volume fraction is determined by the amount of solute and by the composition and density of the precipitated phase.

The Al-Li system is an example of the first system in which there is extensive solid solubility of Li in Al so that the alloy can be solution treated, quenched and aged in the conventional way, and rapid solidification is not required to achieve a high volume fraction of precipitate. Extensive studies have been made of this system (see Section 2.4) which shows the highest specific modulus for a given solute content of any aluminum alloy system. The precipitate which forms at low aging temperatures is $Al_3Li$, and very high volume fractions can be obtained, giving a high modulus. Difficulties have been experienced with the Al-Li system in the conventionally cast and wrought condition, in particular low toughness at peak strength, and segregation in large ingots. Rapid solidification of powders should enable significant improvements in the strength and toughness of these alloys to be achieved, by decreasing segregation, and producing a very fine grain size.

The Al-Mn system is an example of the second type of system, with limited solid solubility, in which conventional casting will not achieve sufficient supersaturation to give a large volume fraction of fine precipitate. Rapid solidification is needed to achieve this requirement. This alloy in the cast and wrought condition has shown a higher modulus than most other aluminum alloys (34). Rapid quenching of Al-Mn alloys will give a supersaturated solid solution, and if the precipitation of second phase ($Al_6Mn$) can be controlled during consolidation and subsequent processing, to give a fine dispersion, then a high modulus and improved secondary properties should be obtained. Other alloy systems (Al-Ca) have shown increased modulus values in

15

preliminary studies (see Section 3), and would also be expected to show significant improvements as a result of rapid quenching.

## Alloys Showing Decreased Density

Alloy elements of low density can be added to aluminum alloys to decrease the density, and to a first approximation the final density can be calculated from the law of mixtures (35). The common alloying elements Li, Mg, Si, and B decrease the density and Cr, Cu, Fe, Mn, Ni, Ti and Zn result in an increase. Li has the greatest effect in decreasing the density for a given alloy content, and since it also has the greatest effect in increasing the modulus, it clearly is the outstanding system for improvement in specific modulus. In other systems in which the element forming the high modulus phase is of high density, it may be necessary to add other elements of low density (e.g. Mg) to decrease the final alloy density.

## Alloy Elements Influencing Strength

Strengthening of aluminum alloys can be achieved by a number of different mechanisms including solid solution strengthening, precipitation hardening dispersion hardening, work hardening and use of a fine grain size. Precipitation hardening is the most effective and is achieved by solution heat treatment, quenching and aging to precipitate coherent G-P zones, partially coherent intermediate precipitates or incoherent equilibrium precipitates, depending on the aging conditions. In the 2000 series aluminum alloys Cu is the principal alloy element and gives precipitation strengthening by zones, intermediate precipitates, or the equilibrium precipitate $CuAl_2$. In the 7000 series alloys Zn and Mg are the principal alloying elements and provide zones and precipitates of the $MgZn_2$ type.

In addition to direct strengthening which is achieved by precipitates interacting with dislocation movement, alloy elements can provide indirect strengthening by the formation of fine stable dispersoids which stabilize a fine grain structure.

16

Rapid quenching of aluminum alloys can result in significant strength increases being obtained, firstly as a result of increasing the solid solubility and thereby increasing the volume fraction of precipitate which forms on aging, and secondly as a result of the very fine grain size ($\sim 1\mu m$) which is well below the size ($\sim 5\mu m$) at which significant strengthening starts to occur.

## Factors Affecting Fracture Toughness

Alloy elements affecting fracture toughness in aluminum alloys are predominantly those which form brittle insoluble intermetallic compounds (36). These brittle particles fracture at low strains and initiate microvoids which coalesce to cause failure. The role of various alloying elements in affecting both strength and fracture toughness has been studied by many workers, for example in 7178 Al alloy by Piper, et al (37), who found that Fe degraded toughness to the greatest extent. Recent work (38,39) has shown that the most significant elements influencing toughness of aluminum are both Fe and Si. This has lead to the development of new alloys having the same nominal chemistry as previous ones but with Fe and Si contents kept to an absolute minimum. Examples are 2124 (the counterpart of 2024) and 7475 (the counterpart of 7075) which have the same strengths as their counterparts, but enhanced toughness. Both the particle size and volume fraction of the intermetallics are important and large particles are particularly detrimental. Rapid quenching can eliminate the formation of large intermetallic particles and result in the formation of a very fine dispersion with significant increase in fracture toughness.

The reduction in grain size which is achieved by rapid quenching may be even more important than the reduction in the intermetallic particle size, since it represents a unique opportunity by which the material may be both strengthened and toughened. This is particularly attractive in view of the generally observed inverse relationship between strength and toughness. The fine grain size will also be stabilized by the fine dispersion of intermetallic particles. Data are reported by Hahn and Rosenfield (36) and by Thompson (40) that show significant increases in fracture toughness with

17

decrease in grain size for a number of 7000 series alloys in both the under-
aged and overaged conditions. Similar data are also shown by Nes (41) for
Al-Zn-Mg alloys in the naturally aged and peak aged conditions. Rapid soli-
dification by splat quenching produces grain sizes $\sim 1\mu m$ which are signifi-
cantly smaller than those developed in conventional casting. A quantitative
analysis of the grain refinement resulting from solidification at the high
cooling rates ($> 10^5$ K/sec) encountered in splat quenching has been made by
Boswell and Chadwick (42), and good agreement was obtained between observed
and predicted grain sizes for rapidly quenched aluminum. Significant in-
creases in toughness should be realized if the fine grain size obtained by
the splat quenching can be retained through subsequent consolidation.

## Factors Affecting Fatigue Crack Propagation

Many studies of fatigue crack growth rates in the intermediate growth rate
regime have shown that metallurgical factors such as monotonic yield strength,
thermomechanical treatment and preferred orientation do not have a significant
effect on the crack growth rate in aluminum alloys. The most significant
finding has been that the fatigue crack growth rates in engineering alloys
depend on the modulus of elasticity. By normalizing the stress intensity
factor range by the modulus, differences in fatigue crack growth rate are
largely eliminated (43). One of the significant benefits of the production
of high modulus aluminum alloys from rapidly solidified powders is the reduc-
tion in fatigue crack growth rate which should be achieved. Results reported
in the literature (23) have shown significantly improved fatigue lifetimes
in rapidly quenched aluminum alloys which are probably a result of decreased
crack growth rate.

## Factors Affecting Environment-Assisted Cracking

The environment assisted cracking of aluminum alloys has been recently reviewed
by Speidel (44). The main metallurgical factors affecting environment assisted
cracking in aluminum alloys are alloy chemistry, heat treatment and thermo-
mechanical treatment. Many studies have shown that overaging is the most
effective way to improve the environment assisted cracking behavior of aluminum

18

alloys. Overaging also decreases the yield strength but increases the fracture toughness. The same factors that apply in conventionally cast and wrought materials will likely apply in rapidly quenched aluminum alloys. The resistance to environment-assisted cracking generally improves with decreasing size of constituent particles (44). Rapid solidification produces very fine constituent particles and should therefore improve these properties.

## Factors Affecting Elevated Temperature Strength

One of the requirements for elevated temperature strength is a fine dispersion of thermodynamically stable, coherent, coplanar precipitates or second-phase particles (Fine (45)). The intermediate size precipitates which are found in 7075 containing Cr are stable, partially coherent precipitates, and $ZrAl_3$ is also partially coherent with the Al matrix. The volume fractions of both these particles are limited in conventionally cast systems but may be significantly increased by rapid solidification. $Al_3Ni$ is also a very stable phase used to obtain elevated temperature strength and normally only small volume fractions can be obtained. The presence of Fe in conventionally cast Al alloys normally has a deleterious effect on properties as a result of the relatively coarse intermetallic particles which are formed. However, rapid solidification of Al-Fe alloys has been shown to result in a very fine dispersion of stable $FeAl_3$ particles, and better high temperature properties than existing commercial high temperature alloys (27). In binary Al-Mg alloys, $Mg_2Al_3$ is a reasonably stable phase and large volume fractions may be formed in conventional casting. However rapid solidification would give a much finer dispersion and would be expected to improve elevated temperature strength. Similarly in the Al-Cu system where the stable $CuAl_2$ phase is used to improve elevated temperature properties in alloys containing Cu in excess of the solid solubility limit, rapid solidification would be expected to improve the properties by providing a much finer dispersion of the $CuAl_2$ particles.

19

## 2.4 Aluminum-Lithium Alloys

Al-Li alloys are being evaluated for aerospace applications as a result of the significant increase in specific modulus (i.e., modulus/density ratio) which can be achieved in this alloy system. Recent progress in the development of Al-Li alloys has been reviewed by Sanders and Balmuth (46). Difficulties have been experienced in the conventional casting of these alloys, in particular segregation of alloy elements, and low values of fracture toughness. For this reason alloy X-2020 was withdrawn as a commercial product. As a result of these difficulties, attempts are currently being made to produce Al-Li alloys from rapidly solidified powders (Webster (47), Sankaran (48)). Rapid solidification is being used primarily for its ability to reduce segregation and produce a fine grain size, rather than to extend solid solubility which is not necessary for the Al-Li system. Previous research on Al-Li alloys can be divided into work on the precipitation effects in the alloys, and work on the mechanical properties. Research has been reported mainly on binary Al-Li alloys and on two ternary systems, Al-Cu-Li and Al-Mg-Li.

### Precipitation Studies

### Al-Li Binary Alloy

The decreasing solid solubility with temperature of Li in Al renders the system capable of age hardening. TEM studies (Noble and Thompson (49), Williams and Edington (50)) have shown that the precipitation sequence is: solid solution $\rightarrow \delta' \rightarrow \delta$, where $\delta'$ is a metastable ordered precipitate which has the $LI_2$ type superlattice structure (similar to $Cu_3Au$) and the composition $Al_3Li$, and $\delta$ is the equilibrium f.c.c. phase of composition AlLi. Noble and Thompson (49) found that the $\delta'$ precipitation occurred over a temperature range of 293-513 K in a 2 wt. % Li alloy and formed a spherical precipitate which had a volume fraction of 0.04, and over a temperature range of 293-573 K in a 4 wt. % Li alloy forming an irregular shaped precipitate with a volume fraction of 0.4. They also found that variation of the quench rate had little effect on $\delta'$ formation. The precipitate size and dispersion

20

after aging at 473 K were essentially the same after furnace cooling or water quenching from the solution treatment temperature. The size of the $\delta'$ precipitate varied from 0.01μm after aging for 24 hr. at 373 K to 0.03μm after aging for 24 hr. at 473 K. This latter treatment produced considerable strengthening and the maximum hardness. Above 473 K $\delta'$ coarsened rapidly according to an $r^3$ relation. Continued aging below the $\delta'$ solvus, or aging above the $\delta'$ solvus (513 K in the 2 wt. % alloy and 573 K in the 4 wt. % alloy) resulted in the heterogeneous formation of the equilibrium (f.c.c.) $\delta$ precipitate. The $\delta$ precipitates were found to add little to the strengthening of the alloy due to the large size and coarse dispersion of the particles.

### Al-Cu-Li Alloys

Early work on this system was performed by Hardy (51) and Silcock (52). They used alloys containing up to 5 wt. % Cu and up to 2.5 wt. % Li. The precipitates formed on aging at 438 K were identified as $\theta''$ and $\theta'$ as in binary Al-Cu alloys, $\delta'$ as in binary Al-Li alloys, and $T_1$ ($Al_2CuLi$). The equilibrium precipitates formed by aging at 623 K were identified as $\theta$ ($CuAl_2$), $T_1(Al_2CuLi)$, $T_3(Al_7Cu_4Li)$ and $\delta(AlLi)$. The effect of Cd additions on aging was also investigated. Noble and coworkers (53) investigated the aging of Al-4.5 wt. % Cu alloys containing between 0.8 and 1.5 wt. % Li. Natural aging resulted in GP zones with the Li remaining in solution. At elevated temperatures Li suppressed the formation of $\theta''$ while promoting the formation of $\theta'$. In alloys with Li contents above 1 wt. % fine $\delta'$ was also precipitated. In 2020 alloy (Al-4.5 wt. % Cu - 1.5 wt. % Li) Sanders and Balmuth (46) reported that the Cu precipitated independently of the Li and followed the sequence of the Al-Cu binary system, while the Li precipitated as $\delta'$.

### Al-Mg-Li

The aging sequence in Al-Mg-Li alloys has been determined as: solid solution $\rightarrow \delta'\rightarrow Al_2MgLi$ (Sanders (54), Thompson and Noble (55)). The strengthening precipitate is the $\delta'$ phase; it is essentially unaltered by the presence of the

21

Mg, the beneficial effect of which is attributed to solid solution strengthening. The equilibrium $Al_2MgLi$ precipitate, which is incoherent and transforms from $\delta'$ upon prolonged aging, does not significantly strengthen the alloy.

## Mechanical Properties

The most attractive feature of Al-Li alloys for aerospace structural applications is that they possess a higher elastic modulus and lower density than commercial high strength Al alloys, giving significantly higher values of specific modulus. The specific modulus of a 2.84 wt. % Li alloy is 21% higher than that for 2024-T351 and 26% higher than that for 7075-T651 (Sanders and Balmuth (46)). The alloys also show high yield strength and good corrosion resistance; however values of fracture toughness are currently lower than desired, and research is in progress to improve the toughness of these alloys.

## Al-Cu-Li Alloys

The earliest commercial alloy containing Li was developed in 1957; it had a nominal composition of Al 4.5% Cu 1.3% Li 0.5% Mn 0.02% Cd and was designated X2020. This alloy was stronger than 7075-T6, and possessed a 3% lower density and an 8% higher modulus. The fatigue properties were superior to those of 7075-T6 and the stress rupture properties were superior to those of all other high strength Al alloys. The fracture toughness, however, was low, particularly in the peak strength temper; a significant improvement in toughness could be obtained by slightly underaging the alloy (Sanders (56)).

The Russian alloy VAD23 similar in composition to X2020, was developed in 1962, and its properties are similar to those of X2020 (Fridlyander (57)). Both X2020 and VAD23 contain about 0.2 wt. % Cd, which has been shown to increase the strength at all temperatures, and to improve the stress-rupture properties. It is thought that the strengthening arises from a reduction in the matrix-precipitate interfacial energy which results in a finer precipitate distribution; the resistance to coarsening of the precipitates is also increased thereby improving the elevated temperature properties.

22

## Al-Mg-Li Alloys

Alloys with compositions in the two phase solid solution + $Al_2MgLi$ region are age hardenable, and this feature was utilized in the development of the Russian alloy 01420 in 1968 by Fridlyander et al (58). The alloy has similar strength, 12% lower density, 8% higher modulus, and better corrosion and fatigue properties than 2024-T4.

Recent work has been performed at ALCOA on Al-Mg-Li alloys strengthened by the precipitation of $\delta'$, and has resulted in high strength alloys with very high values of specific modulus (Evancho (59), Sanders (54), Sanders and Balmuth (46)). The alloys possess lower than desirable values of fracture toughness. It has been proposed that this is a result of the ordered structure of $\delta'$ which limits cross slip so that high stress concentration can occur at grain boundaries, where there is heterogenous precipitation of $Al_2MgLi$. This can lead to intergranular failure and low values of toughness (Sanders (54)).

## Rapidly Solidified Al-Li Alloys

Webster (47) examined the properties of Al-2024, Al-2024-1-1/2% Li and Al-2024-3% Li alloys, consolidated from rapidly quenched powders made by a melt spinning process. The alloys showed that a 28% improvement in specific modulus could be obtained with 3% Li while maintaining a high strength (yield strength 62 ksi). Impact toughness was low at peak strength but could be increased to Al-7075-T6 levels by underaging with a consequent loss in strength. The Al-Li alloys were easy to hot work and machine, showed acceptable corrosion resistance in 3-1/2% NaCl solution, and could be welded. The properties of an Al-5% Li alloy consolidated from gas atomized powders are currently being examined.

Sankaran (48) examined the properties of Al-2024-1% Li and Al-2024-3% Li alloys consolidated from splat quenched flakes made by a roll method with a cooling rate of $10^4$ K/sec. A grain size of $2\mu m$ was obtained in the 1% Li alloy and a dendritic structure with a dendrite arm spacing of $2.5\mu m$ was

23

obtained in the 3% Li alloy. The alloys were consolidated by cold compaction and hot extrusion; both alloys recrystallized to a grain size of 1-2μm. A fine dispersion (1-2μm) of second phase particles was also obtained in both alloys; the dispersion did not coarsen much during subsequent solution heat treatments. The 1% Li alloy had a 3% lower density and 8% higher modulus than Al-2024; the 3% Li alloy had 9% lower density and 18% higher modulus. The yield strengths of the alloys in the T-6 condition were 63.5 ksi for the 1% Li alloy and 83 ksi for the 3% Li alloy. The toughness values of the alloys in the T-6 condition, particularly the 3% Li alloy were rather low, even though the grain size was very fine. It was suggested that this was a result of the presence of a significant volume fraction of second phase particles, resulting from the low solubility of Cu in the 3% Li alloy. It was also suggested that the toughness might be improved by underaging or overaging. The refined microstructures in both the alloys resulted in better S-N fatigue properties, particularly in the 3% Li alloy; however, the presence of the insoluble second phase particles resulted in poor fatigue crack growth behavior in the 3% Li alloy. The stress rupture properties of the 1% Li alloy were superior (at 423 K) or comparable (at 473 K) to those of 2024; those of the 3% Li alloy were inferior; the inferior properties at 473 K were attributed to rapid coarsening of the $\delta'$ precipitate.

## 2.5 Powder Metallurgy of Aluminum Alloys

Extensive research investigations have been performed by ALCOA (Lyle and Cebulak (60), Otto (61)) aimed at developing powder metallurgy mill products with superior mechanical and physical properties compared to products produced by conventional ingot metallurgy. Outstanding combinations of strength, toughness, fatigue and stress corrosion resistance have been achieved by the use of atomized powders which have been compacted into various products forms by a process involving vacuum preheating, hot pressing, and hot deformation. The aim of recent work has been to establish the optimum processing sequence to provide improved property levels, and the process has been scaled up to 1450 kg. (3200 lb.) hot compacted billets.

The powder metallurgy approach has been developed for two main reasons, firstly because of the fine metallurgical structures which can be obtained by the rapid solidification of the powders, and secondly because alloy compositions can be used which cannot be made by ingot metallurgy. The atomization process used by ALCOA results in cooling rates $\sim 10^3 - 10^5$ K/sec. (Lyle and Cebulak (60)). By the use of a splat quenching process which gives cooling rates of $10^6$ K/sec. or greater, further refinement of the microstructure and improvements in properties can be anticipated.

Early work indicated that the Al-Zn-Mg-Cu system was the most promising for developing high strength at room temperature. It was also found that phases containing Co or Fe+Ni were more resistant to coarsening during fabrication than phases containing Cr, Ti, V, Zr, Mo and W. Additions of Co or Fe+Ni were therefore made to these alloys to produce fine dispersoids of $Co_2Al_9$ or $FeNiAl_9$. P/M alloy MA67 had the composition Al-8% Zn-2.5% Mg-1% Cu-1.6% Co. Alloy MA87 was then developed with lower Zn and Co levels which resulted in better toughness for the same yield strength; the composition of MA87 is Al-6.5% Zn-2.5% Mg-1.6% Cu-0.4% Co.

Atomized powders were consolidated by a process involving the following steps: Sieving of powders, cold compaction, preheating in flowing argon or vacuum to degas, hot pressing, extrusion to forging stock and forging. Alloys were then solution heat treated, quenched and aged. Development work showed that preheating in vacuum gave better final toughness than preheating in argon.

The microstructures of MA67 were compared with those of 7000 series alloys, particularly 7050 made by ingot metallurgy. The grain size of the P/M alloys was very much finer, and the grain boundaries were very irregular as a result of the presence of the dispersoid of $Co_2Al_9$ particles; these particles ranged in size from 0.05 to 2μm, depending upon the size of the atomized powder, and on the thermal and mechanical process used. Oxide particles were another

25

feature of the structures of P/M alloys as seen by TEM. They were substantially finer than the $Co_2Al_9$ particles, ranging in size from 0.01 to 0.04μm, and appeared frequently in clusters and in grain boundaries. The amount of oxygen present was determined by a neutron activation method, and depended on the size of the powder particles. For a particle size of 20μm the volume fraction of oxide was 0.5%. Electron microprobe analysis indicated that a substantial part of the oxide was present as MgO. Porosity did not appear to be a problem in P/M alloys which had been given the vacuum preheat-hot pressing treatment.

Lyle and Cebulak (60) found that the P/M alloys MA67 and MA87 had superior combinations of high strength and stress-corrosion cracking resistance compared to I/M 7075 and 7050 alloys. The fracture toughness was equal to that of 7075 but somewhat lower than that of 7050, partly as a result of a larger volume fraction of second phase particles. The improvement in stress-corrosion properties was attributed to a more favorable grain morphology and to the presence of the $Co_2Al_9$ particles; it was suggested that they could serve electrochemical, catalytic and mechanical functions in retarding crack propagation. Otto (61) performed further work on alloy MA87 and established optimum powder production and consolidation processes. The improved alloy showed slightly higher strength, equal ductility and substantially higher toughness than 7050. The most significant improvement observed was in the fatigue crack growth behavior particularly at low values of ΔK; crack growth rates were 15-1000% slower than 7050. The most influential factors affecting the fatigue performance were the amount of secondary hot working and the cobalt content.

The final properties of alloys produced from splat quenched powders will be strongly influenced by the consolidation and processing parameters, as with the alloys produced from gas atomized powders. Both the temperature of deformation and the amount of deformation will affect the precipitation of second phase particles, and rapidly quenched splat powders, as a result of the higher supersaturation of alloy elements and excess vacancy concentrations, will behave differently from gas atomized powders. For those alloy systems

26

which cannot be solution treated after processing the precipitation of disper-
soid will have to be carefully controlled. For alloys which can be solution
treated and aged after processing (e.g. Al-Li system) the processing require-
ments may not be so critical, except that a fine grain size and grain stabi-
lizing dispersoid will have to be maintained. Other primary factors which
will affect toughness are degree of bonding between particles and amount of
oxide included. Sufficient hot working will be required to break up and
disperse the oxide and achieve good inter-particle bonding. The difference
in shape between splat quenched particles (flat) and gas atomized particles
(spherical) will affect the amount of hot working required.

## Section 3
## ALLOY DEVELOPMENT

### 3.1 Objective

To examine the feasibility of producing aluminum alloy powders of novel composition that would be difficult to produce by conventional casting processes.

### 3.2 Approach

Five alloys were selected for investigation. The requested compositions are shown in Table 3.

### TABLE 3

#### SPECIFIED CHEMICAL COMPOSITION OF RAPIDLY SOLIDIFIED ALLOY POWDERS (WT. %)

| ALLOY | Fe | Ca | Mg | Zn | B | Si | Cu | Ti | Cr | Mn | Zr |
|-------|----|----|----|----|----|----|----|----|----|----|----|
| Al-2Ca | | 2 | 1 | 5 | 0.01 | 1 | 4 | 0.05 | 0.2 | 0.5 | 0.25 |
| Al-4Fe | 4 | | 1 | 5 | 0.01 | 1 | 4 | 0.05 | 0.2 | 0.5 | 0.25 |
| Al-20Mg | | | 20 | | 0.01 | 1 | | 0.05 | 0.2 | 0.5 | 0.25 |
| Al-1B | | | 1 | 5 | 1 | 1 | 4 | 1 | 0.2 | 0.5 | 0.25 |
| Al 7075 | | | 2.5 | 5.6 | | | 1.6 | | 0.3 | | |

The first four of these alloys are of novel composition; the abbreviated designations identify the principal element not conventionally used to the extent herein. The alloys represented varying degrees of manufacturing difficulty due to their intrinsic reactivity or the high casting temperature required to take alloying elements into solution. Al 7075 was investigated to allow observation of the effect of rapid solidification and evaluation of powder processing procedures for a well-characterized commercial alloy. The

first four alloys shown in Table 3 were requested from both Pratt and Whitney Aircraft Corporation (PWA) and Battelle Columbus Laboratories (BCL) in order to compare the two widely differing powder manufacturing techniques. The fifth alloy (7075) was requested from PWA.

## 3.3  Experimental Procedure

### 3.3.1  Powder Manufacture

Powder was manufactured at both PWA and BCL. The PWA process uses a high speed rotating disc to atomize a stream of molten metal followed by cooling in helium gas which produces spheroidal particles of less than 100$\mu$m dia. The BCL process uses melt spinning onto a rotating copper disc and produces flakes approximately 25$\mu$m thick and 1mm long x 1mm wide.

### 3.3.2  Consolidation and Extrusion

The flow chart for procedures involved in vacuum hot pressing and extrusion of the powders evaluated on this program is shown in Figure 1. The temperature used for pressing and extrusion for each alloy is shown in Table 4.

TABLE 4

CONSOLIDATION PARAMETERS FOR ALUMINUM ALLOY POWDERS

| Alloy No. | Alloy (Nominal Composition) Weight Percent | Supplier | Pressing & Extrusion Temperature ( K) | Maximum Pressure During Pressing (MPa) |
|---|---|---|---|---|
| 1 | Al-2Ca | BCL | 700 | 76 |
| 4 | Al-20Mg | BCL | 644 | 76 |
| 1 | Al-2Ca | PWA | 700 | 76 |
| 4 | Al-20Mg | PWA | 644 | 23 |
| 3 | Al-1B | PWA | 727 | 23 |
| 7 | Al-7075 | PWA | 727 | 76 |

This temperature was selected after consideration of the following parameters.

Weigh And Dry Al
Alloy Powder

↓

Load In Graphite Die
Vacuum Degas At
R.T. 0.5-1 Hrs.

↓

Vacuum Degas
On Heating
0.5-1 Hr.

↓

Vacuum Hot Press In
Graphite Die at Selected
Temperature, 3.3 ksi
2 Hrs.

If 100% Dense

If Not 100% Dense

↓

Vacuum Hot Press In
Steel Die At Temperature
11 ksi, 1 Hr.

↓

Machine Pressing
For Extrusion

↓

Extrude At
VHP Temperature
With a 10:1 Reduction
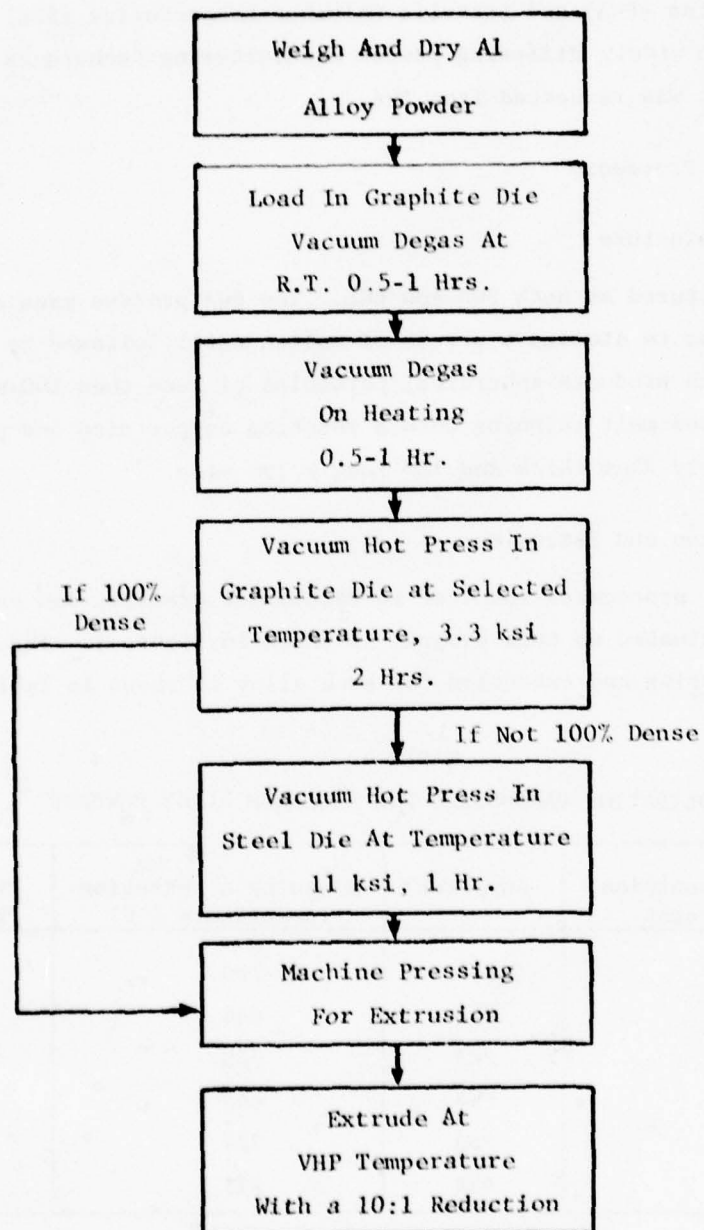
Figure 1   Flow Chart for Consolidation of Rapidly Solidified Aluminum
Alloy Powders

1. Melting range of the alloy. The alloys were processed below their solidus temperatures.

2. Stability of dispersed phases. In the case of the Al-20Mg and Al-2Ca alloys the pressing temperature was selected to be below the temperature at which significant growth of the precipitated phases occurred. This temperature was determined by transmission electron microscopy of heat-treated powders.

The vacuum hot-pressing was carried out in two stages so that a graphite die with a low wall friction could be used followed by higher pressure consolidation in a steel die. The 20 percent magnesium and 1 percent B alloys were fully dense after pressing in graphite so they were extruded without further consolidation.

The compacted alloys were then enclosed in an aluminum 6061 cylinder with Al 7075 tail and nose pieces and hot extruded at the temperature shown in Table 4. The initial extrusion billet was 50mm diameter which was extruded at an extrusion ratio of 10:1 to give a rectangular cross section 41mm x 5.6mm.

3.4 Results

3.4.1 Composition of As-Received Powders

The actual chemical compositions of the as-received powders are given in Table 5. The Al-4Fe alloy could not be produced by PWA due to technical difficulties. BCL could not produce either the Al-4Fe or the Al-1B alloys due to technical difficulties.

3.4.2 Microstructure

A. Powders

The microstructures of the as-received powders from both suppliers are shown in Figures 2-10. The powders can be characterized by their secondary dendrite arm spacing (SDAS) which for a given composition is related to the cooling rate, and by the precipitate particle size in the case of the B, Ca and Mg

31

TABLE 5

ACTUAL CHEMICAL COMPOSITION OF RAPIDLY SOLIDIFIED POWDER ALLOYS

| SUPPLIER | ALLOY | PRODUCT | WT. PERCENT | | | | | | | | | | |
|---|---|---|---|---|---|---|---|---|---|---|---|---|---|
| | | | Cu | Mg | Zn | Fe | Ti | Ca | O | Si | Cr | Mn | Zr |
| PWA | Al-7075 | Extrusion | 1.65 | 2.9 | 5.71 | 0.23 | 0.07 | 0.05 | 0.089 | | | | |
| PWA | Al-2Ca | " | 3.95 | 1.06 | 4.87 | 0.46 | 0.11 | 2.26 | 0.081 | | | | |
| PWA | Al-1B | " | 3.07 | 0.91 | 4.02 | 0.59 | 0.53 | 0.12 | 0.126 | | | | |
| PWA | Al-20Mg | " | 0.07 | 21.82 | 0.01 | 0.41 | 0.02 | 0.04 | 0.108 | | | | |
| PWA | Al-2Ca | Ingot | 4.11 | 1.05 | 5.17 | 0.47 | 0.05 | 2.39 | | 0.66 | 0.25 | 0.47 | |
| PWA | Al-1B | " | 3.98 | 1.16 | 5.13 | 0.58 | 0.87 | | | 1.48 | 0.19 | 0.50 | |
| PWA | Al 7075 | " | 1.50 | 2.46 | 5.36 | 0.18 | 0.09 | | | 0.25 | 0.19 | 0.025 | |
| BCL | Al-2Ca | Powder | 4.58 | 1.02 | 4.97 | 0.52 | | 1.45 | | | 0.17 | 0.41 | 0.25 |
| BCL | Al-20Mg | " | 0.14 | 20.34 | 0.02 | 0.48 | | | | | 0.24 | 0.48 | 0.25 |
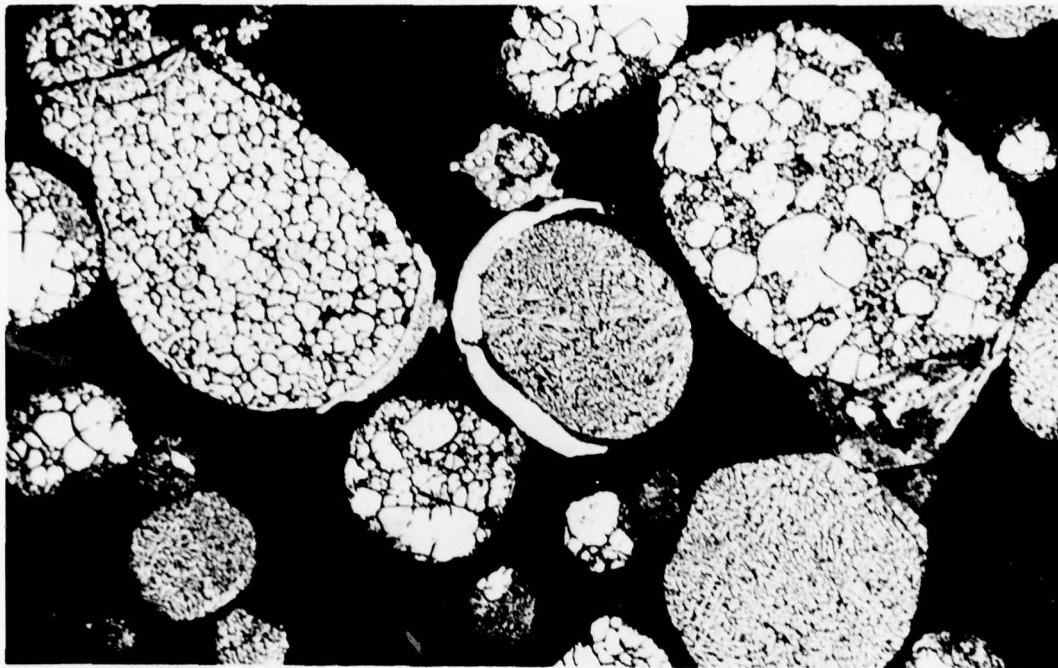
D2471                                    (a)
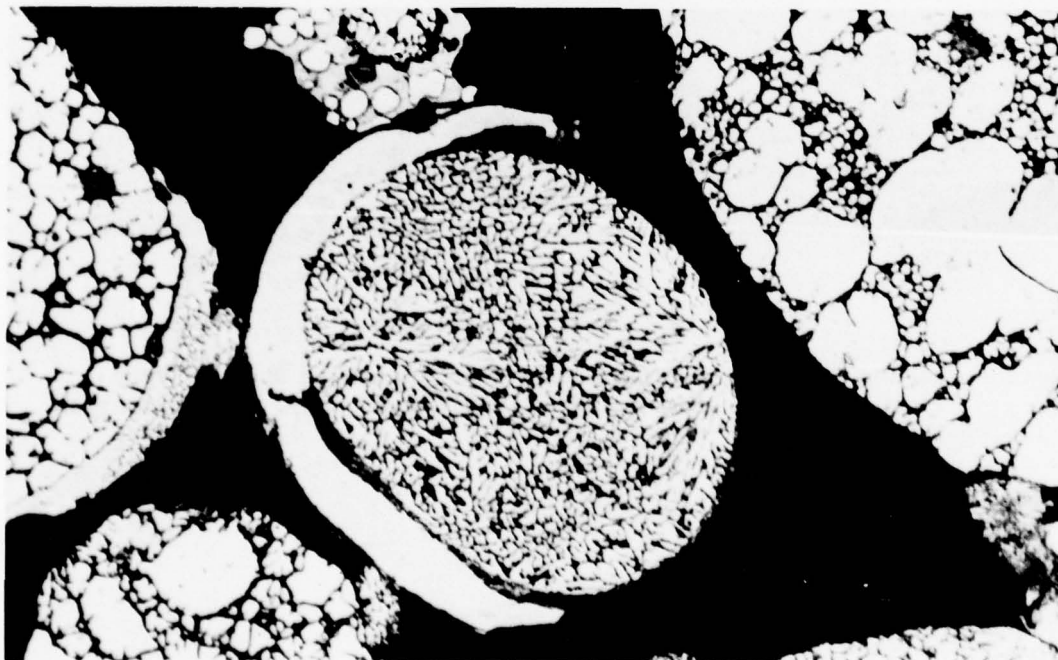


D2470                                    (b)

Figure 2    Al-1B Powder from PWA.  A wide variation in cooling rate is
            indicated by the particle to particle changes in dendrite
            spacing.  Magnification   (a) 500X, (b) 1000X
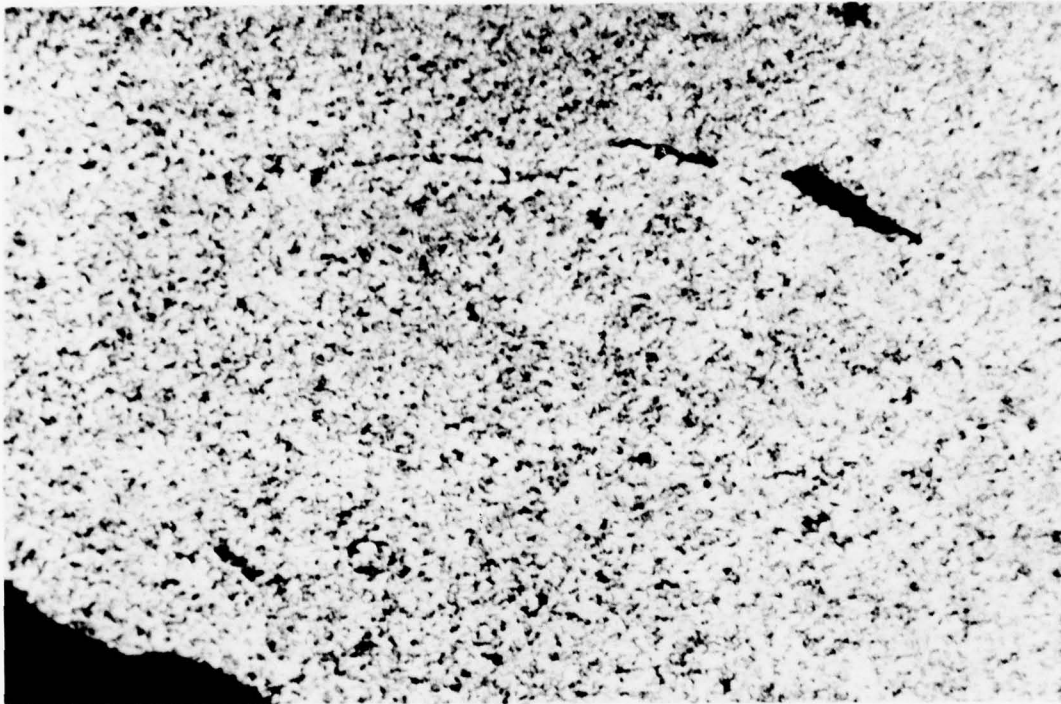
D1458

Figure 3   Al-2Ca Powder Flake from BCL.   The structure shows a very
           fine grain size almost unresolvable optically.   Magnification
           1000X

J895

Figure 4   Al-2Ca Powder Flake from BCL.   Transmission electronmicro-
graph shows a very fine matrix precipitate, 5-10nm diameter
with a few larger particles at subgrain boundaries.
Magnification  60,000X

35
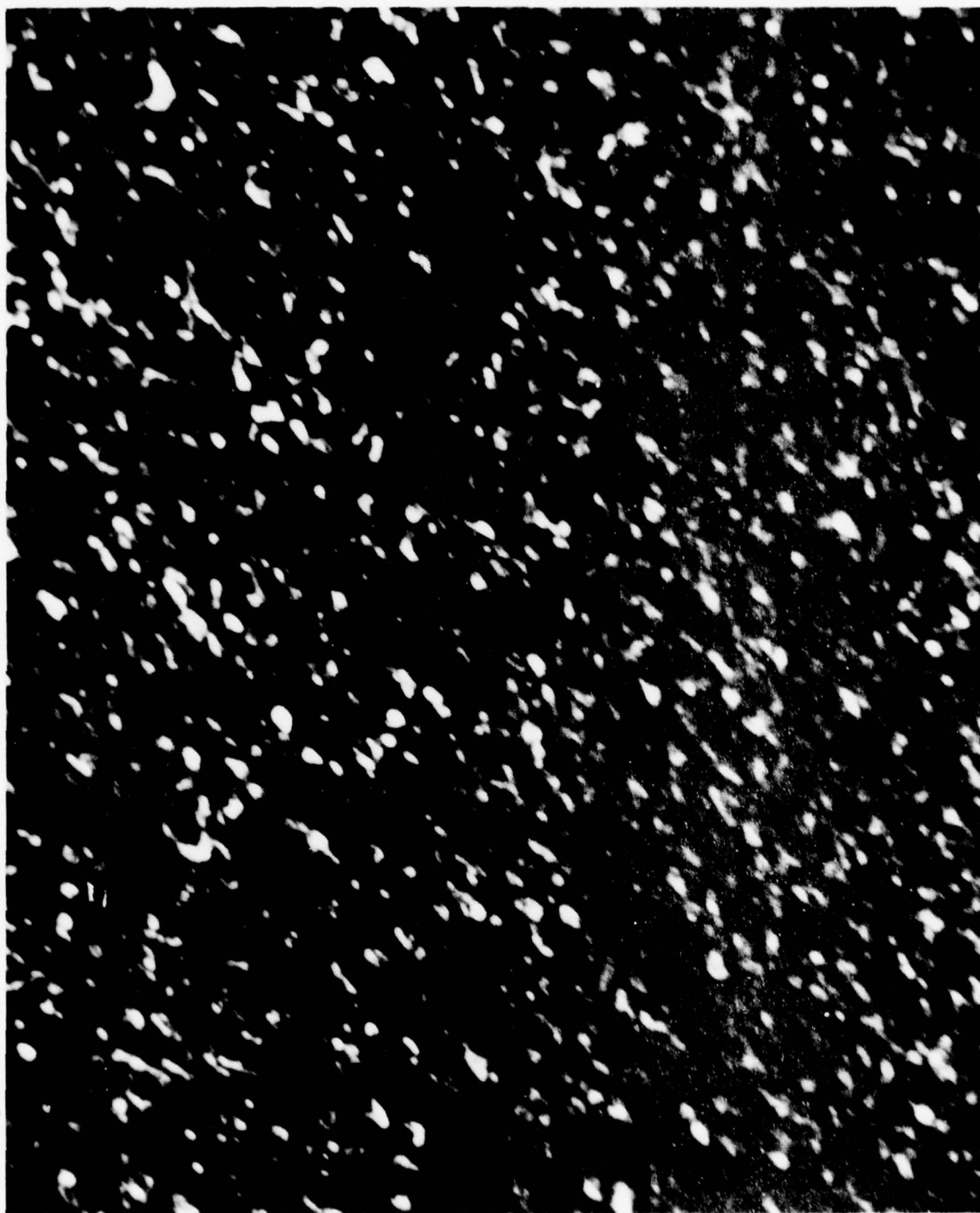
J906

Figure 5  Al-2Ca Powder Flake from BCL.  Dark field transmission electron micrograph showing the high volume fraction of 5-10nm diameter matrix precipitates.  Magnification 230,000X
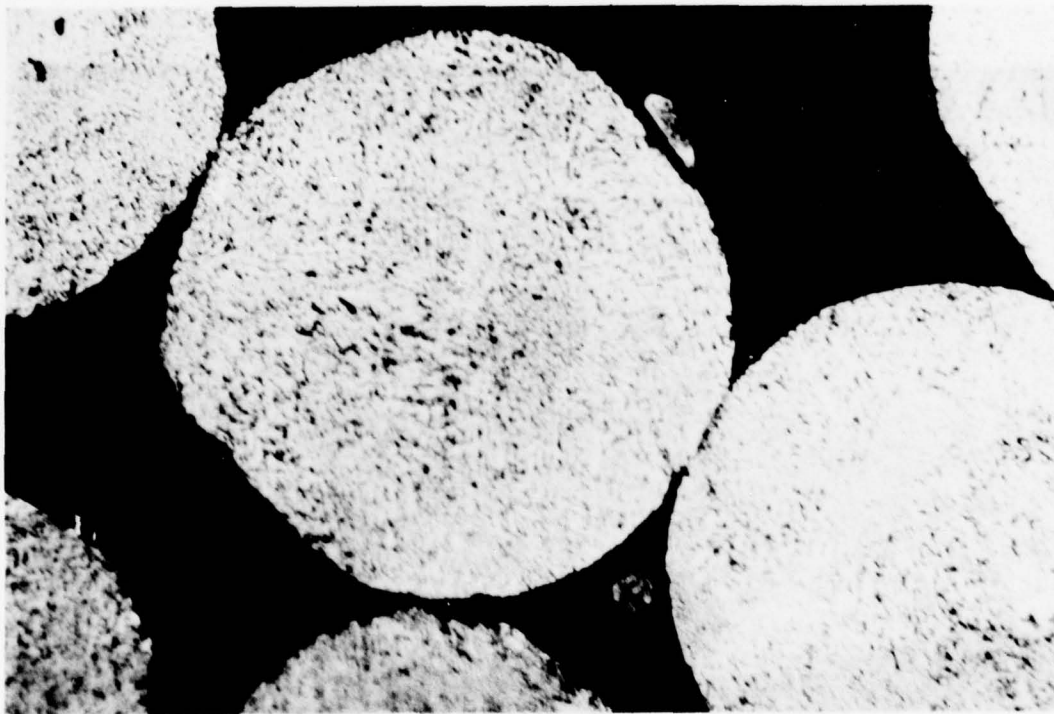
D2348

Figure 6  Al-2Ca Powder from PWA.  A very fine dendrite spacing
typical of calcium alloys can be seen in all particles.
Magnification 1000X
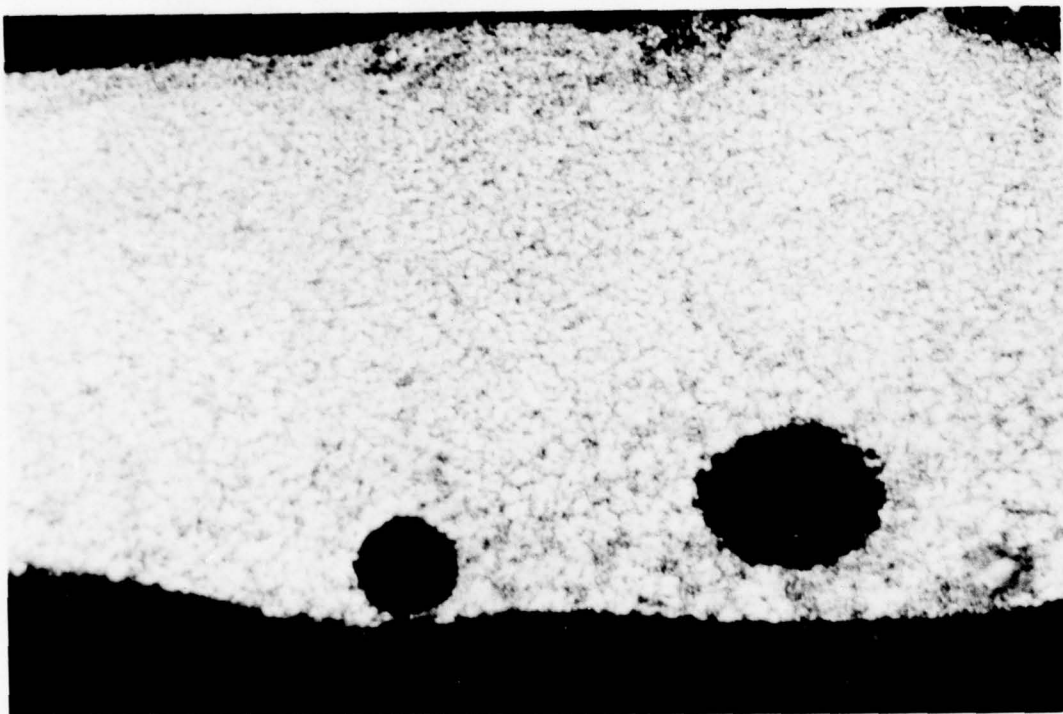
D1465

Figure 7 Al-20Mg Powder Flake from BCL. The flake shows a grain
structure which coarsens as the distance away from the
flake surface in contact with the rotating metal wheel
(top side in photo) increases. Magnification 1000X

J886

Figure 8  Al-20Mg Powder Flake from BCL.  Transmission electron micro-
graph showing acicular particles (possibly $Mg_2Si$) about
20nm thick.  Magnification 60,000X
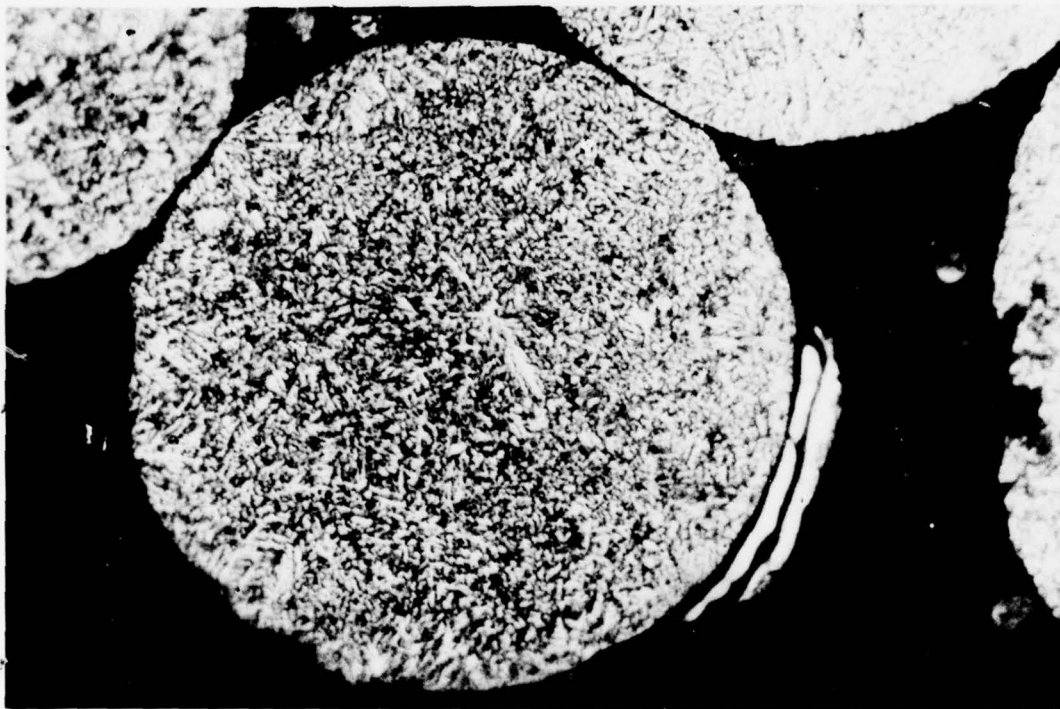
D2413

Figure 9   Al-20Mg Powder from PWA.   Structure shows a very fine
dendrite size in all particles with little variation
from edge to center.   Magnification 1000X

40
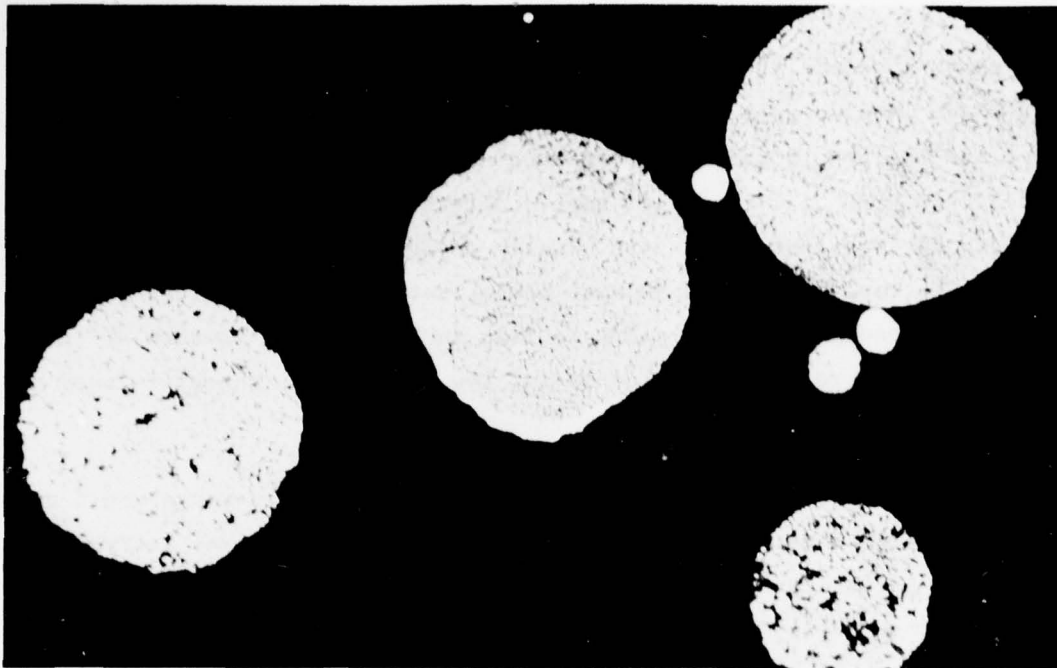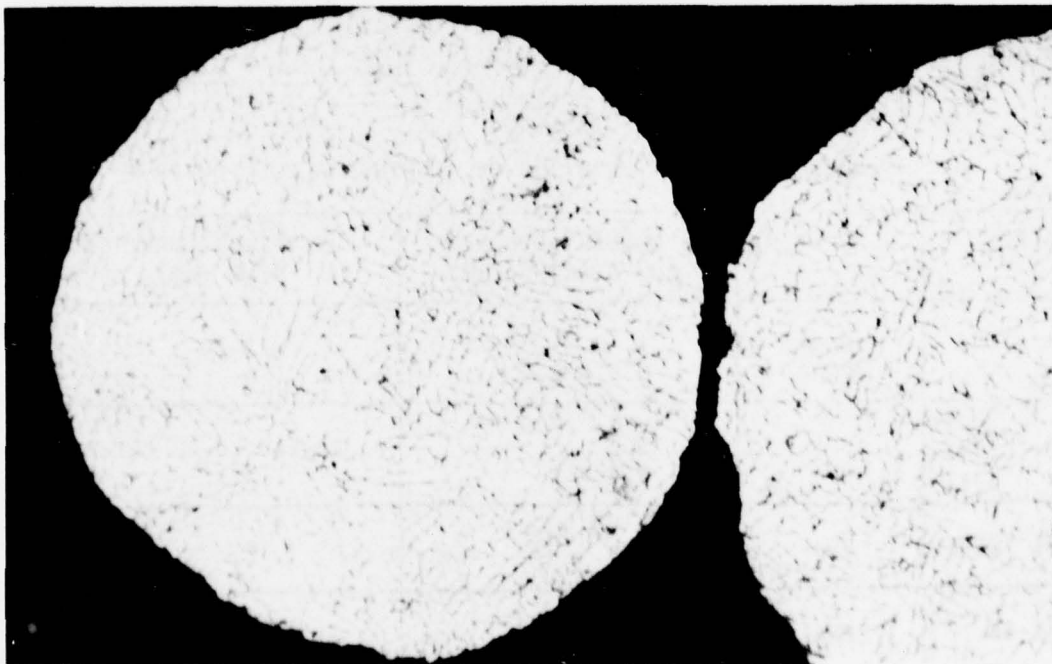
Figure 10 Al 7075 Powder from PWA. A uniform dendrite size is observed, but some particles have 20-30% porosity. Magnification (a) 500X (b) 1000X

41

alloys where a second phase of low solubility is formed. The size of the second phase is also related to the cooling rate. The secondary dendrite arm spacing and the precipitate particle size are listed in Table 6. It is not expected that SDAS will in itself have a direct effect on mechanical properties since the apparent grains are usually separated by low angle boundaries which are destroyed during subsequent consolidation and mechanical working. On the other hand precipitate particle size in as-received powders defines, in those cases where the particles are of low solubility, the efficiency and application of the alloy system.

The production of a stable dispersion in the 100-500nm size range would allow the production of a very fine grained material by cold work and recrystallization since particles in this size range efficiently prevent grain boundary migration. In a still finer particle size range alloys that produce a stable dispersion less than 50nm during rapid cooling would be suitable for elevated temperature application where a conventional precipitated phase would agglomerate and reduce the strength of the alloy.

TABLE 6

MICROSTRUCTURAL CHARACTERISTICS OF ALUMINUM ALLOY POWDER

| ALLOY | SUPPLIER + | SECONDARY DENDRITE ARM SPACING ($\mu$m) | PRECIPITATE PARTICLE SIZE (nm) |
|-------|-----------|------------------------------------------|-------------------------------|
| Al-2Ca | BCL<br>PWA | 1<br>0.5 - 2.5 | 5-10<br>* |
| Al-20Mg | BCL<br>PWA | 1-2<br>0.5 - 1 | Plates 10-20 thick.<br>* |
| Al 7075 | PWA | 1.5 - 10 | * |
| Al-1B | PWA | 1-26 | Up to 60,000 |

+ BCL Powders produced as flakes ~ 25$\mu$m thick by melt spinning process in Argon. PWA powders produced as 5-100$\mu$m dia. spheroids by atomization, quenching in helium.

* Not determined.

Small amounts of porosity were observed in some of the as-solidified powders. In PWA powders the porosity was observed predominantly in the Al-2Ca alloys, with smaller amounts in the Al-1B and Al 7075 (Fig.10). In BCL powders porosity was observed predominantly in the Al-2Ca alloy (Fig. 3), and also in the Al-20Mg alloy.

Of the alloys evaluated on this program the Al 7075, Al-2Ca and Al-20Mg appear to be free of massive inclusions. The Al-1B alloy contains inclusions up to 60µm diameter which would be expected to cause embrittlement. The large borides were not able to be dissolved before casting owing to temperature limitations on the PWA equipment which required casting at 1373 K rather than the desired 1573 K needed to put the alloy in a single phase liquid field.

The Al-2Ca and Al-20Mg powders have dispersoids in the size range suitable for dispersion hardening. These dispersoids grow slightly during consolidation but appear to be suitable constituents for high temperature aluminum alloys.

B.   As-Extruded

The microstructures of the as-extruded alloys are shown in Figures 11-18. The consolidation procedure for all materials was successful in eliminating porosity; however, a considerable degree of growth of the intermetallic particles has occurred in some alloys which would be expected to reduce toughness and strength of these alloys. The actual grain size of the extrusions is not resolvable optically but is expected to be in the submicron range. The Al-1B alloy from PWA (Figs. 11 and 12) showed a fine grain size, but rather coarse second phase particles, up to 50µm in size, which would be expected to reduce the toughness. The Al-2Ca alloys from both BCL (Fig. 13) and PWA (Figs. 14 and 15  showed a fine grain size and a fine particle dispersion. In the PWA alloy the dispersion was finer in the alloy extruded at the lower temperature. The Al-20Mg alloy (Fig. 16) showed a fine script-like microstructure with occasional coarse intermetallic particles. The Al 7075 alloy (Fig. 17) showed a fine grain structure and a fine dispersion of intermetallic particles; the particles, however, were coarser than those in the

43
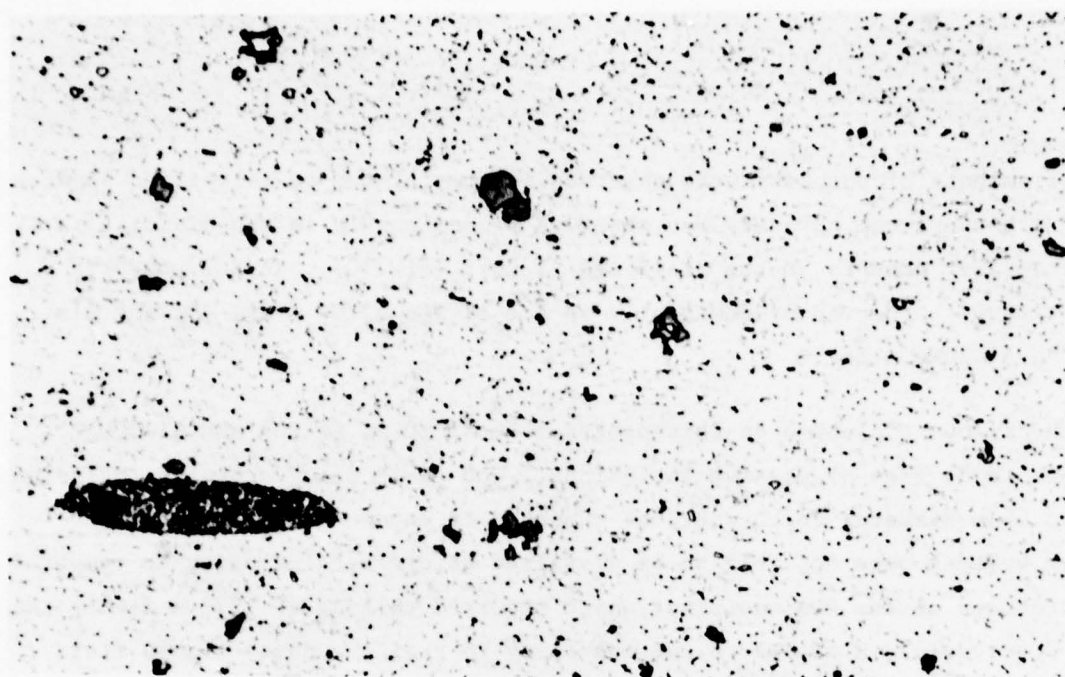
D3275                                    (a)



D3286                                    (b)

Figure 11   Microstructure of Al-1B Alloy from PWA, Hot Pressed and
            Extruded at 728K.   Shows fine grain size, and second-phase
            particles.   Magnification (a) 500X   (b) 3000X

44
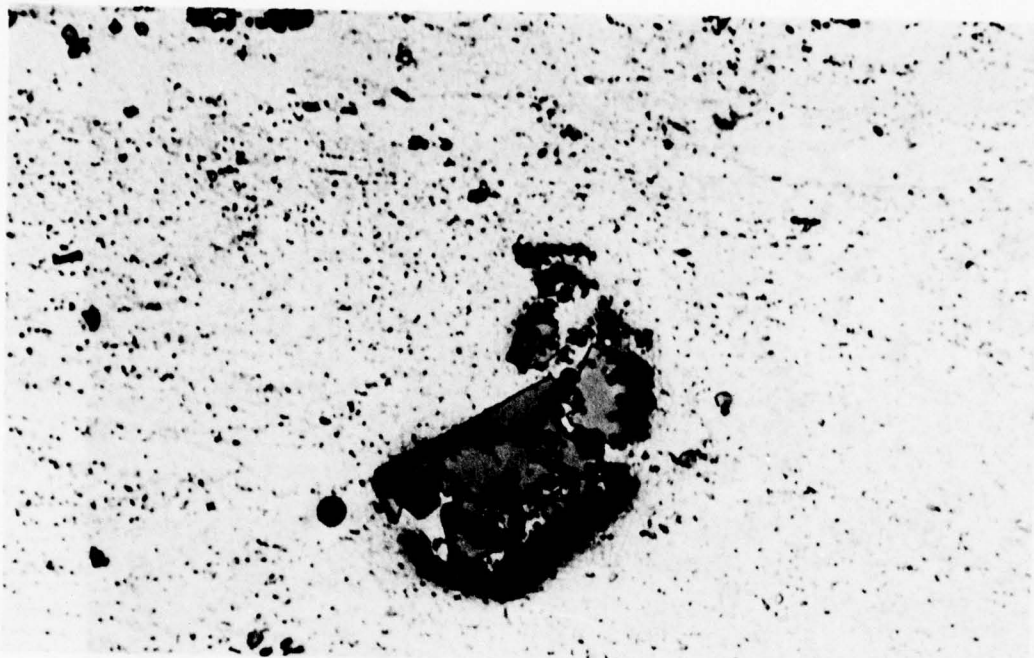
D3566                                    (a)



D3567                                    (b)

Figure 12   Microstructure of Al-1B Alloy from PWA, Hot Pressed and
            Extruded at 728K.  Second phase particles as large as 50μm
            (a) and regions containing high volume fraction of particles
            (b) are present.  Magnification 500X for (a) and (b)

45
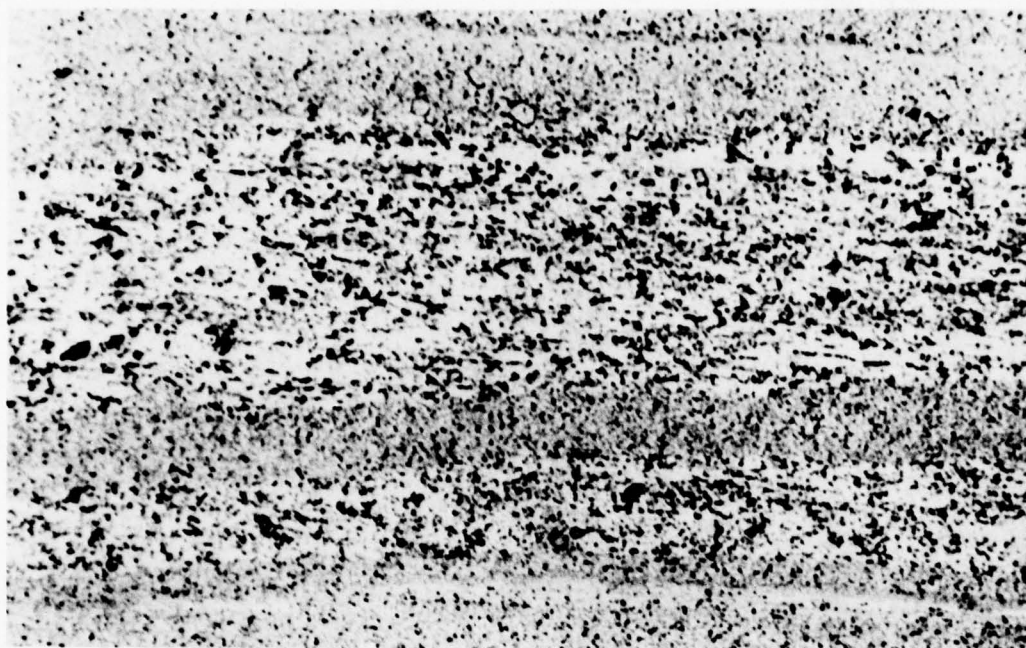
D3589                     (a)
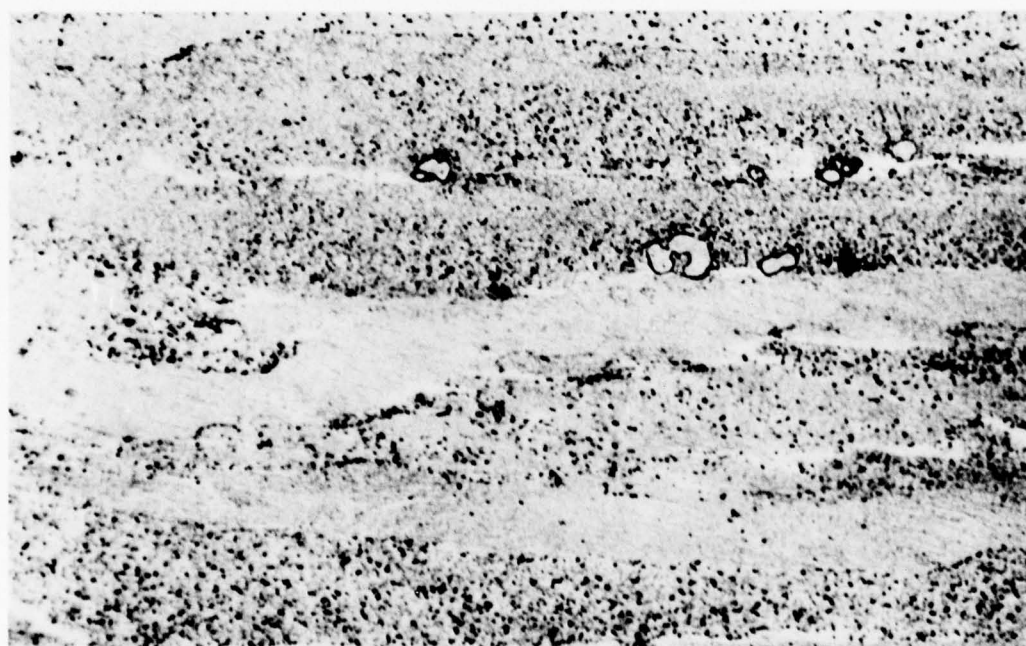
D3590                     (b)

Figure 13   Al-2Ca Alloy from BCL, Hot Pressed and Extruded at 700K.
Fine grain size and particle size of rapidly solidified
powder apparently retained through hot pressing and
extrusion at 700K.  Magnification (a) 500X  (b) 500X

46
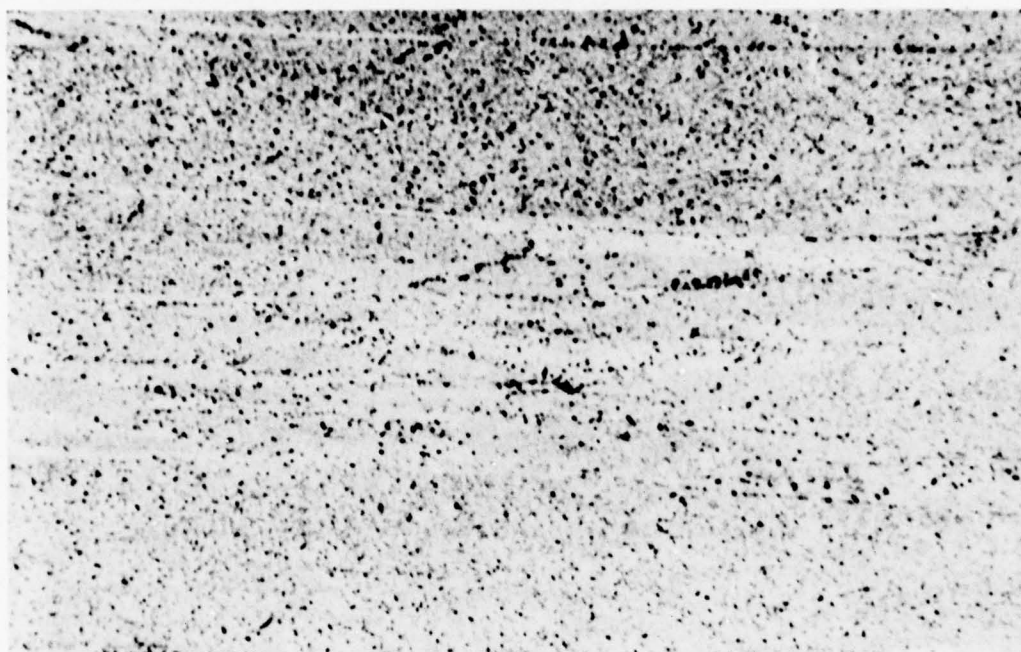
D3579                              (a)
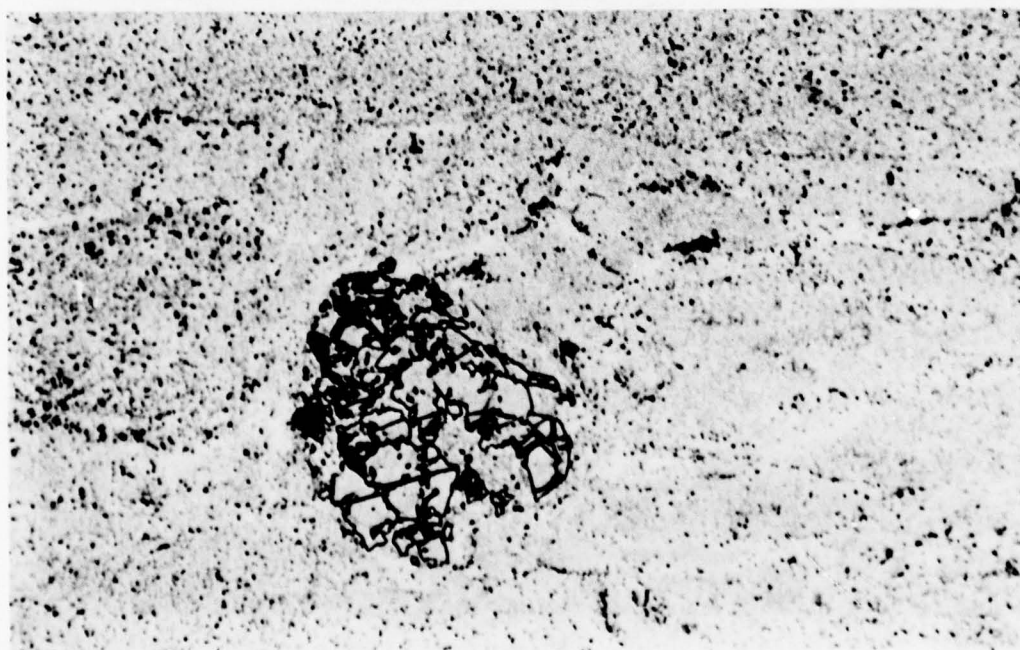


D3580                              (b)

Figure 14    Al-2Ca Alloy from PWA, Hot-Pressed and Extruded at 700 K.
             Microstructure as-extruded contains rather homogeneous
             sub-micron size particles (a).  Occasionally, coarse,
             fragmented intermetallic particles are found (b).
             Magnification (a) and (b) 500X

47
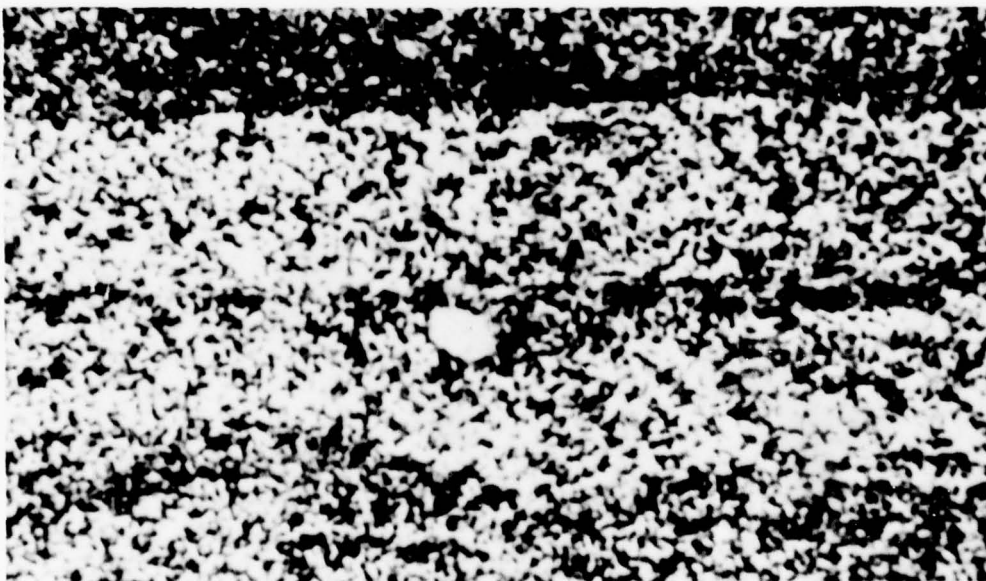
Figure 15   Al-2Ca Alloy from PWA, Hot-Pressed and Extruded at
            587K.  Microstructure contains fine sub-micron size
            size particles.  Magnification (a) 500X  (b) 3000X

48
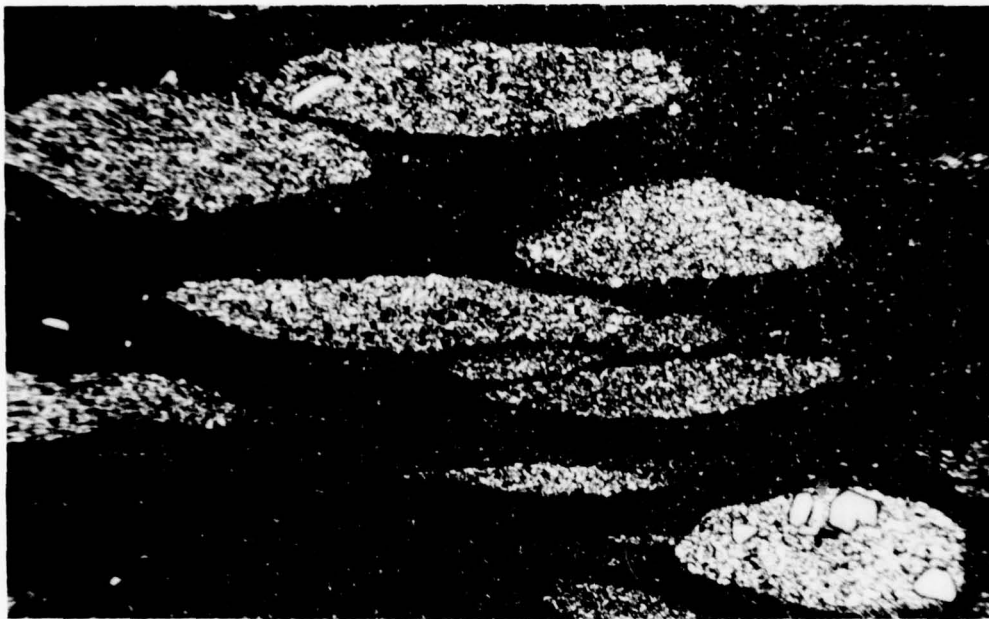
D2150            (a)
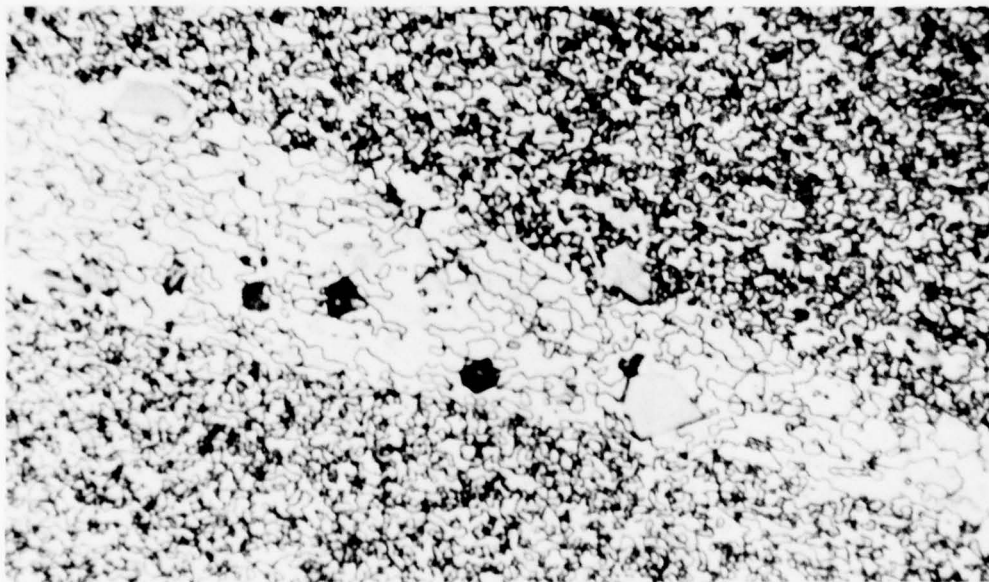


D2155            (b)

Figure 16   Al-20Mg Alloy from BCL, Hot-Pressed and Extruded at
644K.   Fine script-like microstructure may be two-
phase field and contains occasional relatively
coarse intermetallics after hot pressing and extrusion.
Magnification (a) 200X   (b) 2000X

49

D3557                                    (a)
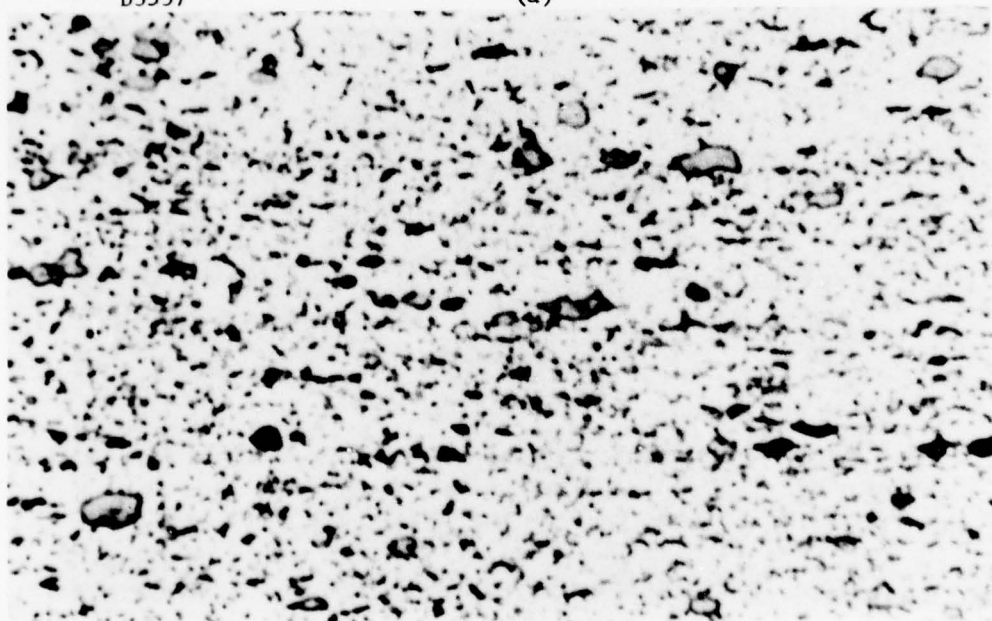


D3279                                    (b)

Figure 17    Al 7075 Alloy from PWA, Hot-Pressed and Extruded at
             700 K.   Most intermetallics are less than $1\mu m$ after
             hot pressing.   Magnifications (a) 500X   (b) 3000X

50

D3546

Figure 18 Al 7075 Alloy from PWA, Hot-Pressed and Extruded at
700 K. Solution Treated 1 hr. at 739 K, WQ and Aged
25 hr. at 394 K. Microstructural appearance similar
to as-extruded condition. Magnification 500X

Al-2Ca and Al-20Mg alloys. The microstructure of the Al 7075 alloy in the STA condition was similar, but showed fewer intermetallic particles.

### 3.4.3 Physical Properties - Density

The densities of the alloys made on this program are given in Table 7. The densities were measured in the hot pressed and extruded condition which was found to have negligible porosity. The only alloy of significantly reduced density is the Al-20Mg alloy with a 13 percent lower density than Al 7075.

TABLE 7

DENSITY OF RAPIDLY SOLIDIFIED POWDER ALLOYS
AFTER VACUUM HOT PRESSING AND EXTRUDING

| DENSITY AT 293 K | | | |
|---|---|---|---|
| ALLOY | POWDER SOURCE | $g/cm^3$ | $lbs/in^3$ |
| Al 20Mg | BCL | 2.454 | .0887 |
| Al 2Ca | BCL | 2.872 | .1038 |
| Al 20Mg | PWA | 2.446 | .0884 |
| Al 2Ca 600 | PWA | 2.873 | .1038 |
| Al 2Ca 800 | PWA | 2.871 | .1037 |
| Al 1B | PWA | 2.868 | .1036 |
| Al 7075 | PWA | 2.815 | .1017 |

### 3.4.4 Mechanical Properties

Aging Response

The aging response of rapidly cooled powder extrusions of Al-20Mg and Al-2Ca is shown in Figure 19. The response of Al 7075 alloy commercial sheet is also shown for comparison; aging response of rapidly cooled powder extrusions of 7075 was identical to the commercial sheet. The Al-Mg and Al-Ca alloys do not show the loss of hardness after elevated temperature exposure shown by conventional alloys such as Al 7075. This indicates that very little particle agglomeration is occurring in the new alloys which is a requirement for a stable high temperature material.

52
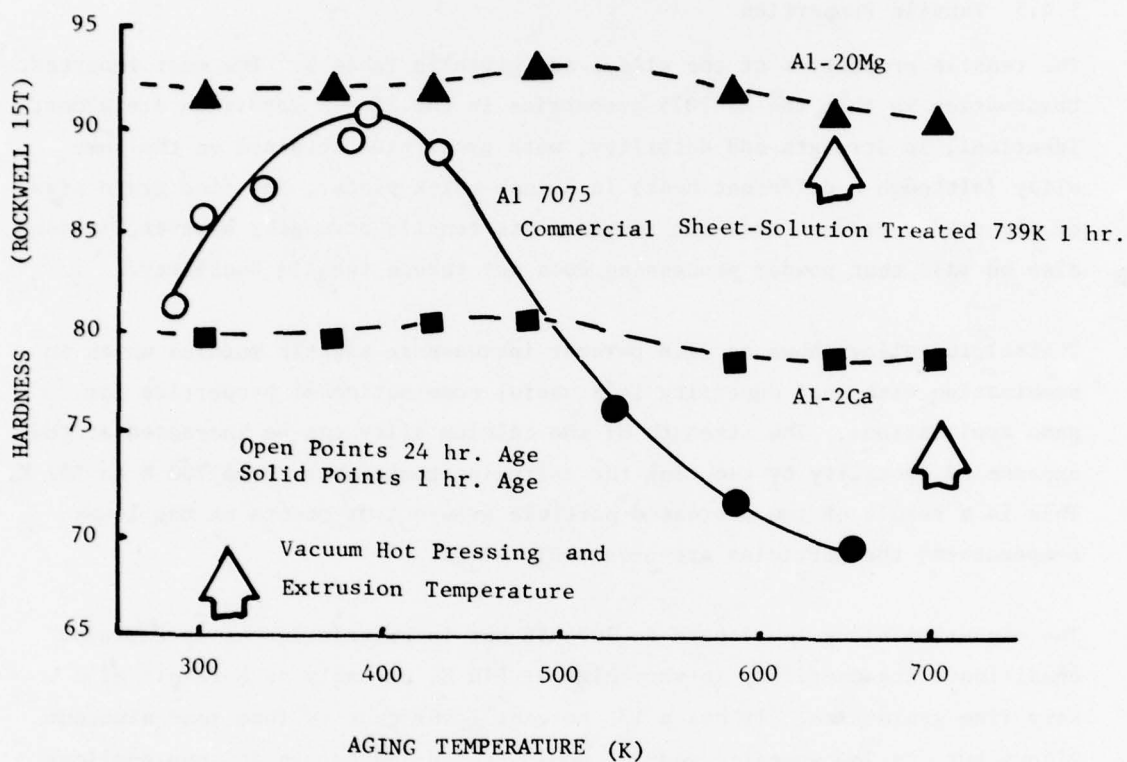
Figure 19  Room Temperature Hardness Versus Aging Temperature
for Aluminum Alloys Prepared From Rapidly Solidified
Powders.  Commercial Al 7075 aging response is shown
for comparison.

53

### 3.4.5 Tensile Properties

The tensile properties of the alloys are given in Table 8. The most important observation is that the Al 7075 properties in the STA-T6 condition are almost identical, in strength and ductility, with properties obtained on the same alloy (although a different heat) in 3-inch thick plate. The fine grain size of the powder product does not increase its tensile strength, however, it can also be said that powder processing does not reduce tensile ductility.

The calcium alloy shows an 11.8 percent increase in elastic modulus which in combination with good ductility is a useful combination of properties for some applications. The strength of the calcium alloy can be increased at the expense of ductility by reducing the extrusion temperature from 700 K to 587 K. This is a result of the decreased particle growth that occurs at the lower temperature; the particles are presumably $Al_4Ca$.

The magnesium alloy is as hard as 7075-T6 but is brittle in the as-extruded condition. Its ductility is very high at 616 K, probably as a result of a very fine grain size. It has a 13 percent lower density than most aluminum alloys but its low specific modulus would be a disadvantage in some applications. The elastic modulus of Al-Mg alloys over the full range of composition has been determined by Köster and Rosenthal (62). This work showed that the addition of Mg to Al decreases the modulus more rapidly than would be predicted from the law of mixtures. The decrease is approximately linear for Mg contents up to about 38 wt. percent, at which concentration the modulus is as low as that of pure Mg. Assuming a similar decrease in the present Al-20Mg alloy, and interpolating for a Mg concentration of 20 wt. percent gives a value for the modulus of about 56 GPa, which is close to the experimental value of 52 GPa (Table 8).

### 3.4.6 Toughness Properties

Indications of fracture-toughness of the alloys were obtained from slow bend tests of fatigue pre-cracked Charpy specimens. The specimens were too thin to produce plane strain conditions with alloys of the yield strengths

# TABLE 8

## TENSILE PROPERTIES OF EXTRUDED RAPIDLY COOLED POWDERS

| ALLOY | CONDITION | UTS MPa | 0.2% YS MPa | El % | E GPa | TEST TEMPERATURE K |
|---|---|---|---|---|---|---|
| A1-1B PWA | As Extruded 728K | 311<br>311 | 173<br>173 | 17<br>18 | 72<br>72 | 300 |
| A1-2Ca PWA | As Extruded 700K | 373<br>380 | 228<br>228 | 14<br>13 | 79<br>79 | "<br>" |
|  | As Extruded 587K | 455<br>435 | 297<br>283 | 6<br>7 | 77<br>79 | " |
| A1 7075 PWA | As Extruded 700K | 455<br>428 | 283<br>283 | 13<br>12 | 70<br>70 | " |
|  | STA-T6 | 614<br>635 | 545<br>573 | 13<br>11 | 70<br>70 | " |
| A1 7075 3 in. Plate From Ingot for Comparison | STA-T6    a<br>b | 600<br>628 | 573<br>600 | 11<br>8 |  | " |
| A1-20Mg BCL | As Extruded 644K | 290*<br>19 | -<br>27 | -<br>204 | 52 | 300<br>616 |
| A1-2Ca BCL | As Extruded 700K | 380 | 262 | 14 | 80 | 300 |

\*   Premature Failure.

a   Plate Center.

b   Plate Edge.

obtained in this program. However taken in conjunction with the impact
results given below they present a qualitative indication of the resistance
to crack initiation and propagation in the alloys. The fracture toughness
results calculated in five different ways are given in Table 9. $K_Q$ was
obtained from the ASTM E-399-74 test method pertaining to 3-point bend.
Application of this method involving a secant intercept equivalent to a 5 per-
cent change in compliance did not satisfy requirements for $K_{Ic}$ in any case
here. All specimens were inadequate in size, thereby exhibiting insufficient
elastic constraint to obtain plane strain conditions at the crack tip. Only
in one case, Al 7075, solution treated and aged to peak hardness, was the
specimen size close to being large enough: specimen thickness was 0.48 cm
nominally and would have to be at least 0.77 cm, according to the ASTM
standard. However, the $K_Q$ values of 31 and 32 for Al 7075 STA-T6 are probably
within 10 percent or less of actual $K_{Ic}$.

$K_{SR}$ was obtained by methods described in general in ASTM E-399 and for pre-
cracked Charpy slow bend testing are described in detail in a recent NMAB
committee report (63). This method has been shown to be useful for extrapo-
lation of $K_{Ic}$ by correlation with subsize specimen results up to a limit.
In the present case, the results are probably a useful estimate of $K_{Ic}$ for the
Al-2Ca alloy from PWA, hot pressed and extruded at 587 K. This estimate is
25 MPa $m^{\frac{1}{2}}$ ± 20 percent.

$K_1$ and $K_2$ are by methods first proposed by Orner and Hartbower (64), where
$K_1$ pertains to integrated energy only up to maximum load and $K_2$ pertains to
total integrated energy. In the latter case, the total integrated energy
was obtained to beyond maximum load to the end of recorded load-displacement
on the chart, or to where the load dropped off to 20 percent of maximum load.
Thus in all cases, the integrated energy did not include the entire "tail"
of the load-deflection record. When specimen size comes close to satisfying
size conditions required by ASTM procedure E-399, then $K_1$ is probably a close
estimate of $K_{Ic}$. For example, $K_1$ and $K_Q$ values for both Al-2Ca extruded at
587 K and Al 7075 STA-T6 are in close agreement. In the other cases, $K_2$ is
a qualitative indication of $K_c$ for sheet thickness the same as specimen

TABLE 9

QUALITATIVE FRACTURE TOUGHNESS VALUES

| ALLOY | CONDITION | $K_Q$* | $K_{SR}$* | $K_1$* | $K_2$* | $K_3$* | 0.2% YS |
|-------|-----------|--------|-----------|--------|--------|--------|---------|
| | | | | $MPa\ m^{\frac{1}{2}}$ | | | MPa |
| Al-1B PWA | As Extruded 728K | 15 15 | 24 23 | 50 50 | 66 66 | 46 | 173 |
| Al-2Ca PWA | As Extruded 700K | 22 22 | 28 26 | 41 34 | 88 80 | 62 57 | 228 |
| | As Extruded 587K | 21 22 | 25 24 | 25 23 | 40 39 | 28 28 | 290 |
| Al 7075 PWA | As Extruded 700K | 23 22 | 28 29 | 39 37 | 82 84 | 58 59 | 283 |
| | STA-T6 | 32 31 | 37 39 | 29 31 | 40 36 | 27 26 | 559 |
| Al 2Ca BCL | As Extruded 700K | 22 29 | 29 30 | 49 40 | 78 73 | 55 52 | 262 |

* $K_Q$ calculated from 5 pct. secant intercept method per ASTM E-399, 3-point bend.

$K_{SR}$ calculated from ASTM E-399 residual strength method and correlation: $K_{SR} = 0.3\ R_{Sb-cv}\sigma_Y$ where $R_{Sb-cv} = \sigma_N/\sigma_Y$ and $\sigma_N = 3\ P_{max}\ S \div 2B(W-a_o)^2$

$K_1$ calculated from energy to max load $\div$ propagation area, $(W/A)max$; $K_1^2 = E(W/A)max \div (1-\nu^2)$

$K_2$ calculated from total energy $\div$ propagation area, $K_2^2 = E(W/A) \div (1-\nu^2)$ per Orner and Hartbower (64).

$K_3$ calculated from total energy $\div$ propagation area, $K_3^2 = \dfrac{E(W/A)}{2} \div (1-\nu^2)$ per Ronald, Hall and Pierce (65).

57

thickness, nominally 0.48 cm. See Ref. 64 for illustration and Ref. 63 for discussion of this correlation.

$K_3$ is obtained by energy integration similar to that used for $K_2$, but assumes a different correlation between total work per unit crack propagation area, W/A. ( 63, 65). Ronald et al have found a correlation between $K_3$ and $K_{Ic}$ for various aluminum alloys (65) that would include results obtained here only for the Al-2Ca, extruded at 587 K and the Al 7075 STA-T6 alloys. Note the relatively close agreement between $K_3$ and $K_Q$ or $K_{SR}$ values for these two alloys in Table 9. Obviously, it would be advantageous to test larger size specimens to assess toughness more accurately than permitted in the present study. This was not possible because of the limited amount of rapidly quenched powders available, as well as the extrusion tooling and reduction ratio selected. Alternatively, one might use other methods of subsize testing than employed herein, but some degree of verification would still be required between experimental results and $K_{Ic}$.

Impact results for subsize notched Charpy specimens are given in Table 10. The Al 7075 (STA-T6) is slightly less tough than an equivalent ingot product but this may be a result of non-optimized compacting procedures. As would be expected the weaker alloys have the highest impact strength.

The fracture surfaces of the slow bend Charpy specimens are shown in Figures 20-27. The Al-1B, Al-2Ca and Al 7075 alloys all showed transgranular, ductile rupture. The dimple size in the Al-2Ca alloys was smaller than in the other two alloys, as a result of the finer intermetallic particle dispersion. The Al-20Mg alloy appeared to fail by transgranular cleavage. The Al-2Ca alloys, and the Al 7075 alloy in the STA-T6 condition, showed delaminations which were probably fractures along prior particle boundaries. This suggests that during the extrusion operation, either the temperature was too low, or the amount of deformation insufficient, to promote complete interparticle bonding.

## TABLE 10

### SUBSIZE CHARPY IMPACT VALUES

| ALLOY | CONDITION | THICKNESS (mm) | IMPACT ENERGY* (J) |
|-------|-----------|----------------|--------------------|
| A1-1B PWA | As Extruded 728K | 4.25 | 15.3 |
| A1-2Ca PWA | As Extruded 587K | 4.44 | 2.7 |
| A1-2Ca PWA | As Extruded 700K | 4.76 | 9.5 |
| A1-2Ca BCL | As Extruded 700K | 3.89 | 6.9 |
| A1-7075 PWA | As Extruded 700K | 4.48 | 11.1 |
| A1 7075 PWA | STA-T6 | 4.37 | 3.9 |

\* Normalized to Standard Charpy Size.

8ESS                            (a)
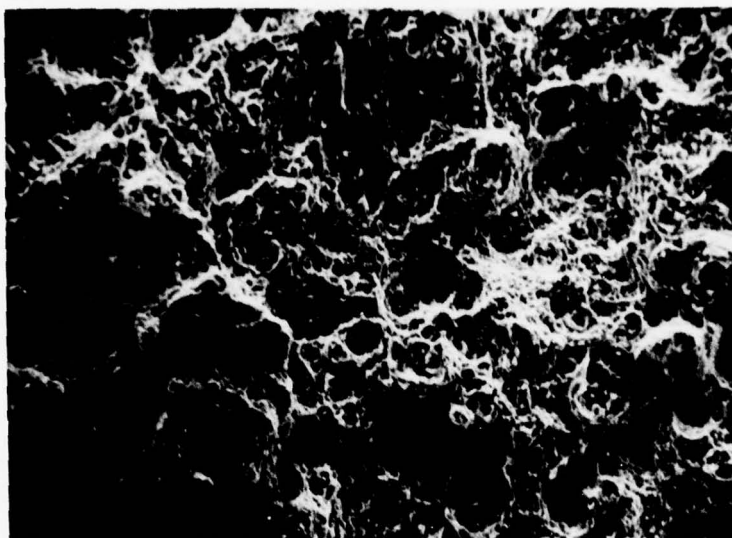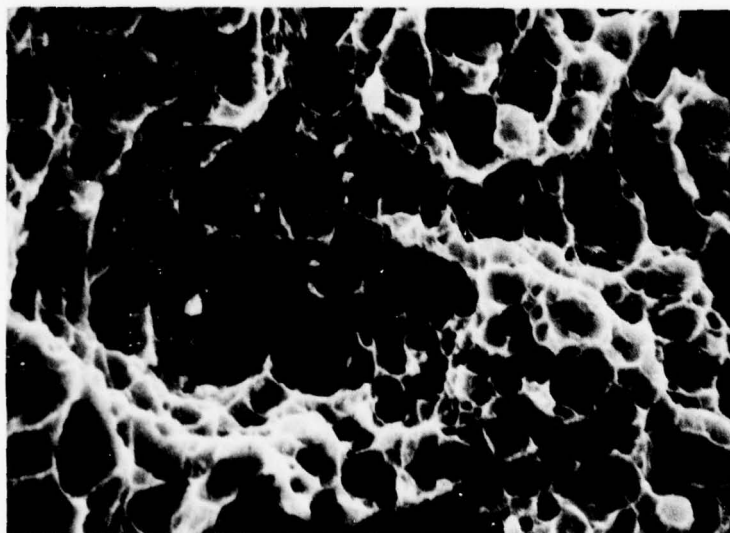


8EST                            (b)

Figure 20   Fracture Surface Appearance of Al-18 Alloy from PWA, Hot-
            Pressed and Extruded at 728 K.   Fracture mode is transgran-
            ular, ductile rupture with the coarser intermetallic
            particles nucleating the larger microvoids.   Magnification
            (a) 200X,  (b) 2000X

8ESG                                  (a)
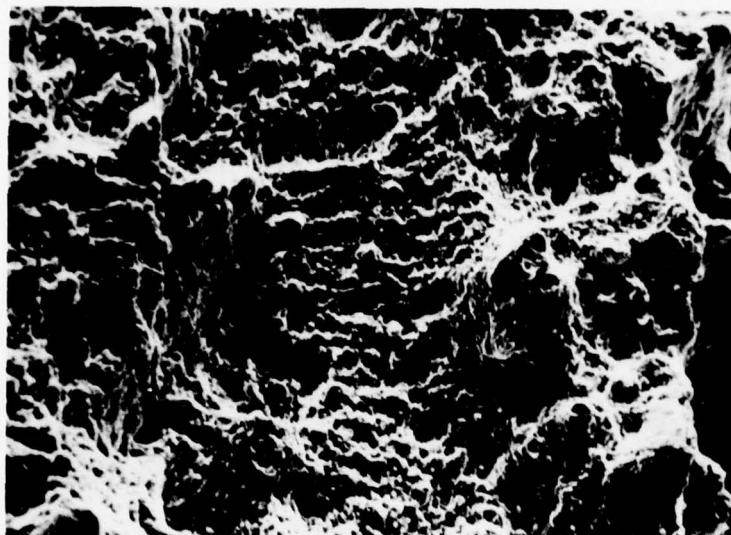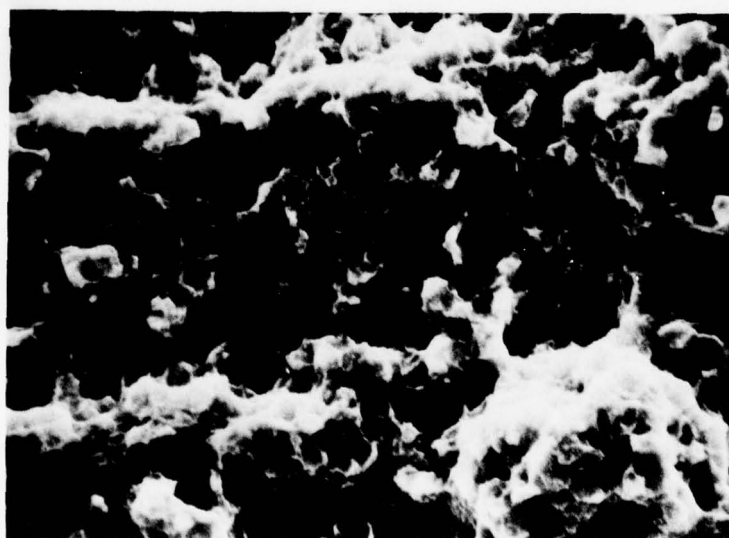


8ESH                                  (b)

Figure 21    Fracture Surface Appearance of Al-2Ca Alloy from BCL, Hot-
             Pressed and Extruded at 700 K.  Fracture mode is relatively
             fine transgranular ductile rupture.  Magnification (a) 200X,
             (b) 2000X

61

8ESD                              (a)
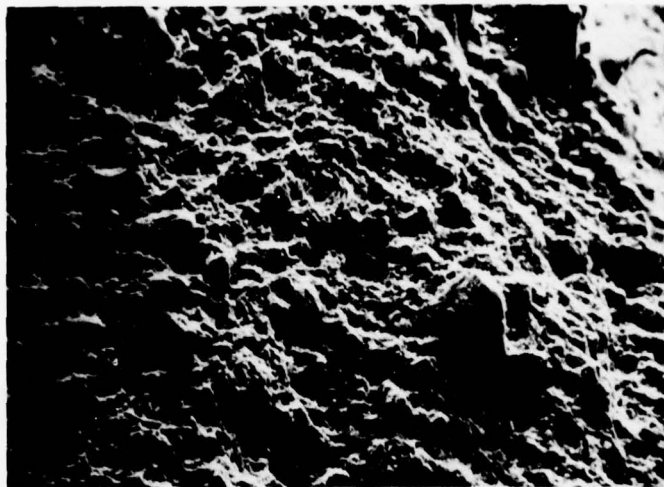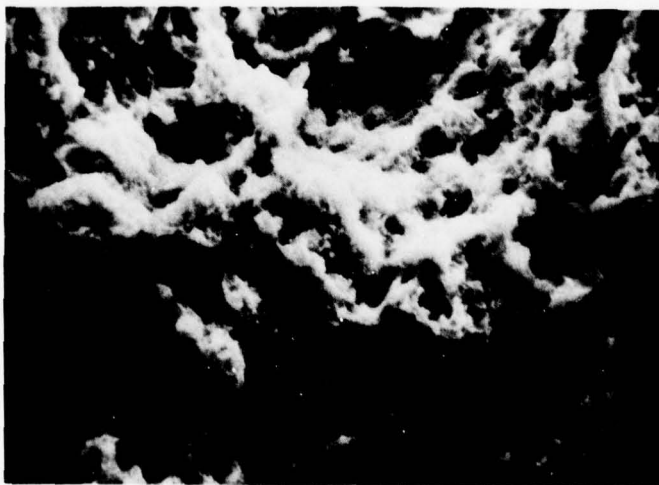


8ESE                              (b)

**Figure** *22* Fracture Surface Appearance of Al-2Ca Alloy from PWA, Hot-
Pressed and Extruded at 700 K. Fracture mode is very fine
transgranular ductile rupture. Occasional splits are
probably boundaries between prior solidified particles
retained through processing. Magnification (a) 200X, (b) 2000X

62
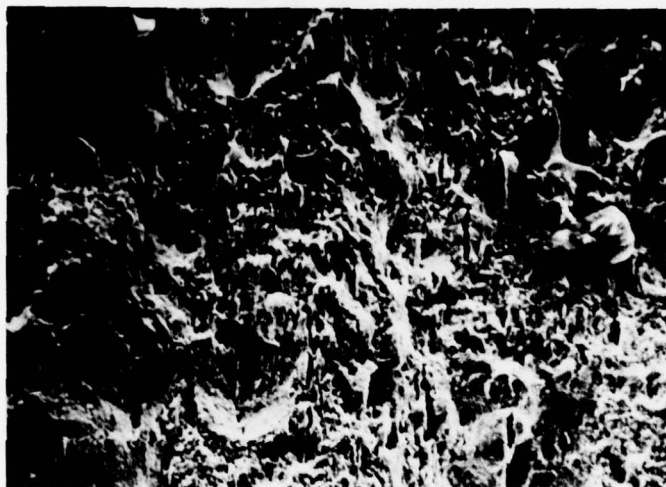
8ESJ                          (a)
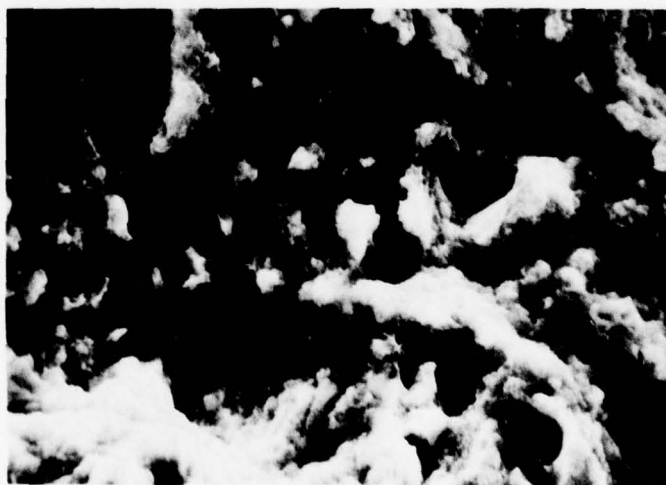


8ESK                          (b)

Figure 23    Fracture Surface Appearance of Al-2Ca Alloy from
             PWA, Hot-Pressed and Extruded at 587 K.  Mixture
             of fine transgranular ductile rupture and splits
             along prior particle boundaries retained through
             processing.  Magnification (a) 200X  (b) 2000X

63

D3596                          (a) as-polished



D3595                          (b) etched
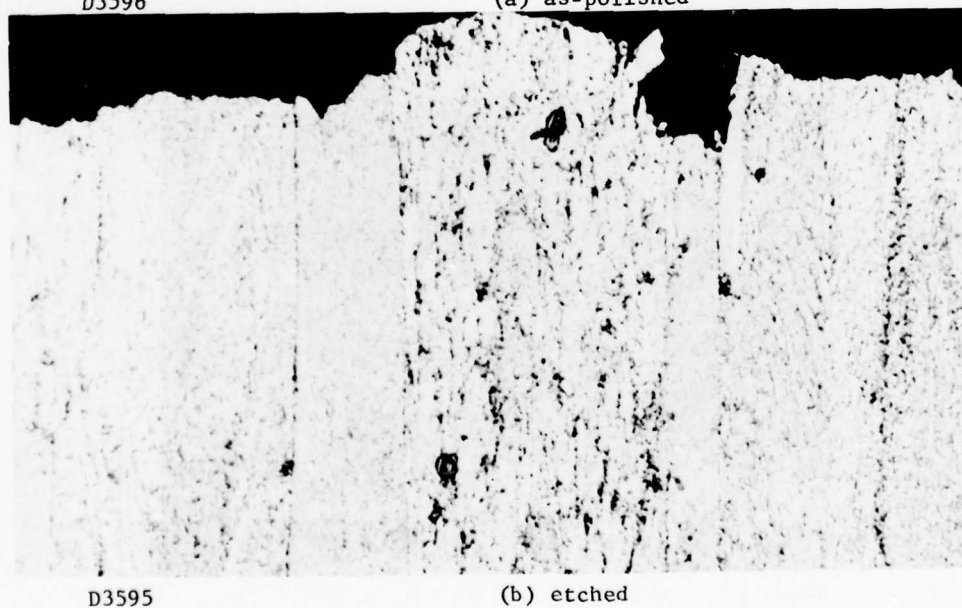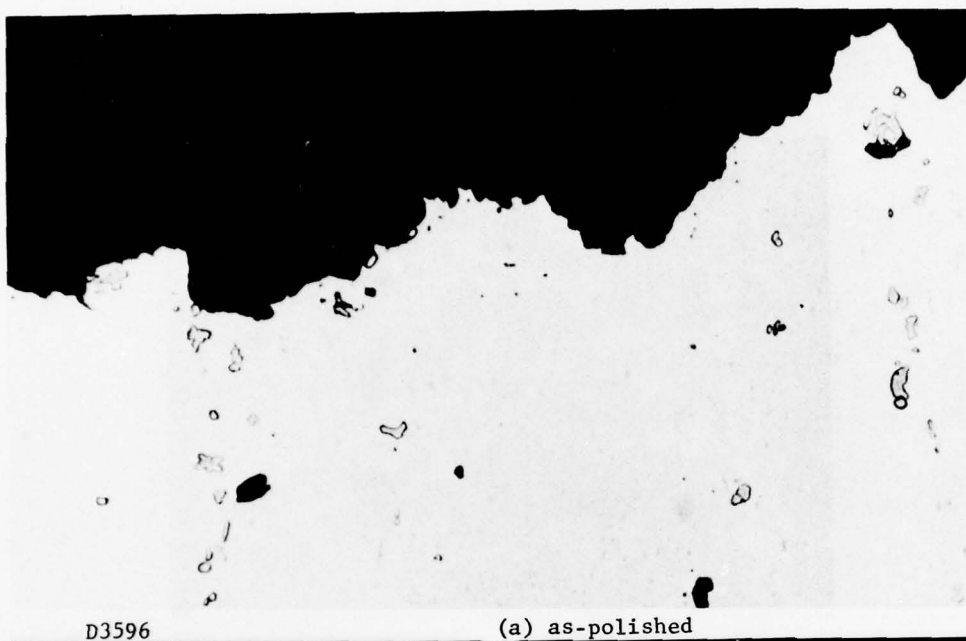
Figure 24    Sections Through Fracture Surface in Al-2Ca Alloy from
             PWA, Hot-Pressed and Extruded at 587 K.  These two
             different fields illustrate fine transgranular ductile
             rupture mode [cusps in (a)] and separation along prior
             particle boundaries (b).  Magnification (a) and (b) 500X
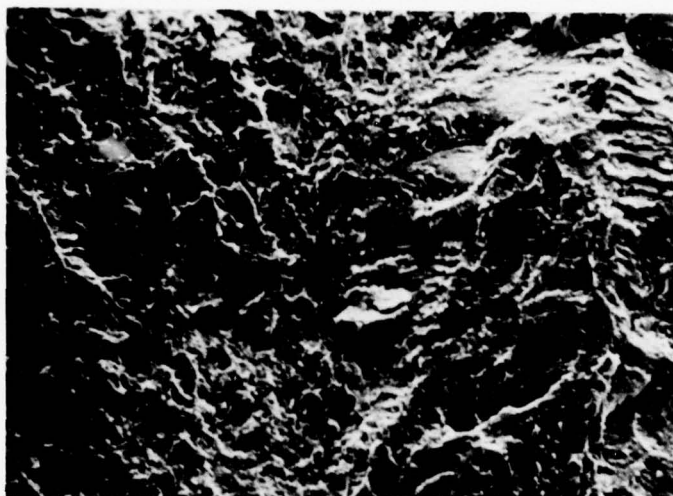
8 ESV                  (a)
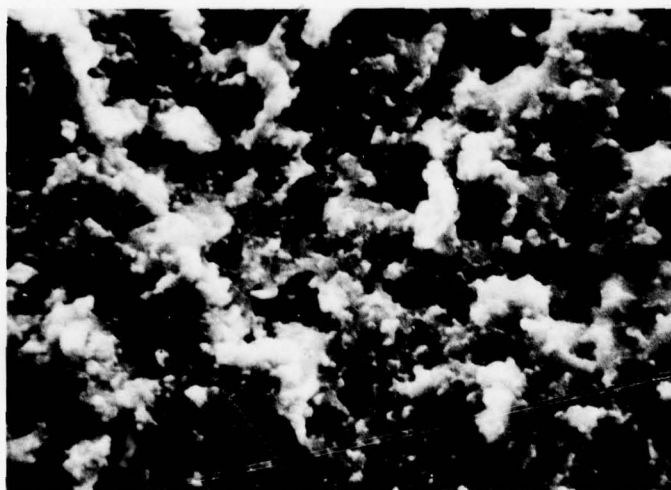
8 ESW                  (b)

Figure 25   Fracture Surface Appearance of Al-20Mg Alloy from
BCL, Hot-Pressed and Extruded at 644K. Fracture
mode appears to be transgranular cleavage.
Magnification (a) 200X   (b) 2000X

65
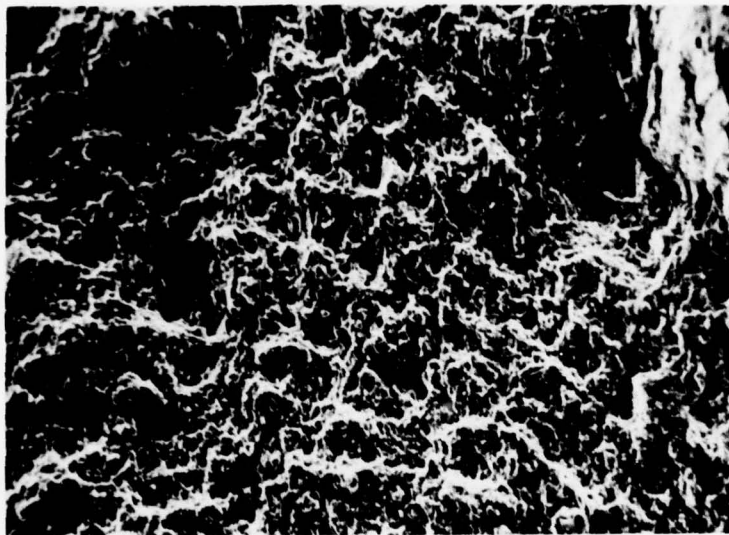
8 ESP                           (a)
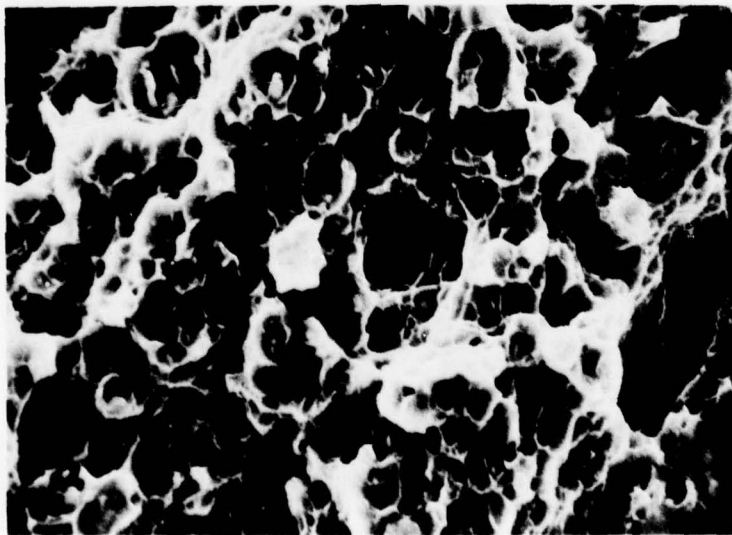


8 ESQ                    (b)

Figure 26  Fracture Surface Appearance of Al 7075 Alloy
           from PWA, Hot-Pressed and Extruded at 700 K.
           Fracture mode is transgranular ductile rupture
           with the coarser intermetallic particles
           nucleating the larger microvoids.  Magnification
           (a) 200X  (b) 2000X

66
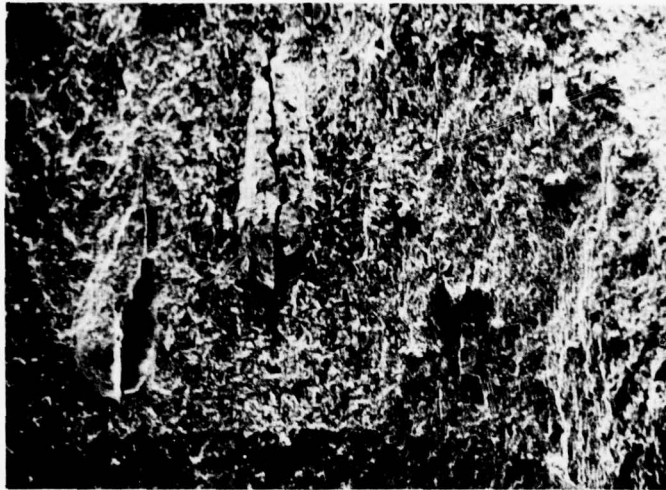
8 ESL                    (a)
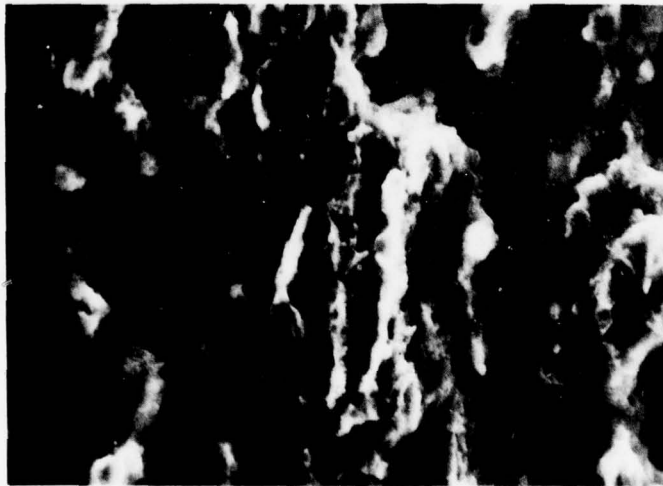


8 ESN                    (b)

Figure 27    Fracture Surface Appearance of Al 7075 Alloy from PWA: Hot-
             Pressed and Extruded at 700 K, Solution Treated and Aged
             to -T6 Condition.  Occasional large slits probably correspond
             to solidified particle boundaries retained through processing.
             Magnifications (a) 50X   (b) 2000X

67

## Section 4
## DESIGN TRADE-OFF STUDIES

The effective development of advanced aluminum alloys for aerospace structural applications requires as a first step the establishment of property goals which would result in major payoffs in specific applications. These property goals may call for improvements in strength, elastic modulus, density, toughness or environmental resistance (fatigue, stress corrosion threshold) singly or in combination. The applications considered are space, missile and aircraft systems that are likely to be designed or to undergo major redesign in the next decade. After a preliminary review was conducted of general material property needs for advanced aerospace structures, three properties were considered for improvement: density, elastic modulus, and strength. It was assumed that other properties would be retained at least to the degree needed for each specific structural application. Selected space, missile and aircraft structures were then studied to determine the effect of the assumed property improvements on weight savings and where possible on payload and range. The following subsections describe the specific studies performed and results obtained. These results, along with design trade-off studies from other sources, were used to establish recommended property improvements goals for the development of advanced aluminum alloys from rapidly solidified powders.

### 4.1 Space Systems Structures

Two different types of space structures were selected for evaluation of weight savings obtained by application of advanced aluminum alloys. The first was the CENTAUR Standard Shroud, a large, lightweight, stiffness-critical assembly. The second structure studied was the SEASAT-A Sensor Module and Module Support Structure, comprised of a complex combination of square and rectangular tubular sections, frames and plates, most of which are strength-critical.

68

### 4.1.1 Assumed Properties

Properties were assumed for advanced aluminum alloys to be evaluated as possible replacements for the existing aluminum alloys used in the two space vehicle systems studied. The baseline alloy considered was 7075-T76. Advanced alloy properties differed in modulus, density or strength, and selected combinations of these. All other properties including fabrication, fatigue, toughness, and corrosion resistance were assumed to be the same as those of Al 7075-T76. The properties assumed are given in Table 11. Major features of these alloys are as follows.

Advanced Alloy A is assumed to have a 20 percent lower density than the baseline alloy. All other properties are the same as baseline.

Advanced Alloy B is assumed to have a 40 percent higher modulus than the baseline alloy, with all other properties being the same as baseline.

Advanced Alloy C is assumed to have both a 40 percent increase in modulus and a 20 percent decrease in density. This results in a modulus-to-density ratio increase of 75 percent compared to the baseline alloy.

Advanced Alloy D is the same as Alloy C but with a significantly higher yield strength and ultimate strength, 60 and 70 percent, respectively.

The effect on weight of each of the space vehicle systems was determined by substituting each of these alloy property sets for the existing aluminum alloys.

### 4.1.2 CENTAUR Standard Shroud

The shroud provides an aerodynamic cover over the payload and second-stage launch vehicle positioned forward of the first stage launch motor. Figure 28 shows a Titan/Centaur Vehicle on take-off. The shroud is the entire top half of the visible structure. The relative size of the shroud is more clearly illustrated in Figure 29, showing the structure during fabrication.

TABLE 11

ADVANCED ALUMINUM ALLOY PROPERTIES
ASSUMED FOR SPACE VEHICLE STRUCTURES
APPLICATION STUDY

| ALLOY | ULTIMATE TENSILE STRENGTH MPa (ksi) | TENSILE YIELD STRENGTH MPa (ksi) | COMPRESSIVE YIELD STRENGTH MPa (ksi) | MODULUS OF ELASTICITY GPa ($10^3$ ksi) | SHEAR MODULUS GPa ($10^3$ ksi) | POISSON'S RATIO | COEFFICIENT OF THERMAL EXPANSION $10^{-6}$/°C ($10^{-6}$/°F) | DENSITY g/cm$^3$ (lb/in$^3$) |
|---|---|---|---|---|---|---|---|---|
| 7075-T76 (Baseline) | 538 (78) | 483 (70) | 476 (69) | 69 (10.0) | 26 (3.8) | 0.33 | 23.2 (12.9) | 2.768 (0.10) |
| A | 303-386 (44-56) | 248-345 (36-50) | 476 (69) | 69 (10.0) | 26 (3.8) | 0.33 | 23.4 (13.0) | 2.214 (0.08) |
| B | 538 (78) | 483 (70) | 476 (69) | 97 (14.0) | 37 (5.3) | 0.33 | 23.4 (13.0) | 2.768 (0.10) |
| C | 538 (78) | 483 (70) | 476 (69) | 97 (14.0) | 37 (5.3) | 0.33 | 23.4 (13.0) | 2.214 (0.08) |
| D | 862 (125) | 827 (120) | 827 (120) | 97 (14.0) | 37 (5.3) | 0.33 | 23.4 (13.0) | 2.214 (0.08) |
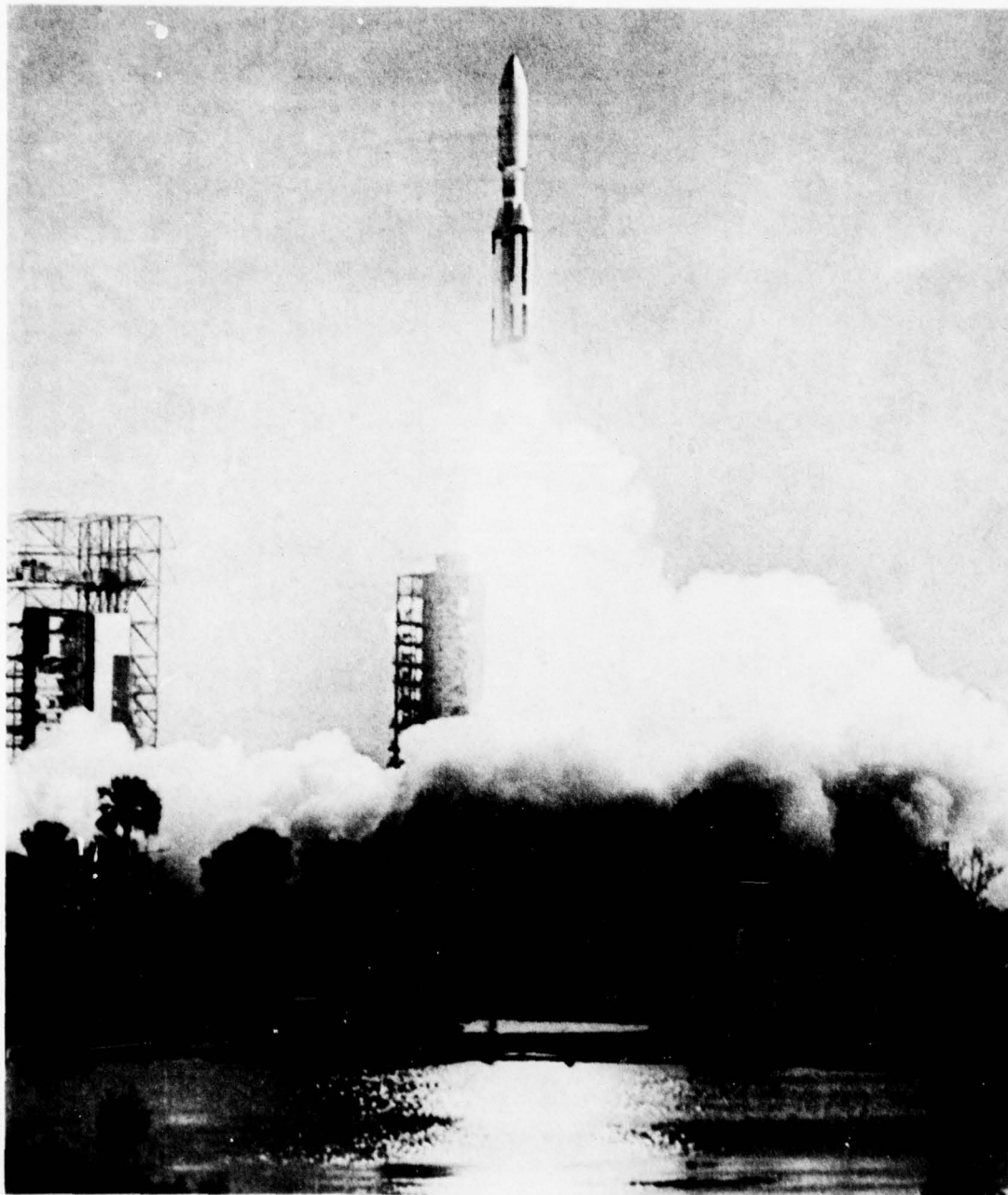
Figure 28 TITAN/CENTAUR - 1 Take-Off. Payload on top of rocket is covered by CENTAUR Standard Shroud

71
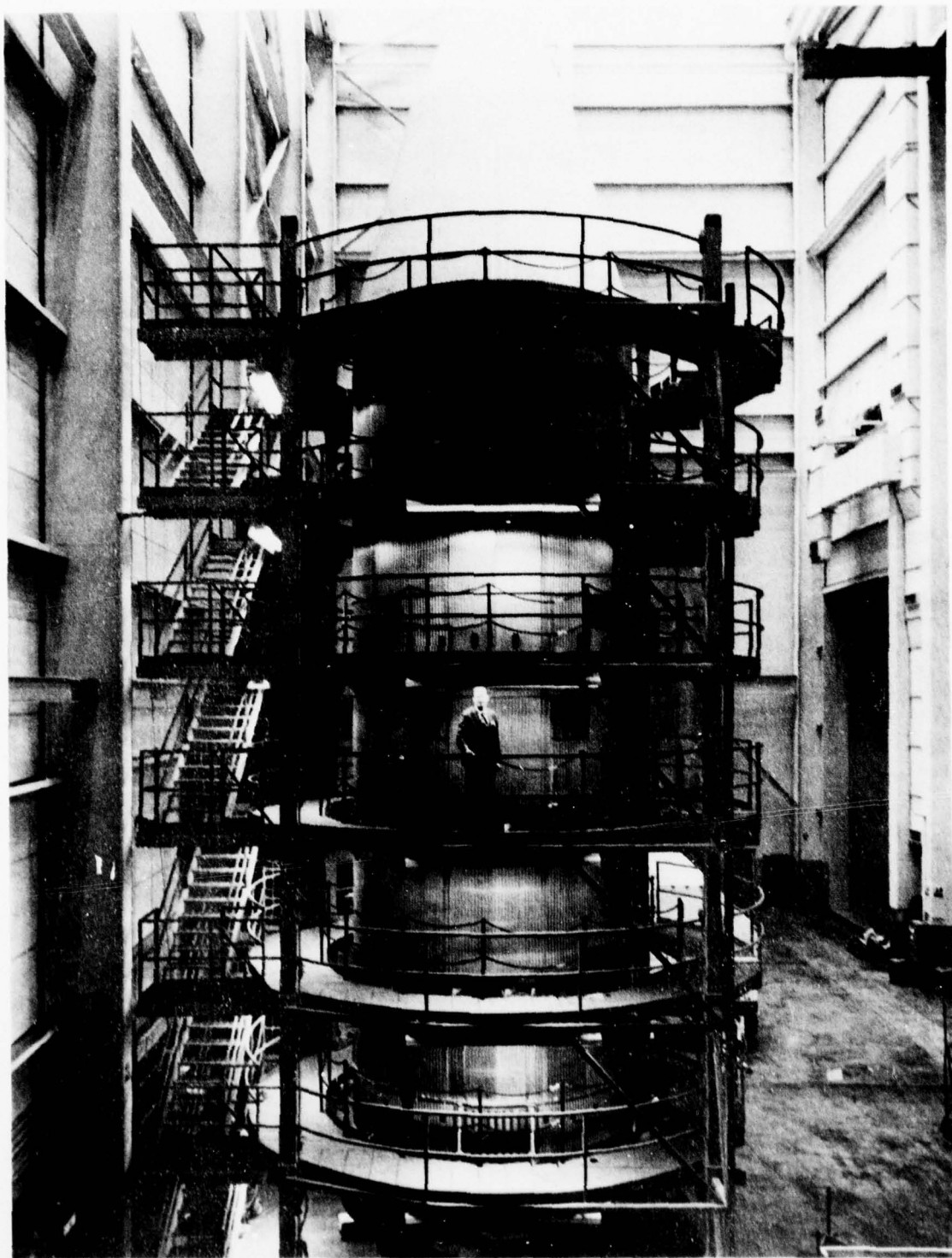
Figure 29 CENTAUR Standard Shroud in Fabrication

Construction features of the shroud are shown in Figure 30. Three main sections of the shroud were evaluated by substitution of the advanced aluminum alloys. These are the bi-conic nose, cylindrical center section, and conic boattail aft end. The bi-conic nose is of semi-monocoque construction and for purposes of this study an aluminum alloy construction was substituted for the existing magnesium alloy when weight reduction could be effected. The cylindrical shell is stiffened internally by circular ring frames, as shown in Figure 30. The boattail aft shell is reinforced externally by hat stiffeners, as shown in Figure 30. Design loading criteria for the CENTAUR Standard Shroud are presented in Figures 31 and 32. Additional key design criteria are the external and internal space envelopes, assembly requirements, including access parts, and separation requirements. Upon launch, the shroud provides aerodynamic cover and support of the payload, until at a predetermined altitude, the shroud is plit into two halves lengthwise by pyrotechnic super-zip joints and separated from the launch vehicle.

Bi-Conic Nose

The primary design criterion for the nose is shell instability due to external pressure loading (see Fig. 32). Critical pressure on the cone is:

$$P_{cr} = \frac{\gamma C_p \pi^2 E_c}{12 \sqrt{1-\nu^2} Z} (\frac{t}{b})^2$$

where;

$\gamma$ = 0.78, a "knock-down" factor for monocoque cones

$C_p$ = buckling coefficient, experimentally determined

$E_c$ = compressive modulus

$\nu$ = Poissons' ratio

$t$ = shell thickness

$b$ = shell width normal to primary loading direction

$Z$ = $\frac{L^2}{Rt} \sqrt{1-\nu^2}$

$L$ = equivalent cylinder length

73
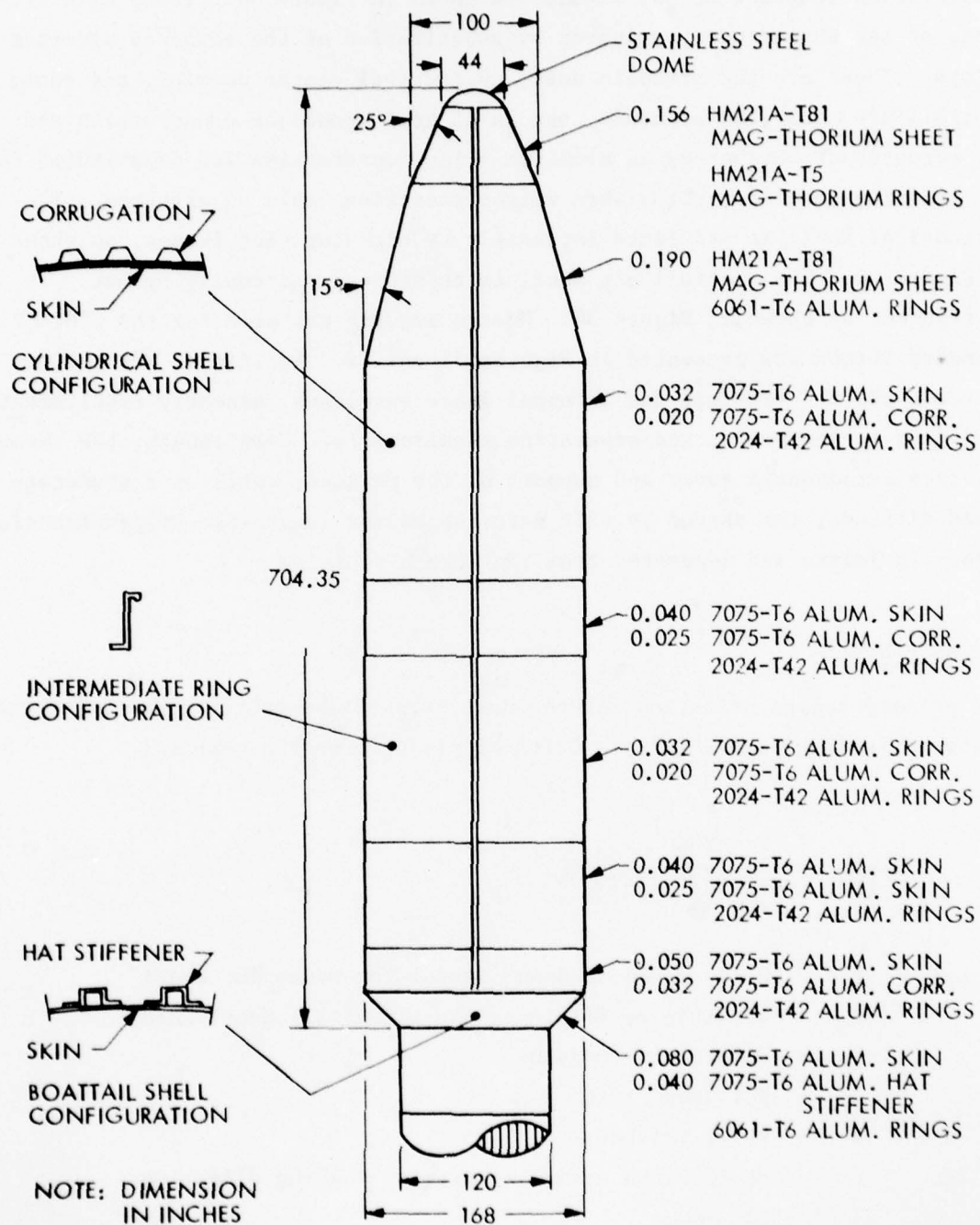
Figure 30 Construction Features of CENTAUR Standard Shroud
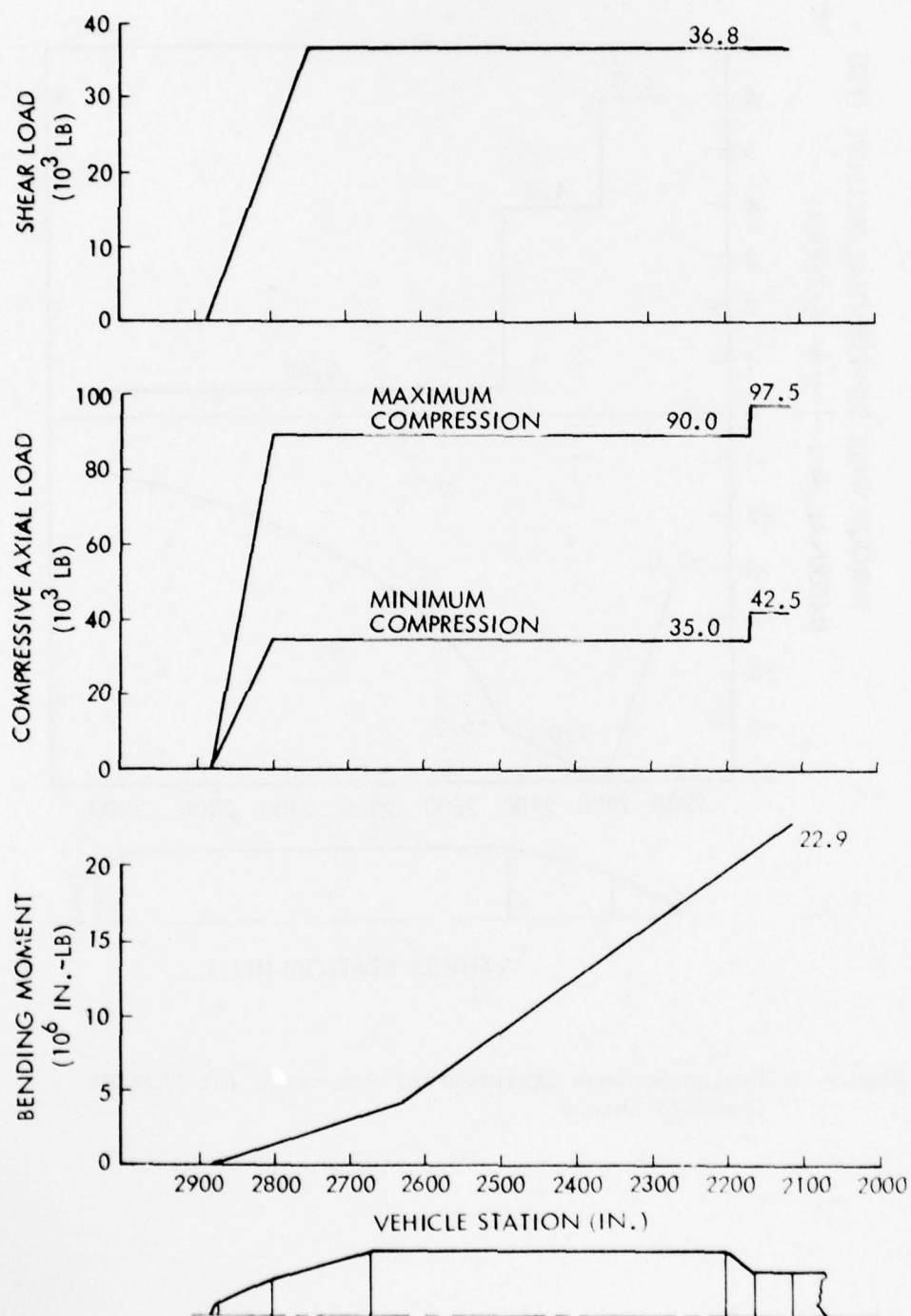
Figure 31 Design Limit Loads for CENTAUR Standard Shroud
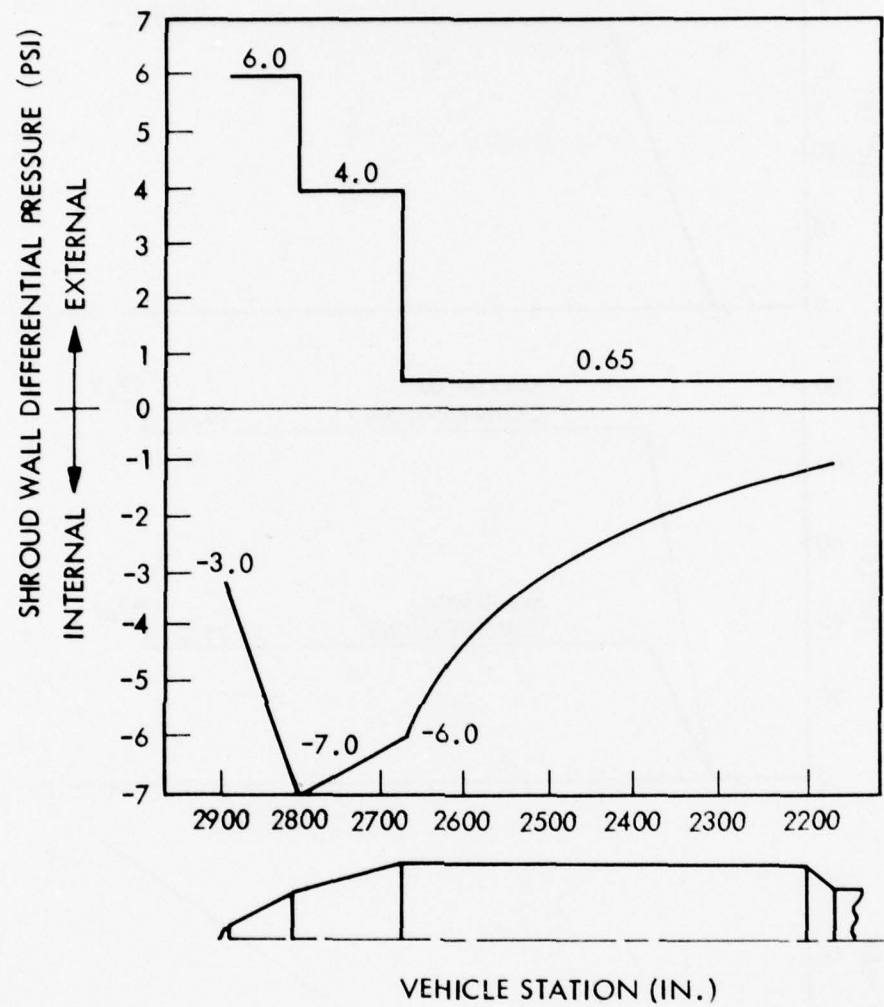
Figure 32  Design Maximum Differential Pressures for CENTAUR
Standard Shroud

$$R = \frac{R_{min} + R_{max}}{2 \cos \alpha}$$

$R_{min}$, $R_{max}$ = min and max cone radii

$\alpha$ = half cone angle

Thus, advanced alloys that have increased modulus or decreased density would result in weight savings in this component.

## Cylindrical Shell

The primary design criterion for the shell structure is compression loading resulting from axial load and bending on the leeward side at maximum air loading (see Fig. 30). The critical buckling stress was used for analysis.

$$\sigma_{cr} = \frac{\pi^2 E_t \, \rho^2}{L^2}$$

where: $E_t$ = tangent modulus

$\rho$ = radius of gyration of shell corrugation

$L$ = internal ring spacing, 38.1 cm (15 in.)

Thus, advanced alloys exhibiting higher modulus or lower density would result in weight savings of this component.

## Boattail Shell

The primary design criterion for the boattail shell is compressive load resulting from longitudinal bending (see Fig. 31). The critical mode for the hat stiffener is the inter-rivet buckling between fasteners. In both cases, flat plate column critical buckling stress is used for design analysis.

$$\sigma_{cr} = \frac{K \pi^2 E}{12(1-\nu^2)} \left(\frac{t}{b}\right)^2$$

where:    k = sheet buckling coefficient

t = sheet thickness

b = sheet width normal to direction of load

Thus, for the same critical buckling stress an increased modulus or decreased density would result in weight savings of both the conical shell and the hat stiffeners.

## Internal Ring Frames

The primary design criterion for internal ring frames in the bi-conic cylindrical sections is elastic stability during external pressure loading (see Fig. 32). For the bi-conic section, the critical pressure condition was calculated from a theory assuming failure of two-hinged rings in the second buckling mode.

$$P_{cr} = \frac{3 \, E \, I}{R^3} \text{ , where } I = \text{section moment of inertia}$$

In the cylindrical section, redesign of the ring frames was calculated from the first buckling mode of two hinged rings. Critical pressure is:

$$P_{cr} = \frac{0.8 \, EI}{R^3}$$

Thus, for the same critical pressure weight savings would result for rings made from an alloy exhibiting either a higher modulus or lower density.

## Longerons, Splices, Doublers

A variety of additional structural elements are used in the shroud assembly and which are strength critical, rather than stiffness critical. These are longerons, used for door cutout reinforcing, splices across manufacturing joints, and miscellaneous doublers, stiffeners and reinforcements for various cutouts.

## Summary of Weight Savings

The calculated weight saved in the shroud by substitution of each of the advanced aluminum alloys listed in Table 11 is summarized in Table 12. Construction features of the shroud obtained by redesign resulting from application of the optimum stiffness advanced alloy (Alloy C) are shown in Figure 33.

78

TABLE 12

SUMMARY OF WEIGHT SAVINGS IN CENTAUR STANDARD SHROUD
BY
APPLICATION OF ADVANCED ALUMINUM ALLOYS

WEIGHT SAVED, kg(lb)

| Key Property Changes Compared to Baseline (ref., Table 11)  STRUCTURAL ELEMENTS | Alloy A  20 pct Lower Density | Alloy B  40 pct Higher Modulus | Alloy C  (A+B) | Alloy D  C+ 70 pct Higher Yield Strength |
|---|---|---|---|---|
| SHELL STRUCTURE (Nose, Cylindrical Centerbody, Aft Boattail) | 152 (335) | 265 (585) | 364 (803) | 364 (803) |
| RINGS (ALL) | 144 (318) | 195 (429) | 300 (661) | 300 (661) |
| LONGERONS, SPLICES MISC. DOUBLERS | 86 (189) | 52 (114) | 127 (281) | 168 (371) |
| TOTAL WEIGHT REDUCTION   (a)   kg (lb)   (b)   Pct. of Aluminum Structure | 382 (842)  20% | 512 (1128)  27% | 792 (1745)  41% | 832 (1835)  44% |
| EQUIVALENT INCREASE IN ORBITING PAYLOAD, kg (lb) (14:1 RATIO) | 27 (60) | 37 (81) | 57 (125) | 59 (131) |

STAINLESS STEEL DOME

CORRUGATION

SKIN

CYLINDRICAL SHELL CONFIGURATION

704.35

INTERMEDIATE RING CONFIGURATION

HAT STIFFENER

SKIN

BOATTAIL SHELL CONFIGURATION

|  | ADVANCED ALUMINUM ALLOY | |
|---|---|---|
| SHEET | CORR | RINGS |
| 0.125 | - | X |
| 0.143 | - | X |

|  | ADVANCED ALUMINUM ALLOY | |
|---|---|---|
| SKIN | CORR | RINGS |
| 0.016 | 0.012 | X |
| 0.020 | 0.016 | X |
| 0.020 | 0.016 | X |
| 0.025 | 0.016 | X |
| 0.025 | 0.020 | X |
| 0.071 | 0.032 | X |
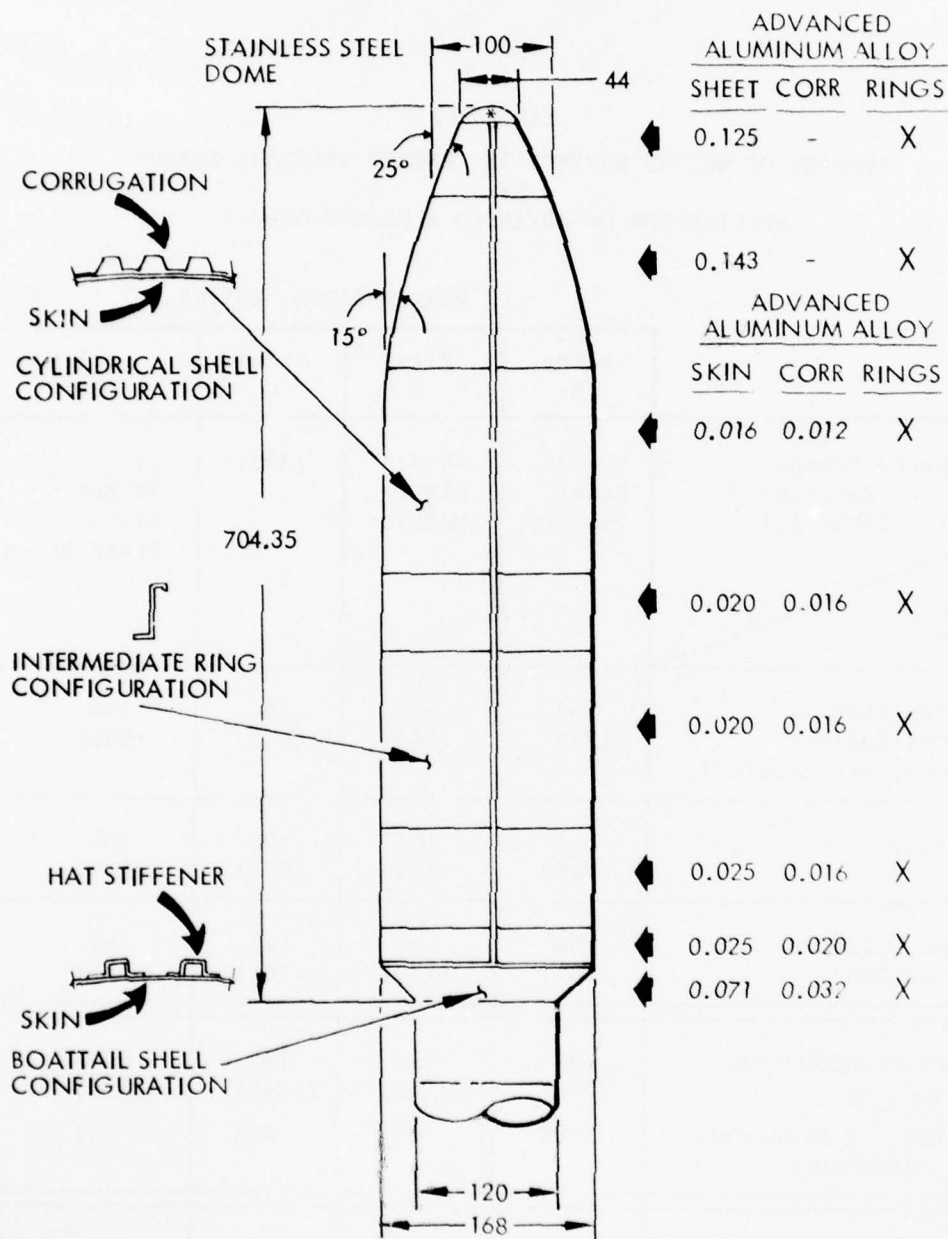
NOTE: DIMENSIONS IN INCHES

X INDICATES VARIOUS THICKNESSES OF ADVANCED ALLOY USED

Figure 33 Construction Features of Redesigned CENTAUR Standard Shroud

80

The CENTAUR Standard Shroud total weight is 2972 kg (6552 lb), of which 64 percent (1910 kg) is aluminum. Substitution of advanced aluminum alloys exhibiting decreased density, increased modulus, or increased strength will save weight in the shroud, thereby allowing an increase in orbiting payload weight. The most effective property in effecting a weight change of the shroud is density, with modulus less effective, and strength having negligible effectiveness. Table 13 shows average weight changes per one percent change in each of these three properties. Thus, the most effective advanced aluminum alloy to be developed for increasing design efficiency in the Centaur Standard Shroud would be a combination of decreased density and increased modulus. Some advanced aluminum alloys selected for development incorporate both these property changes, Al-Li being a prime example.

TABLE 13

SENSITIVITY OF WEIGHT CHANGE TO
PROPERTY CHANGE IN ADVANCED ALUMINUM
ALLOYS APPLIED TO CENTAUR STANDARD SHROUD

|  | STRUCTURE AND PAYLOAD WEIGHT CHANGE* PER ONE PERCENT CHANGE IN SELECTED PROPERTIES | | |
|---|---|---|---|
|  | Density Decrease | Modulus Increase | Strength Increase |
| Weight Savings In Shroud, kg(lb) | 19.1(42.1) | 12.8(28.2) | 0.6(1.29) |
| Orbiting Payload Weight Increase ** kg(lb) | 1.4(3) | 0.9(2) | 0.04(0.1) |

\*   Average, approximated by assuming linear relationship
     between property change and weight change.

\*\*  Assumes same take-off thrust available and 14:1 shroud
     weight reduction to orbiting payload increase ratio.

4.1.3 SEASAT-A Structure

SEASAT-A, shown in Figure 34, is an experimental ocean-survey satellite being developed by Lockheed Missiles and Space Company for the National Aeronautics and Space Administration. SEASAT-A will circle the earth 14 times daily and cover 95 percent of global ocean area every 36 hours. A large variety of sensors, transmitters, and antennas are supported by a complex framework fabricated from aluminum alloys. This framework, shown in Figure 35, is composed of a Sensor Module Structure (SMS) and Sensor Module Support Structure (SMSS). The aluminum alloys presently used in SMS and SMSS include 2XXX, 5XXX and 6XXX alloys, selected for their ease of fabrication, stress corrosion resistance and relatively high strength. Substitution of higher strength or lower density alloys for those presently used would save weight in both the SMS and SMSS.

The SEASAT-A is launched into orbit by a large booster rocket. The axial loads, shear loads, and bending moments imposed on the SMS and SMSS during launch constitute the critical design loading requirements. These are shown in Figure 36. For most of the components, design analysis for weight savings resulting from application of advanced aluminum alloys are based upon strength and density of the alloys and the stresses due to combined axial load and bending moment. Thus, the maximum stress at any location along the structure is:

$$\sigma_{max} = \frac{P_{max}}{A} + \frac{M_{max} C}{I}$$

where:    $P_{max}$    =    max axial load

            $A$    =    cross-sectional area of structural section

            $M$    =    applied bending moment

            $C$    =    distance from neutral axis to outer fiber

            $I$    =    section moment of inertia
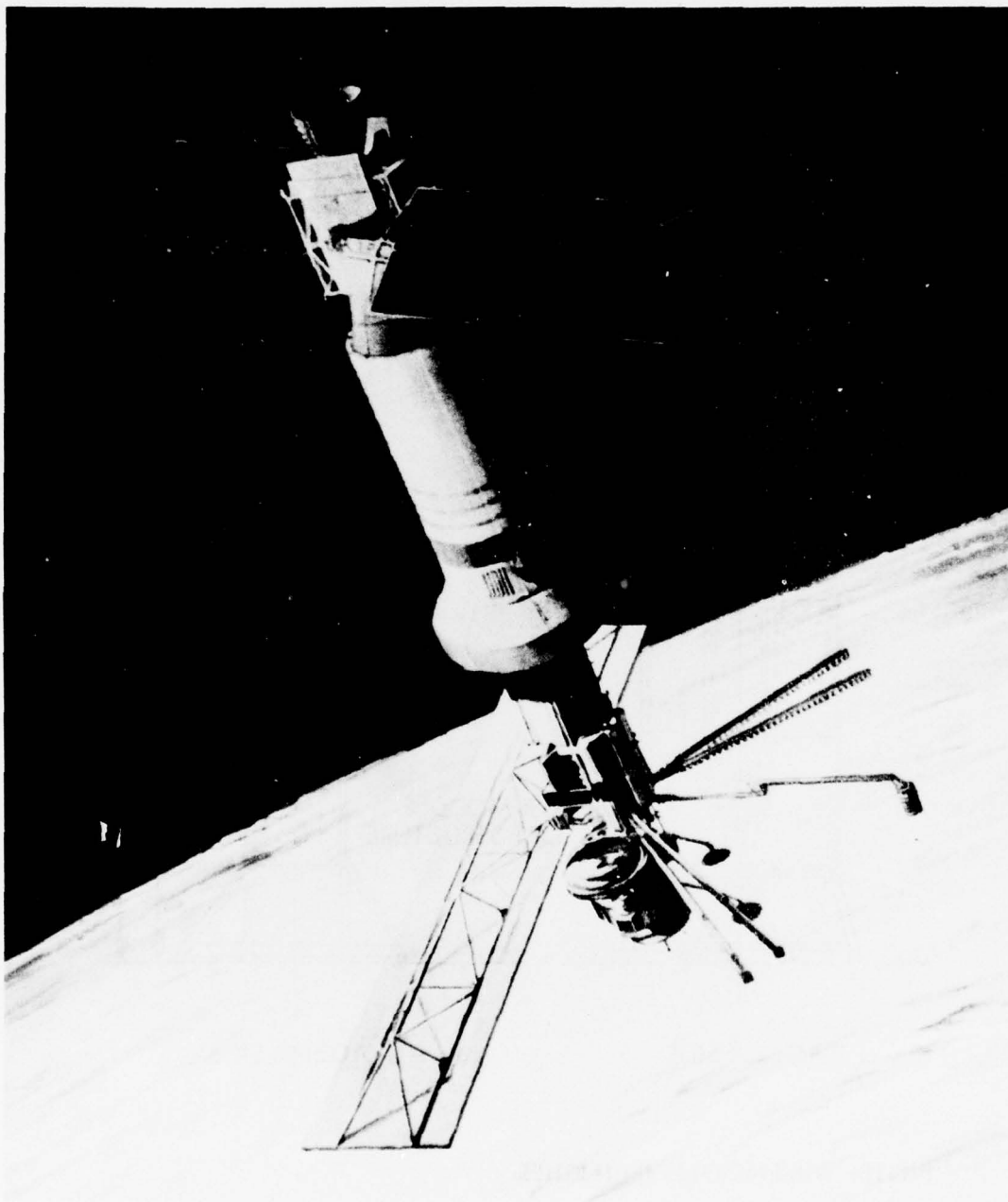
Figure 34  SEASAT-A in Orbit.  Artist's Rendition

83

SENSOR MODULE
MAST ASSY

206.90
REF.

92.70
REF.

SENSOR MODULE
SUPPORT STRUCTURE

+ Z AGENA SIDE                    - Y AGENA SIDE
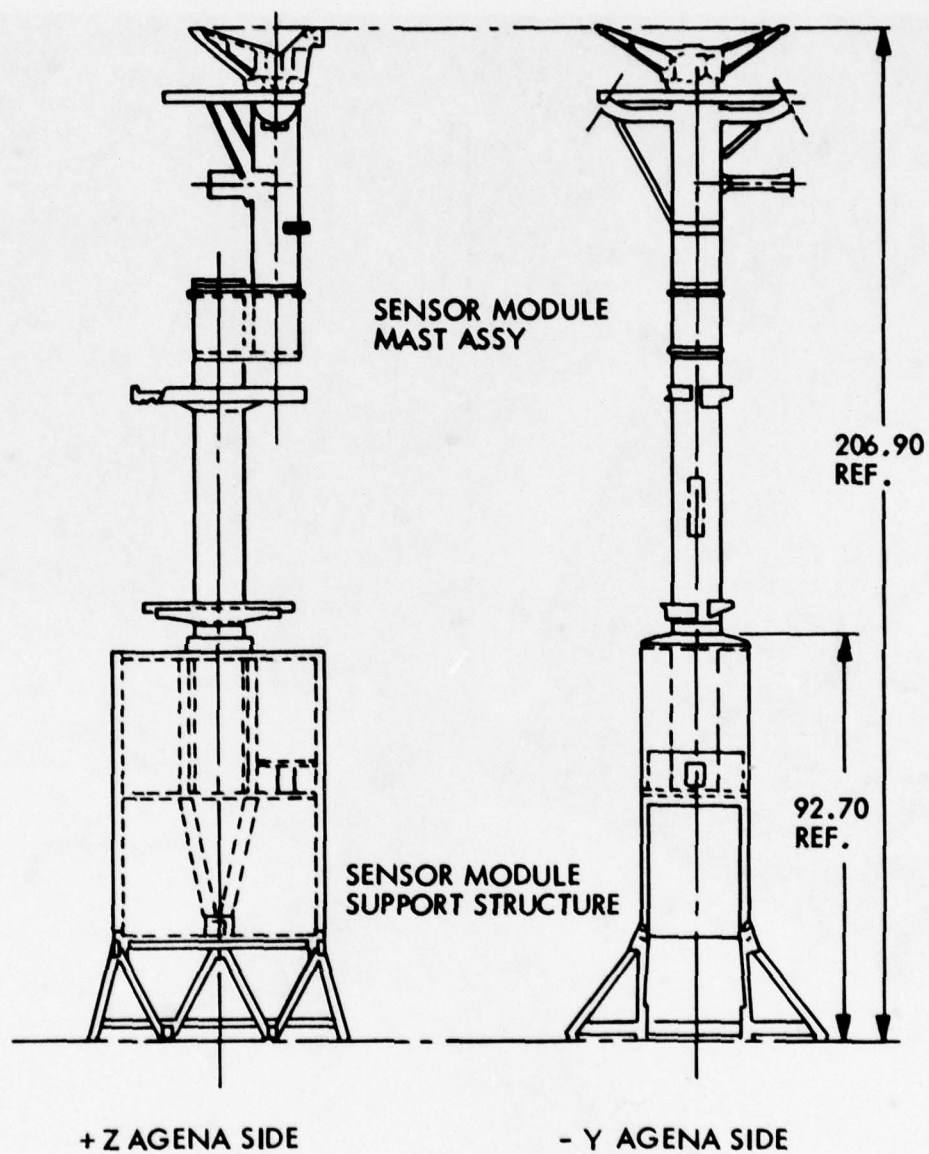
NOTE: DIMENSIONS IN INCHES

Figure 35 SEASAT-A Structural Framework

84

STATION

AXIAL
LOAD
(10³ LB)

SHEAR
(10³ LB)

BENDING
MOMENT
(10⁶ IN-LB)
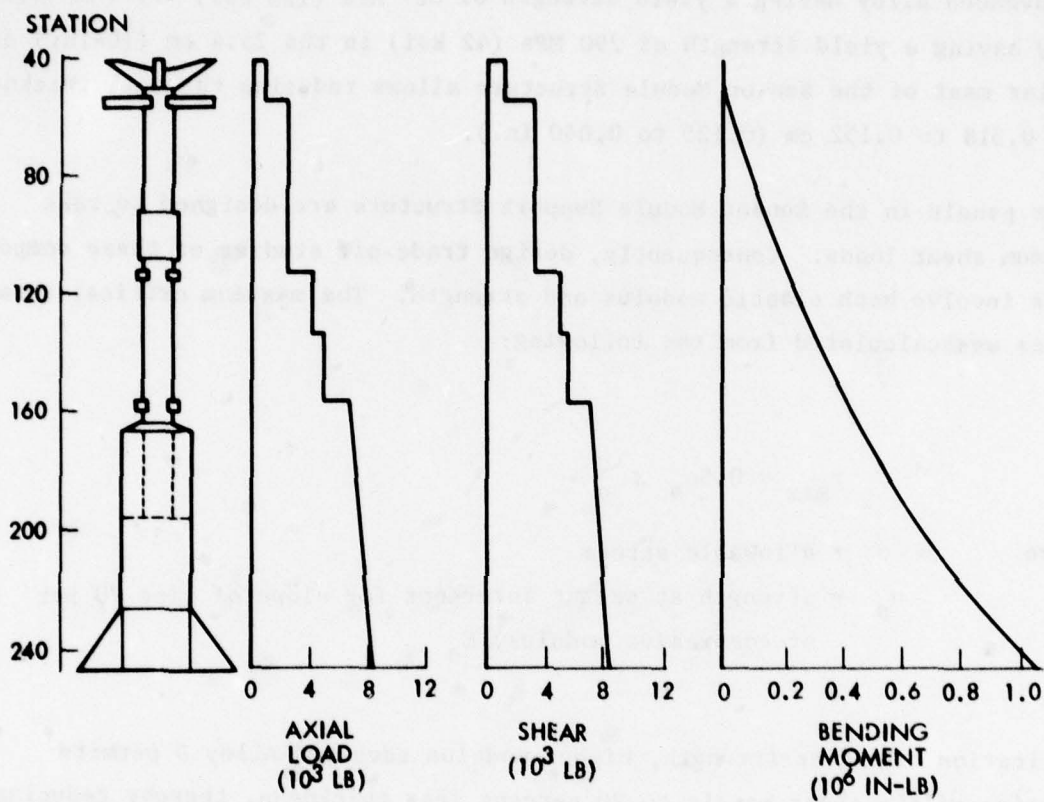
Figure 36 Design Limit Loads for SEASAT-A Structure

Weight savings result from reduced section size of particular components
if fabricated from a higher strength alloy. For example, substitution of
an advanced alloy having a yield strength of 827 MPa (120 ksi) for the 6061-T6
alloy having a yield strength of 290 MPa (42 ksi) in the 25.4 cm (10-in.) dia.
tubular mast of the Sensor Module Structure allows reducing the wall thickness
from 0.318 to 0.152 cm (0.125 to 0.060 in.).

Shear panels in the Sensor Module Support Structure are designed to take
maximum shear loads. Consequently, design trade-off studies of these compo-
nents involve both elastic modulus and strength. The maximum critical shear
stress was calculated from the following:

$$\tau_{max} = 0.5\sigma_s \times \frac{\sigma}{\sigma_s}$$

where      $\sigma$ = allowable stress

           $\sigma_s$ = strength at secant intercept for slope of line 70 pct
              of compresive modulus, $E_c$

Application of higher strength, higher modulus advanced Alloy D permits
redesign of the shear panels to 20 percent less thickness, thereby reducing
weight.

## Summary of Weight Savings

The calculated weight saved in the SEASAT-A Sensor Module Structure (SMS) and
Sensor Module Support Structure (SMSS) is summarized in Table 14. Total
weight of the SEASAT-A, SMS and SMSS is 1189 kg (2622 lb) of which 404 kg
(890 lb) is aluminum structure considered in this study. Weight reductions
from application of advanced aluminum alloys result in a 1:1 ratio of
increased weight for orbiting payload in the form of additional sensors,
transmitters and associated equipment. As shown in Table 14, substitution
of Alloy A with 20 percent lower density than the presently used alloy
results in a 81 kg (178 lb) weight savings. Substitution of Alloy B with

86

39 to 77 percent higher ultimate strength and 40 percent higher elastic modulus than the presently used alloys results in an even larger weight savings, 116 kg (256 lb). This is because a number of the present alloys used in the structure have relatively low ultimate strength, 303-386 MPa (44-56 ksi). The increased modulus of Alloy B contributes to weight reduction only in the SMSS shear panels. Alloy C, combining the lower density of Alloy A and higher modulus of Alloy B and with the strength of 7075-T76 results in a weight savings of 174 kg (383 lb), somewhat less than the additive savings of A and B. The largest savings is achieved by application of Alloy D which is assumed to have an ultimate strength of 827 MPa (125 ksi).

Assuming a linear relationship between selected property change and weight savings, sensitivity factors can be calculated as was done for the Centaur Standard Shroud. These factors are shown in Table 15.

It is evident that change in density is most significant in terms of weight saved per percentage property change. Change in strength is next most significant, followed by change in modulus. These results are in distinct contrast with the results for Centaur Standard Shroud, where the significance of strength change in advanced aluminum alloys on weight saved was negligible. Thus, for the SEASAT-A, the preferred properties to be developed in advanced aluminum alloys would be decreased density and increased strength. If strength increase were not possible, then modulus increase with density decrease would be of next priority. Weight saved by successful application of Alloy C, Table 14, would result in 174 kg (383 lb), which is particularly significant because detector and transmitter payload weight increase is 1:1 with respect to structural weight decrease.

## TABLE 14

### SUMMARY OF WEIGHT SAVINGS IN SEASAT-A
### SENSOR MODULE STRUCTURE AND SENSOR MODULE SUPPORT
### STRUCTURE BY APPLICATION OF ADVANCED ALUMINUM ALLOYS

WEIGHT SAVED, kg(lb)

| KEY PROPERTY CHANGES COMPARED TO BASELINE<br><br>STRUCTURAL ELEMENTS | ALLOY A<br><br>20 pct Lower Density<br>(a) | ALLOY B<br>40 pct Higher Modulus and 50-60 pct Higher Strength<br>(b) | ALLOY C<br><br>A+B | ALLOY D<br>C+ 60 pct Higher Ultimate Strength<br>(c) |
|---|---|---|---|---|
| SENSOR MODULE MAST TUBE | 23 (50) | 58 (128) | 69 (152) | 85 (188) |
| SENSOR MODULE SUPPORT COMPONENTS (d) | 31 (68) | 28 (61) | 53 (116) | 90 (199) |
| SCATTEROMETER, VIRR AND TRANET BEACON (e) | 18 (39) | 21 (46) | 35 (78) | 56 (124) |
| SMSS SHEAR PANELS | 10 (21) | 10 (21) | 17 (37) | 17 (37) |
| TOTAL WEIGHT REDUCTION kg (lb)<br>Pct. of Aluminum Structure | 81 (178) = 20% | 116 (256) = 29% | 174 (383) = 43% | 249 (548) = 62% |
| EQUIVALENT INCREASE IN ORBITING PAYLOAD, kg(lb) (1:1 RATIO) | 81 (178) | 116 (256) | 174 (383) | 249 (548) |

NOTES:  (a)  Alloy A is assumed to have 20 pct lower density than present alloys, but no change in strength or elastic modulus. Present alloys include include 6061, 5083, and others, varying in yield strength from 248 to 345 MPa (36 to 50 ksi) and ultimate strength from 303 to 386 MPa (44 to 56 ksi).

(b)  Alloy B is assumed to have 40 pct higher modulus than present alloys, and the ultimate strength of 538 MPa (78 ksi) typical for 7075-T76, about 50-60 pct higher than present alloys.

(c)  Ultimate strength of 862 MPa (125 ksi) 60 pct higher than the 538 MPa (78 ksi) ultimate strength of Alloy B.

(d)  Includes machined fittings, structural columns, outrigger columns, synthetic aperature radar mainframe and support structure, and miscellaneous brackets and fittings.

(e)  Includes SASS plate, mast and skin panels, Tranet Beacon frame, and support for visual and infrared radiometer.

**TABLE 15**

**SENSITIVITY OF ORBITING PAYLOAD**
**WEIGHT TO PROPERTY CHANGE**
**IN ADVANCED ALUMINUM ALLOYS**
**APPLIED TO SEASAT-A**

|  | PAYLOAD WEIGHT CHANGE kg (lb) PER PERCENT PROPERTY CHANGE | |
|---|---|---|
| Density | 4 | (8.9) |
| Modulus | $\leq 0.9$ | $\leq (2)$* |
| Strength | 1.25 | (2.75) |

\* Rough estimate as weight savings for Alloy
B incorporate both modulus increase and
strength increase above present alloys.
Contribution of modulus increase alone was
estimated to be $\simeq$ 30 pct of total in making
this calculation.

## 4.1.4 Conclusions

For both the predominantly stiffness-critical shroud and strength-critical
SEASAT-A structures, change in density results in the greatest change in
weight on a percent basis. In the case of the CENTAUR Standard Shroud, modulus
of elasticity change is 2/3 rds as effective as density change; strength
change is of negligible effect. Thus, for the shroud, an advanced alloy
exhibiting higher modulus and lower density would be the most effective
combination to save structural weight. Because the shroud is discarded
after launch but before orbit, weight savings in the shroud results in only
a 1:14 ratio of orbiting payload increase. For a number of satellite pro-
grams in the past, a few kg increase in payload has been of major importance
in design development. Successful development of Alloy C, with a 40 pct
higher modulus and 20 pct lower density compared to 7075-T76, for the CENTAUR
Shroud would result in a major contribution of 57 kg to increased payload.

Application of either the higher modulus or higher strength advanced aluminum alloys to the SEASAT-A structure contributes to increase in orbiting payload, but these are only 25 to 31 pct as effective as density decrease, on a percent property change basis. Thus, combined property improvements of increased strength and decreased density or increased modulus and decreased density would both contribute about the same to orbiting payload increase. Weight saved in the SEASAT-A structure has a direct 1:1 effect* on payload, as the structure is part of the orbiting system. Achievement of Alloy D properties in an advanced alloy would result in a major contribution to SEASAT-A payload, 249 kg. This would allow reduction of the booster rocket thrust requirement or addition of more sensors, transmitters, etc., thereby increasing functional capability during service.

4.2 Fleet Ballistic Missile Structures

The next generation fleet ballistic missile (FBM) is the D5 Advanced TRIDENT. This missile will have a longer range and possibly a heavier payload than the existing C4 TRIDENT FBM. The detailed design of the D5 has not yet been initiated. However, two components were selected from the C4 missile for weight savings studies using assumed properties of advanced aluminum alloys. The components selected were based on one being stiffness critical and the other being strength critical; both are structural components likely to be incorporated, with only minor modification, in the D5 FBM.

The intention in applying advanced aluminum alloys to FBM applications is to reduce structural weight, thereby increasing range or payload. In the FBM multistage missile, parts of the structure are carried in the flight for different times. The longer a given structural component is carried, the greater is the penalty of its weight on payload or range. The relative weight/performance sensitivity of major components of a typical FBM is shown in Figure 37. It is interesting to note that the C4 FBM equipment section, which has the highest sensitivity to weight reduction, is made primarily of graphite/epoxy. At the time this component was being designed, neither advanced aluminum alloys nor advanced metal matrix composites were available.

---

* One unit weight saved in structural weight allows one additional unit weight to be added to the orbiting payload.
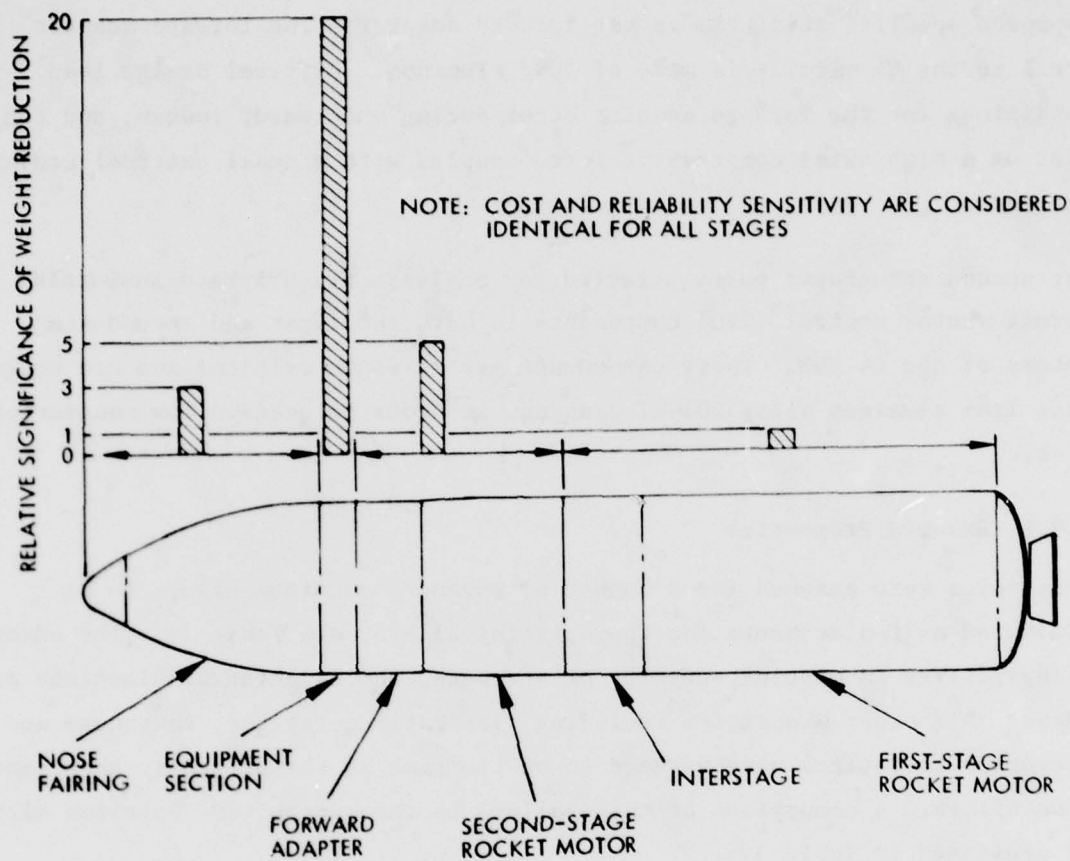
Figure 37   Relative Significance of Structural Component
Weight Reduction on Performance of Typical
Fleet Ballistic Missile

A promising structural component for advanced aluminum alloys exhibiting improved specific stiffness is the forward adapter. The forward adapter shell in the C4 missile is made of 5083 aluminum. Critical design load conditions for the forward adapter occur during underwater launch, and consist of a high axial compressive force coupled with a small external crushing pressure.

The second structural parts selected for analysis are brackets supporting thrust vector control (TVC) components in both the first and second stage motors of the C4 FBM. These components are strength critical and are presently made from aluminum alloy 201-T7 castings in order to achieve low manufacturing cost.

### 4.2.1 Assumed Properties

Properties were assumed for a number of advanced aluminum alloys to be evaluated as replacements for the existing alloys, see Table 16. The advanced alloys differ in modulus, density or strength, and selected combinations of these. All other properties including fabrication, fatigue, toughness and corrosion resistance were assumed to be the same as the presently used baseline alloys. A comparison of these alloys to the appropriate baseline alloy is presented in Table 17.

## TABLE 16

### ADVANCED ALUMINUM ALLOYS PROPERTIES ASSUMED FOR FBM COMPONENTS APPLICATION STUDY

| ALLOY | ULTIMATE TENSILE STRENGTH MPa (ksi) | TENSILE YIELD STRENGTH MPa (ksi) | MODULUS OF ELASTICITY | | POISSONS' RATIO | COEFFICIENT OF THERMAL EXPANSION $10^{-6}$/°C ($10^{-6}$/°F) | DENSITY g/cm³ (lb/in³) |
|---|---|---|---|---|---|---|---|
| | | | TENSION GPa ($10^3$ ksi) | COMPRESSION GPa ($10^3$ ksi) | | | |
| **BASELINE ALLOYS** | | | | | | | |
| 5083-H323 Sheet | 324 (47) | 248 (36) | 70 (10.2) | 72 (10.4) | 0.33 | 24 (13.2) | 2.657 (0.096) |
| 201-T7 Casting | 386 (56) | 331 (48) | 71 (10.3) | 74 (10.7) | 0.33 | 23 (13) | 2.768 (0.10) |
| **ADVANCED ALLOYS** | | | | | | | |
| C | 552 (80) | 483 (70) | 97 (14) | 97 (14) | 0.33 | 23 (13) | 2.214 (0.08) |
| D | 862 (125) | 827 (120) | 97 (14) | 97 (14) | | | 2.214 (0.08) |
| E | 552 (80) | 483 (70) | 83 (12) | 83 (12) | | | 2.464 (0.089) |
| F | 862 (125) | 827 (120) | 62 (9) | 62 (9) | | | 2.491 (0.09) |
| G | 552 (80) | 483 (70) | 97 (14) | 97 (14) | | | 2.768 (0.10) |
| H | 862 (125) | 827 (120) | 97 (14) | 97 (14) | | | 2.768 (0.10) |
| I | 517 (75) | 483 (70) | 69 (10) | 69 (10) | ↓ | ↓ | 2.768 (0.10) |

## TABLE 17

### COMPARISON OF ADVANCED ALLOY PROPERTIES WITH BASELINE ALLOYS

| ADVANCED ALLOY | APPLICATION CONSIDERED | PERCENT CHANGE COMPARED TO BASELINE | | | |
|---|---|---|---|---|---|
| | | DENSITY | YIELD STRENGTH | ULTIMATE STRENGTH | ELASTIC MODULUS (TENSION) |
| C | FWD Adaptor | -17 | + 94 | + 70 | +37 |
| E | | - 7 | + 94 | + 70 | +18 |
| F | | - 6 | +233 | +166 | -12 |
| D | TVC Brackets | -20 | +150 | +123 | +36 |
| F | | -10 | +150 | +123 | -13 |
| H | | 0 | +150 | +123 | +36 |

93

### 4.2.2 Forward Adapter

The forward adapter selected for this study is a good candidate for a high specific modulus material. In addition, a previous study has been made of this structure using graphite/aluminum as the advanced material (66). A cross section of the baseline forward adapter (dwg. No. 3079867) is shown in Figure 38. The shell structure is fabricated of 5083-H323 aluminum sheet with welded end rings and a riveted mid-bay Z ring stiffener. Since there are no longitudinal stiffeners, the structure is a ring stiffened monocoque cylinder. Although there are numerous small cutouts and two large access panels in the structure, these details have been neglected in the present study.

Only the shell portion of the forward adapter was analyzed. The end rings represent a significant portion of the total weight, being about 17 kg (38 lb.) as compared to the shell weight of 25 kg (56 lb.). Therefore, consideration of advanced alloys for the end and mid-bay rings has a future potential for significant additional weight savings. Further, achievement of a high "as welded" strength in the high specific stiffness advanced alloys would provide an additional weight savings.

To evaluate the advanced alloys a bifurcation buckling analysis was performed using the BOSOR computer program to analytically predict the axial load and crushing pressure structural capabilities. Several different alloys were evaluated for different elastic moduli and shell thicknesses. For each configuration, a margin of safety was calculated for the equivalent design loads [P = 809 kN (182 kip), pressure = 12.5 kPa (1.82 psi) limit], and plotted in Figure 39 with respect to shell weight. Also plotted are the results from the graphite/aluminum study performed by Rezin (66). The material properties used in that study are given in Table 18. The results in Figure 40 show that the advanced alloy shell designs are in all cases lighter than the conventional baseline design. For Alloy C, a weight savings of about

94

ALUMINUM ALLOYS:

SHELL: 5083-H323
FORWARD AND AFT RINGS: 5083-H111
MIDRING: 6061-T6

NOTE: DIMENSIONS IN INCHES



11.30

23.55

36.0$^R$

0.875

0.121 $^{+ 0.008}_{- 0.000}$

1.0
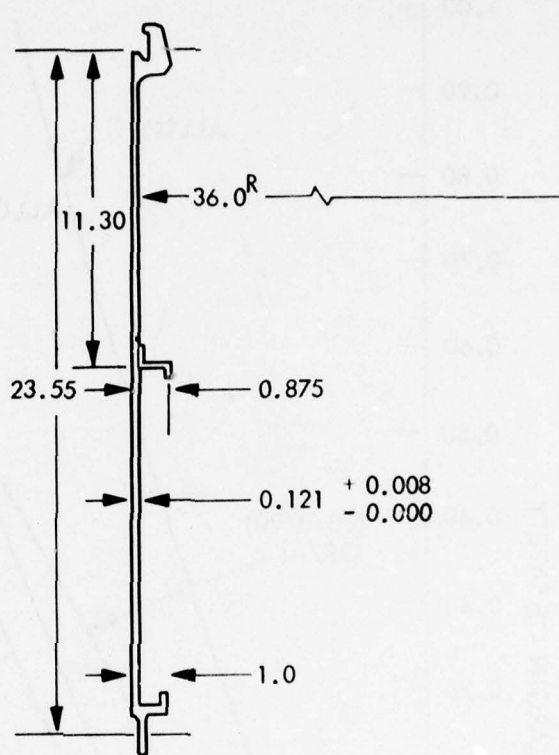
Figure 38  Cross Section of Forward Adapter for
Trident-C4 Fleet Ballistic Missile

95
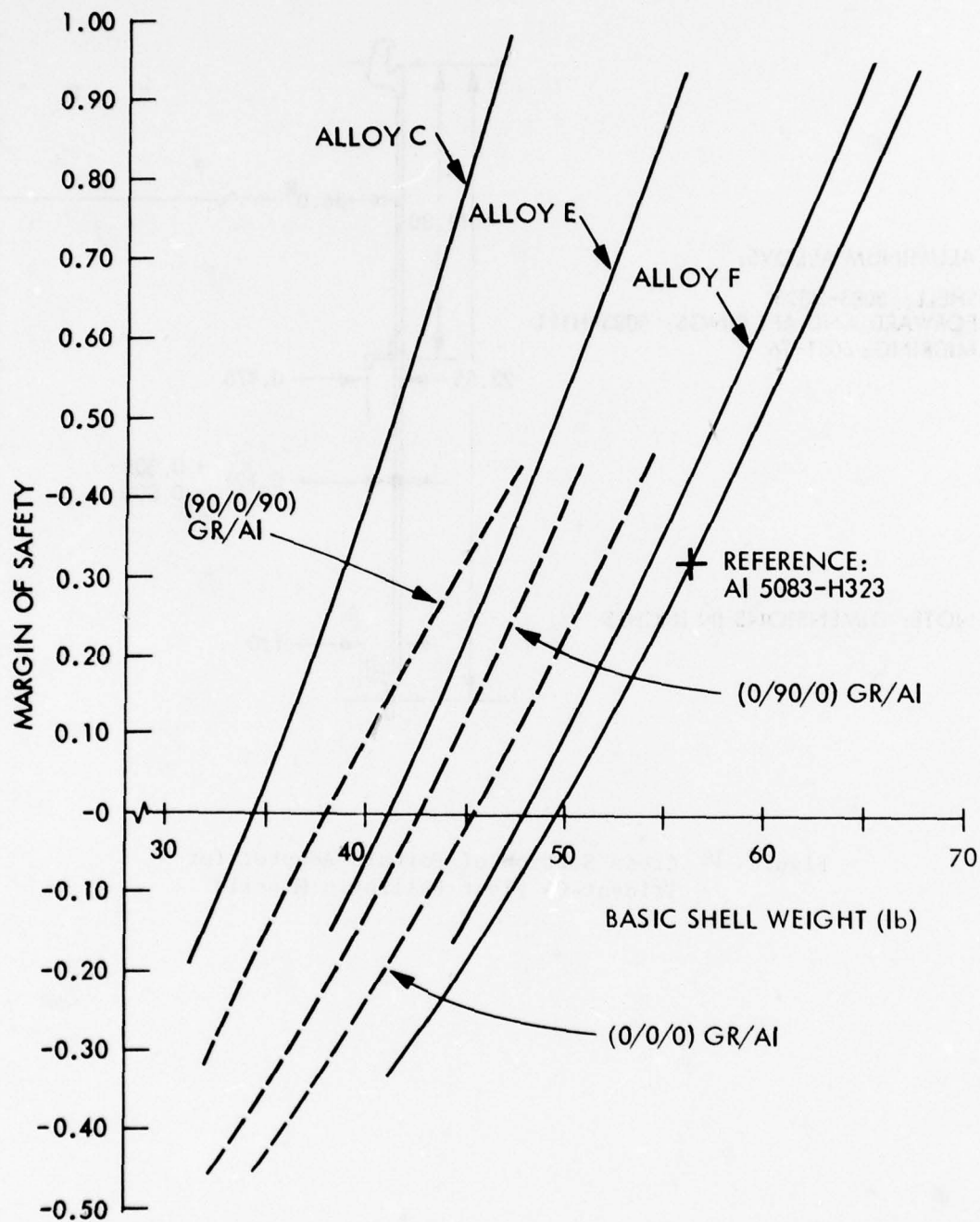
Figure 39   Forward Adapter Margin of Safety Versus Shell Weight

## TABLE 18

## DESIGN ALLOWABLES FOR GRAPHITE/ALUMINUM

| | |
|---|---|
| Name of Material: | Graphite-Reinforced Aluminum |
| Volume Percent of Reinforcement: | 30 |
| Material Density: | 2.38 g/cm$^3$ (0.086 lb/in$^3$) |
| Tensile Stress Allowable | |
|     Longitudinal: | 551 MPa (80 ksi) |
|     Transverse: | 34 MPa (5 ksi) |
| Compressive Stress Allowable | |
|     Longitudinal: | 517 MPa (75 ksi) |
|     Transverse: | 96 MPa (14 ksi) |
| Elastic Constants | |
|     Longitudinal Modulus, $E_{11}$: | 144 GPa (21 x 10$^3$ ksi) |
|     Transverse Modulus, $E_{22}$: | 31 GPa (4.5 x 10$^3$ ksi) |
|     Shear Modulus, $G_{12}$: | 23 GPa (3.4 x 10$^3$ ksi) |
|     Poisson's Ratio, $\nu_{12}$: | 0.26 |

NOTE:  Properties given are for uniaxial ply configuration
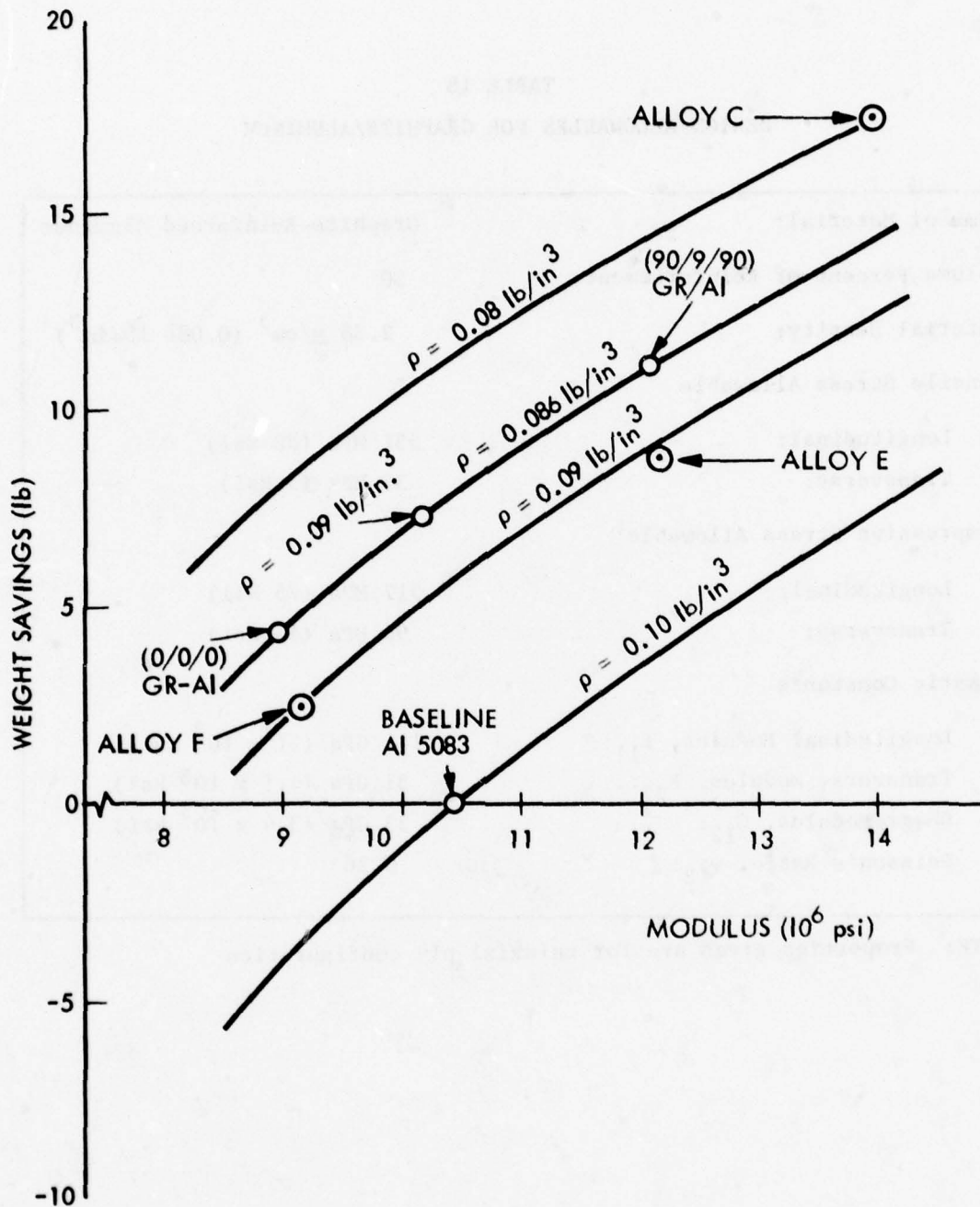
Figure 40    The Effect of Density and Modulus of Elasticity on Weight
Savings in the Forward Adapter Shell for a Margin of Safety
of 0.32

8 kg (17 lb.) is indicated, and, when compared to the graphite/aluminum composites, advanced alloys C and E are both competitive. The isotropic properties of the advanced alloys are an advantage in this particular application. The graphite/aluminum in a quasi-isotropic form has a lower specific modulus than Alloy C. From data in Figure 39, weight savings were determined for the various materials assuming a margin of safety of 0.32, the value used in the present design. Figure 40 presents these weight savings as a function of modulus of elasticity and density. Again, a favorable comparison is indicated for Alloys C and E with the various configurations of graphite aluminum composites.

4.2.3 Thrust Vector Control Brackets

The C4 Thrust Vector Control (TVC) brackets on the first and second stage motors were selected for study on the basis of substituting high strength advanced alloys. These brackets are used to support TVC hardware and are presently made of 201-T7 aluminum castings, insulated to withstand the elevated temperature environment after motor ignition. Figure 41 shows the geometry of these brackets along with the critical design loads.

The advanced alloys selected for evaluation in this application have high specific strength. They are Alloy D, Alloy F, and Alloy H. Critical loading conditions are underwater launch for the first stage bracket, and the first stage separation event for the second stage bracket. Because the brackets are insulated by an overlayer of cork and foam, the maximum temperature experienced by the aluminum is only 338 K.

The TVC brackets are strength critical (bending). Therefore, a simple ratio of the ultimate strengths was used to calculate bracket size. Density of the various alloys was then used to determine weights and potential weight savings. Table 19 is a summary showing the bracket weights and weight saved by the advanced alloys. It is assumed that the insulation weight is constant for all the alloys. Note that on each motor stage there are two brackets; thus the missile weight savings is twice the weight savings for each bracket in each stage.

99

GAS GEN

CG/CP GAS GEN.

$P_Y$ = 5170 lb (LIMIT)

AFT DOME

BRACKET

$P_Y$ 1160 lb (LIMIT)

MOTOR SKIRT

CG/CP BRACKET

(a) FIRST STAGE BRACKET
CRITICAL DESIGN CONDITION: TUBE LAUNCH

$P_S$ = 3260 lb (LIMIT)

$P_T$ = 2950 lb (LIMIT)

MOTOR RING

(b) SECOND STAGE BRACKET
CRITICAL DESIGN CONDITION:
FIRST STAGE SEPARATION,
SECOND STAGE IGNITION
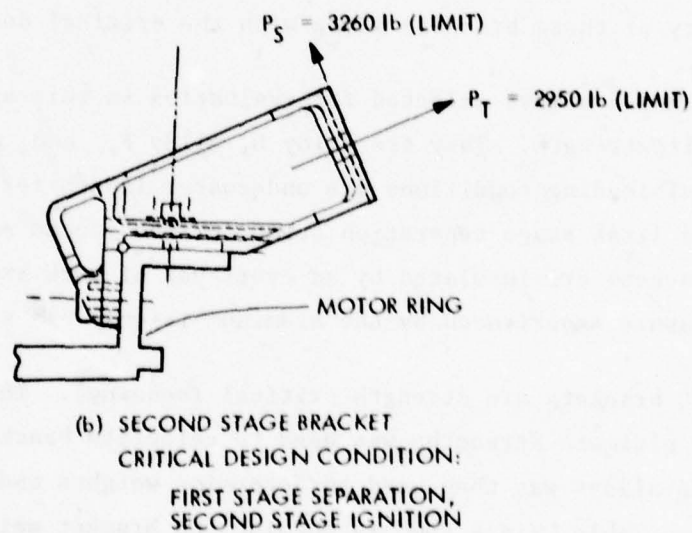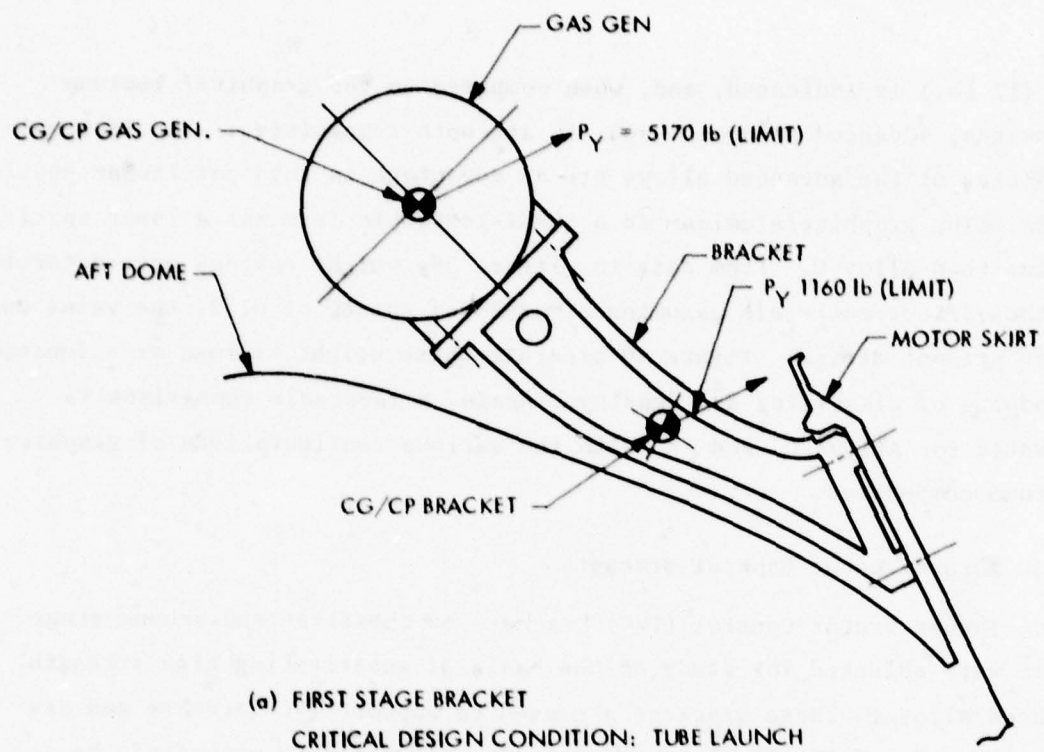
Figure 41   TRIDENT-C4 Thrust Vector Control Brackets With Critical
Design Loads Indicated

In Figure 42, the estimated weight saving per bracket is plotted against ultimate strength and density.

TABLE 19

TVC BRACKET WEIGHT SAVINGS*

| ALLOY | ULTIMATE STRENGTH MPa (ksi) | DENSITY g/cm$^3$ (lb/in$^3$) | FIRST STAGE | | SECOND STAGE | |
|---|---|---|---|---|---|---|
| | | | WEIGHT kg (lb) | WEIGHT SAVINGS kg (lb) | WEIGHT kg (lb) | WEIGHT SAVINGS kg (lb) |
| 201-T7 (BASELINE) | 386 (56) | (0.10) | 3.4 (7.6) | - | (2.15) | - |
| ADVANCED ALLOYS | | | | | | |
| D | 861 (125) | 2.214 (0.08) | 1.2 (2.7) | 2.2 (4.9) | 0.35 (0.77) | 0.63 (1.38) |
| F | 861 (125) | 2.491 (0.09) | 1.4 (3.1) | 2 (4.5) | 0.41 (0.90) | 0.57 (1.25) |
| H | 861 (125) | 2.768 (0.10) | 1.5 (3.4) | 1.9 (4.2) | 0.45 (1.00) | 0.52 (1.15) |

*   Weight and weight savings are per single bracket. Insulation weight not included and is not a variable.

On a percentage basis the sensitivity of weight savings to density is similar for both the brackets and the forward adapter shell, described previously. Both the weight savings per bracket and sensitivity to density and ultimate strength are higher for first stage brackets than for second stage brackets, as shown in Figure 42. With respect to effect on missile range or payload, it should be noted that weight saved in the second stage motor is five times more effective than weight saved in the first stage motor, Figure 37. Thus, substitution of advanced alloys for the 201-T7 aluminum castings in the second stage motor TVC brackets would contribute more to missile range or
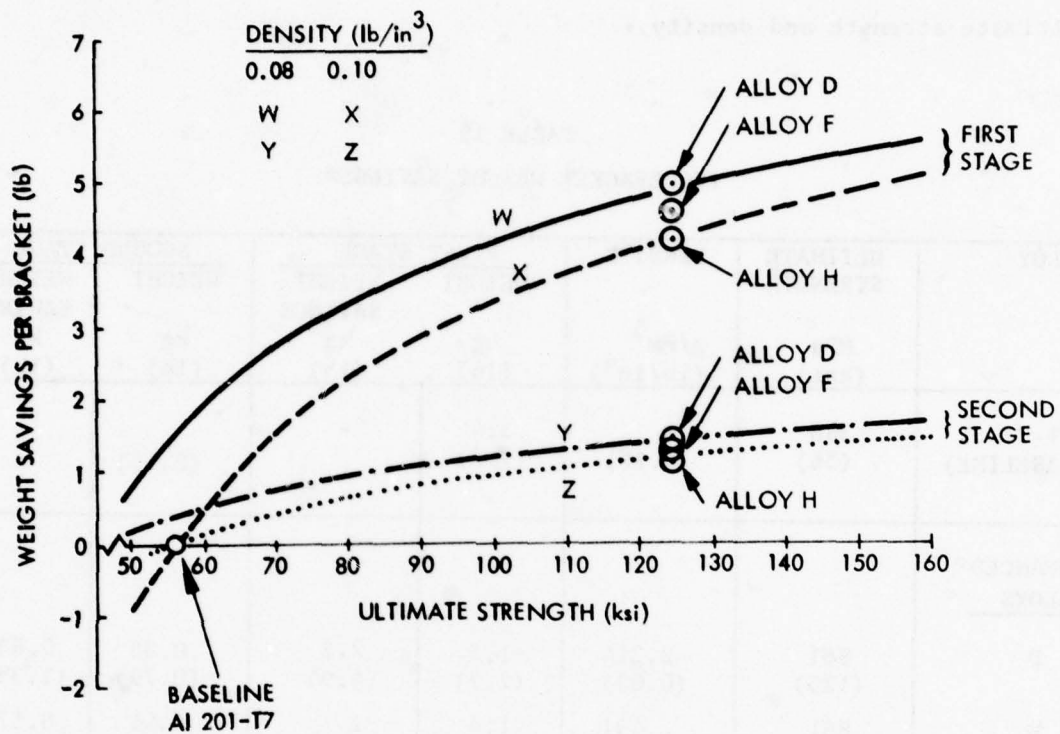
Figure 42   The Effect of Ultimate Strength and Density
on Weight Savings in the TVC Brackets

102

payload than substitution in first stage brackets. Because the brackets are relatively low in total weight, the contribution to missile performance by advanced alloy substitution is limited.

A potential cost limitation in substituting an advanced aluminum alloy for the 201-T7 alloy castings is that the former can not be cast. One approach for low fabrication cost in applying the advanced alloys is to use the HIP (Hot Isostatic Press) process to consolidate the rapidly solidified alloy powders to a near net size part. HIP processing of the 201-T7 bracket castings is now being used to improve their tensile ductility and should be applicable to processing of the advanced alloy powders as well.

## 4.2.4 Conclusions

For both the predominantly stiffness-critical forward adapter shell and strength-critical TVC brackets, successful development of the advanced alloys considered would result in weight savings. In the case of the forward adapter shell, application of Alloy C having 34 percent higher compressive modulus and 16 percent lower density than 5083-H323 sheet presently used would result in a 7.7 kg (17 lb.) weight savings. A higher strength alloy in this case would not result in any weight savings, as the shell is stiffness critical. In the case of the TVC brackets, application of Alloy D having 123 percent higher strength and 20 percent lower density than the 201-T7 castings presently used would result in a 4.4 kg (9.8 lb.) weight savings in the first stage and 1.25 kg (2.76 lb.) weight savings in the second stage. Weight saved in the forward adapter and second stage motor TVC brackets is five times more significant in missile range or payload improvement than in the first stage motor TVC brackets. Because some question exists in economically forming TVC brackets from advanced alloy powders that could compete with the relatively low cost near size casting of the 201 alloy brackets, it is recommended that selection of property goals for advanced alloy development focus on the forward adaptor requirements.

103

Successful development of an improved stiffness alloy such as Alloy C in the form of a rolled ring forging or sheet would provide a weight savings of 7.7 kg(17 lb). However, over a relatively short (three year) period, it is more likely that an advanced alloy would be successfully developed that has an intermediate stiffness improvement. An example is Alloy E, which has a 25 percent higher specific stiffness (compressive modulus-to-density ratio) than the presently used 5086 alloy. Successful application of this alloy would save 3.6 kg (8 lb.) in the forward adapter shell alone, and with additional savings possible by application to the forward adapter rings as well.

## 4.3 Aircraft Structures

Three different aircraft structures were selected for evaluation of weight savings and related performance improvements obtained by application of advanced aluminum alloys. The structures studied were (1) subsonic reconnaissance V/STOL aircraft, (2) supersonic fighter/interceptor V/STOL aircraft, and (3) wide-bodied transport. All three aircraft include stiffness-critical, strength-critical, and fatigue or crack growth rate critical components. Thus, it is appropriate to consider the application of advanced alloys that are higher in strength or stiffness or fatigue resistance than the best commercially available alloys for each aircraft. Because such improved properties are likely to be developed in different alloys rather than all in one, then weight savings may be obtained by selective substitution of advanced alloys each having different properties for different parts of the structure.

The application of advanced alloys exhibiting significantly higher selected properties is intended for new aircraft to be designed in the next decade. Because these aircraft have not yet been designed, except for general size and service requirements, the trade-off studies described herein are

based on two aircraft currently in service. The S-3A Navy carrier-based, anti-submarine patrol aircraft was selected as a structural analog for the future subsonic V/STOL and supersonic V/STOL aircraft; the L-1011 commercial wide-body transport was selected as a structural analog for a future long-range military cargo/transport. This approach is intended to provide a more accurate determination of weight savings/performance improvement from application of advanced alloys than would be obtained from parametric analyses of preliminary designs. Detailed weight and stress analyses as well as extensive in-flight experience are available for all components in the S-3A and L-1011 aircraft.

Analyses of critical and near critical design conditions and failure modes were determined for all structural elements in the two aircraft. Weight savings were then calculated by substituting various advanced alloys for the present aluminum alloys. Substitution was performed by applying improved stiffness alloy properties in stiffness-critical components, improved strength alloy properties in strength-critical components, and so on. In some instances substitution of a particular property set results in shifting from one critical failure mode to another, in which case the limiting condition satisfying structural design requirements and providing the optimum weight reduction was selected.

## 4.3.1 Assumed Properties

Advanced alloys exhibiting two levels of improvement in selected properties were considered. The first level selected is based on a reasonable probability of being developed in a three-year period for scale-up and ready for new systems applications in five to seven years. The second level selected is based on a probability of being developed in five to seven years and ready for application in nine to twelve years. The second level of improvement is twice the first level improvement. The properties and improvement amounts selected for the two levels are as follows.

## Level I

| | |
|---|---|
| Modulus of Elasticity | +20% |
| Strength | +20% |
| Fatigue and da/dN | +20% |
| Density | -10% |

## Level II

| | |
|---|---|
| Modulus of Elasticity | +40% |
| Strength | +40% |
| Fatigue and da/dN | +40% |
| Density | -20% |

It is also assumed that in each instance the properties other than that selected for improvement are not compromised from the presently used alloys. This includes corrosion resistance, machinability, fabricability, etc.

### 4.3.2 V/STOL Aircraft

As described above, weight savings were first determined by substituting alloys assumed to have improved properties for present aluminum structure in the S-3A airplane, then these weight savings were scaled to the two specific V/STOL aircraft configurations, subsonic reconnaissance and supersonic fighter/interceptor, for determination of performance changes. An artist's rendition of one version of the subsonic V/STOL is shown in Figure 43.

Table 20 shows the S-3A weight savings in wing, fuselage, and empennage aluminum structure for levels one and two improvement in strength, modulus of elasticity, and fatigue, but no change in density or other properties. Table 21 shows the percentage by weight of each major structural element that would benefit in strength, stiffness, or fatigue improvement. These percentages represent the portions of existing structure replaced by advanced alloys having selected property improvements. For example, from Table 21, it is seen that 100 percent of the wing spars are strength critical, 38 percent are also stiffness critical, and none are fatigue critical. The weight savings
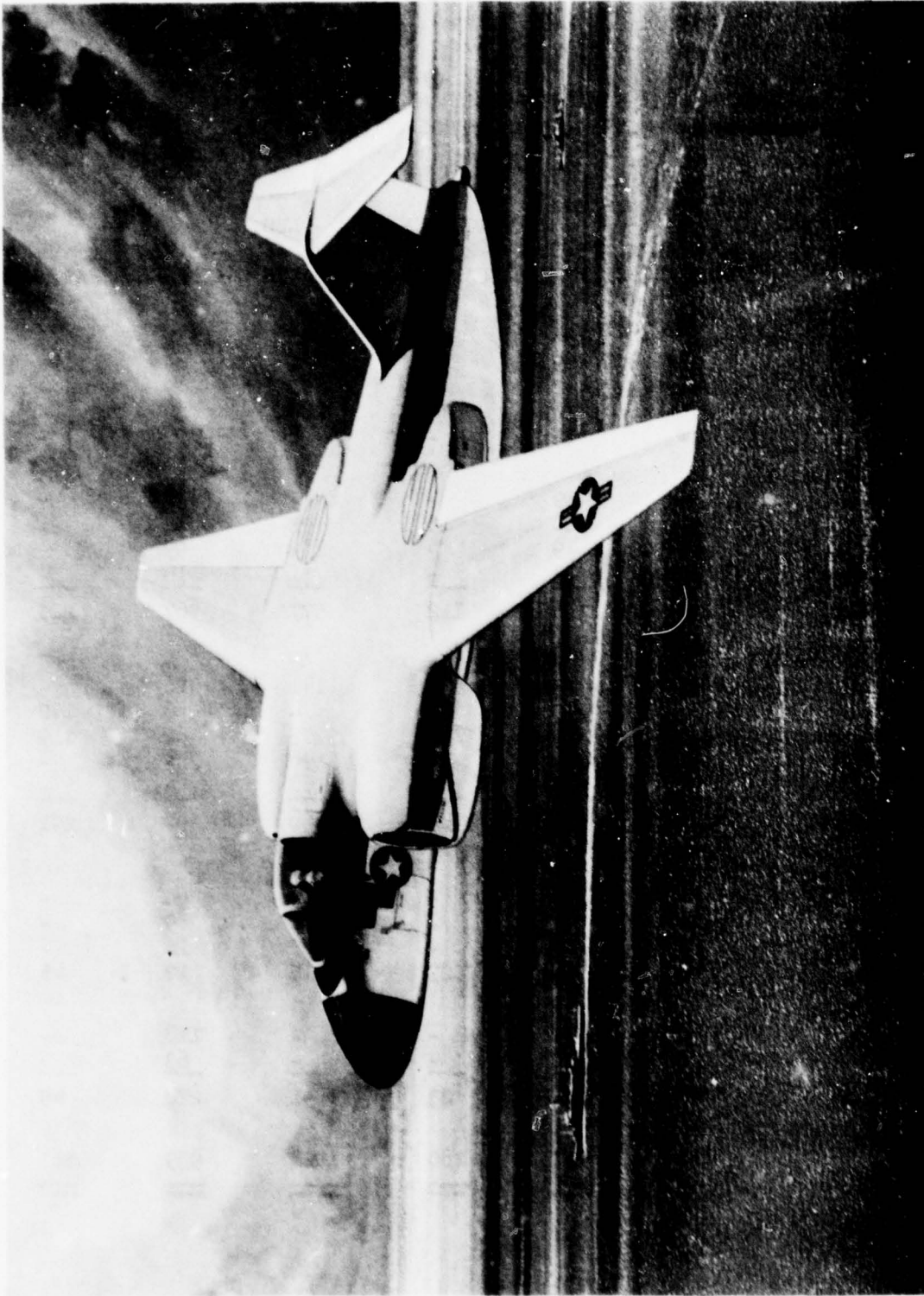
Figure 43  One Version of the Subsonic V/STOL Airplane, Artists' Rendition

## TABLE 20

### S-3A AIRCRAFT WEIGHT SAVINGS RESULTING FROM INDIVIDUAL
### PROPERTY IMPROVEMENTS (NO IMPROVEMENT IN DENSITY)

| | STRUCTURAL ELEMENTS | WEIGHT SAVINGS - LBS. | | | | | |
| --- | --- | --- | --- | --- | --- | --- | --- |
| | | ADV. ALUM.-LEVEL I (-20%) | | | ADV. ALUM.-LEVEL II (+40%) | | |
| | | STRENGTH | STIFFNESS | FATIGUE | STRENGTH | STIFFNESS | FATIGUE |
| WING | Primary Structure | | | | | | |
| | Upper Surface | 18 | 138 | - | 37 | 287 | - |
| | Lower Surface | 23 | 69 | 97 | 31 | 84 | 194 |
| | Spars | 46 | 7 | - | 91 | 9 | - |
| | Ribs | 145 | - | - | 286 | - | - |
| | L.E. | 4 | 11 | - | 8 | 22 | - |
| | Control Surfaces | | | | | | |
| | Aileron | - | 19 | - | - | 38 | - |
| | T.E. Flaps | 47 | 10 | 15 | 93 | 12 | 31 |
| | L.E. Slats | - | 49 | - | - | 99 | - |
| | Spoilers | 16 | 13 | - | 31 | 16 | - |
| | Subtotal - Wing | 299 | 316 | 112 | 577 | 567 | 225 |
| FUSELAGE | Primary Structure | | | | | | |
| | Cover | 71 | 13 | - | 141 | 26 | - |
| | Longerons | - | 3 | 86 | - | 6 | 172 |
| | Blhd. & Frames | 179 | 31 | 59 | 353 | 62 | 119 |
| | Floor & Deck | 99 | - | - | 198 | - | - |
| | Keelson | 84 | - | - | 168 | - | - |
| | Subtotal - Fus. | 433 | 47 | 145 | 860 | 94 | 291 |
| EMPENNAGE | Primary Structure | | | | | | |
| | Surface | - | 33 | - | - | 60 | - |
| | Spars | 26 | 7 | - | 51 | 9 | - |
| | Ribs | 13 | 8 | - | 25 | 16 | - |
| | L.E. & T.E. | 8 | 6 | 23 | 15 | 12 | 45 |
| | Control Surfaces | | | | | | |
| | Elevator | - | 59 | - | - | 118 | - |
| | Rudder | - | 31 | - | - | 63 | - |
| | Subtotal - Emp. | 47 | 144 | 23 | 91 | 278 | 45 |
| | Total | 779 | 507 | 280 | 1528 | 939 | 561 |

108

## TABLE 21

### PROPORTION OF S-3A AIRCRAFT COMPONENT WEIGHT CHANGED
### BECAUSE OF SPECIFIC PROPERTY IMPROVEMENT

| | % STRUCTURE CHANGED | | |
| STRUCTURAL ELEMENT | STRENGTH | STIFFNESS | FATIGUE |
| --- | --- | --- | --- |
| **Wing** | | | |
| Primary Structure | | | |
| Upper Surface | 100 | 100 | - |
| Lower Surface | 100 | 100 | 100 |
| Spars | 100 | 38 | - |
| Ribs | 100 | - | -- |
| L.E. | 100 | 100 | - |
| Control Surfaces | | | |
| Aileron | - | 100 | - |
| T.E. Flaps | 62 | 23 | 17 |
| L.E. Flaps | - | 100 | - |
| Spoilers | 100 | 100 | - |
| **Fuselage** | | | |
| Primary Structure | | | |
| Covering | 98 | 18 | - |
| Longerons | - | 3 | 97 |
| Blhd. Frames | 72 | 10 | 18 |
| Flooring & Decks | 100 | - | - |
| Keelson | 100 | - | - |
| **Empennage** | | | |
| Primary Structure | | | |
| Surfaces | - | 100 | - |
| Spars | 100 | 49 | - |
| Ribs & Fittings | 100 | 86 | - |
| Fixed L.E. & T.E. | 32 | 13 | 51 |
| Control Surfaces | | | |
| Elevator | - | 100 | - |
| Rudder | - | 100 | - |

109

listed for the wing spars, Table 20, are the result of replacing 100 percent of existing alloys with improved strength alloys, or replacing 38 percent of existing alloys with improved modulus alloys, and not replacing any of the structure with improved fatigue strength alloys.

Table 22 presents weight savings for the S-3A aircraft obtained by substituting higher strength or higher fatigue properties but not changing density. For the weight savings obtained by substituting a higher modulus alloy, a change to lower density was also assumed. These latter weight savings were obtained by substituting the higher modulus/lower density alloys for stiffness-critical components and then a lower density alloy was substituted for the balance. For the weight savings in this table attributed to improved strength or fatigue properties, portions of the components not strength critical or fatigue critical, respectively, were changed to a lower density alloy. For example, a structure that is 72 percent by weight strength critical has this portion replaced by a higher strength alloy, and the balance replaced by a lower density alloy in which other properties are unchanged.

In Table 22, weights listed under "Optimum Alloy Selection" are the highest weight savings for each component obtained by alloy substitution. Under the strength, stiffness and density, and fatigue columns, the maximum weight savings are underlined.

The above weight savings data were then transposed to the two V/STOL aircraft configurations and the resulting improvements on aircraft weight, size, and performance were calculated by a proprietary systems analysis program termed ASSET (Advanced System Synthesis and Evaluation Technique). This is an iterative computerized program which is used for aircraft systems analysis and trade-off studies. A schematic of the ASSET synthesis cycle is shown in Figure 44 along with the decision-making flow diagram in Figure 45. ASSET integrates input data describing aircraft geometry, aerodynamics, propulsion, materials and properties, for particular structures, and weights of certain components to obtain optimum aircraft weight, size, and fuel to satisfy previously defined mission and payload requirements. Design options

110

# TABLE 22

## S-3A WEIGHT SAVINGS FOR OPTIMUM COMBINATION OF HIGH STRENGTH, HIGH FATIGUE, AND HIGH MODULUS/LOW DENSITY ALLOYS

| | WEIGHT SAVINGS - LBS. | | | | | | | |
| | ADV. ALUM. - LEVEL I (+20%) | | | | ADV. ALUM. - LEVEL II (+40%) | | | |
| STRUCTURAL ELEMENTS | STRENGTH (1) | STIFFNESS & DENSITY (2) | FATIGUE (3) | OPTIMUM ALLOY SELECTION | STRENGTH (1) | STIFFNESS & DENSITY (2) | FATIGUE (3) | OPTIMUM ALLOY SELECTION |
|---|---|---|---|---|---|---|---|---|
| **WING** | | | | | | | | |
| Primary Structure | | | | | | | | |
| Upper Surf. | 18 | 203 | 79 | 203 | 37 | 388 | 158 | 388 |
| Lower Surf. | 23 | 141 | 97 | 141 | 31 | 225 | 194 | 225 |
| Spar | 46 | 54 | 47 | 54 | 91 | 102 | 94 | 102 |
| Rib | 145 | 94 | 94 | 145 | 286 | 188 | 188 | 286 |
| L.E. | 4 | 19 | 9 | 19 | 8 | 36 | 19 | 36 |
| Control Surfaces | | | | | | | | |
| Aileron | 10 | 27 | 10 | 27 | 19 | 50 | 19 | 50 |
| T.E. Flap | 64 | 54 | 52 | 64 | 127 | 100 | 105 | 127 |
| L.E. Slats | 25 | 69 | 25 | 69 | 49 | 129 | 49 | 129 |
| Spoiler | 16 | 26 | 14 | 26 | 31 | 42 | 29 | 42 |
| Subtotal - Wing | 351 | 687 | 427 | 748 | 679 | 1260 | 855 | 1385 |
| **FUSELAGE** | | | | | | | | |
| Primary Structure | | | | | | | | |
| Covering | 72 | 48 | 36 | 72 | 143 | 93 | 72 | 143 |
| Long | 45 | 47 | 87 | 87 | 89 | 94 | 175 | 175 |
| Blhd. & Frames | 224 | 189 | 190 | 224 | 444 | 372 | 382 | 444 |
| Floor & Deck | 99 | 49 | 49 | 99 | 198 | 99 | 99 | 198 |
| Keelson | 84 | 42 | 42 | 84 | 168 | 84 | 84 | 168 |
| Subtotal - Fuselage | 924 | 375 | 404 | 566 | 1042 | 742 | 812 | 1128 |
| **TAIL** | | | | | | | | |
| Primary Structure | | | | | | | | |
| Surf. | 24 | 54 | 24 | 54 | 48 | 96 | 48 | 96 |
| Spar | 26 | 23 | 17 | 26 | 51 | 41 | 33 | 51 |
| Ribs | 13 | 18 | 10 | 18 | 25 | 34 | 21 | 34 |
| L.E. & T.E. | 23 | 27 | 34 | 34 | 45 | 54 | 66 | 66 |
| Control Surfaces | | | | | | | | |
| Elev. | 29 | 83 | 29 | 83 | 59 | 153 | 59 | 153 |
| Rud. | 16 | 44 | 16 | 44 | 31 | 82 | 31 | 82 |
| Subtotal - Tail | 131 | 249 | 130 | 259 | 259 | 460 | 258 | 482 |
| **Total** | 1006 | 1311 | 961 | 1573 | 1980 | 2462 | 1925 | 2995 |

NOTES:

(1)   The structure is assumed to be made from a high strength material where it is strength critical and a low density material with equivalent properties for the remaining structure.

(2)   The structure is assumed to be made completely from a high stiffness, low density alloy. Thus both weight savings from higher modulus and lower density are included.

(3)   The structure is assumed to be made from a high fatigue strength material where it is fatigue critical and a low density material with equivalent properties for the remaining structure.
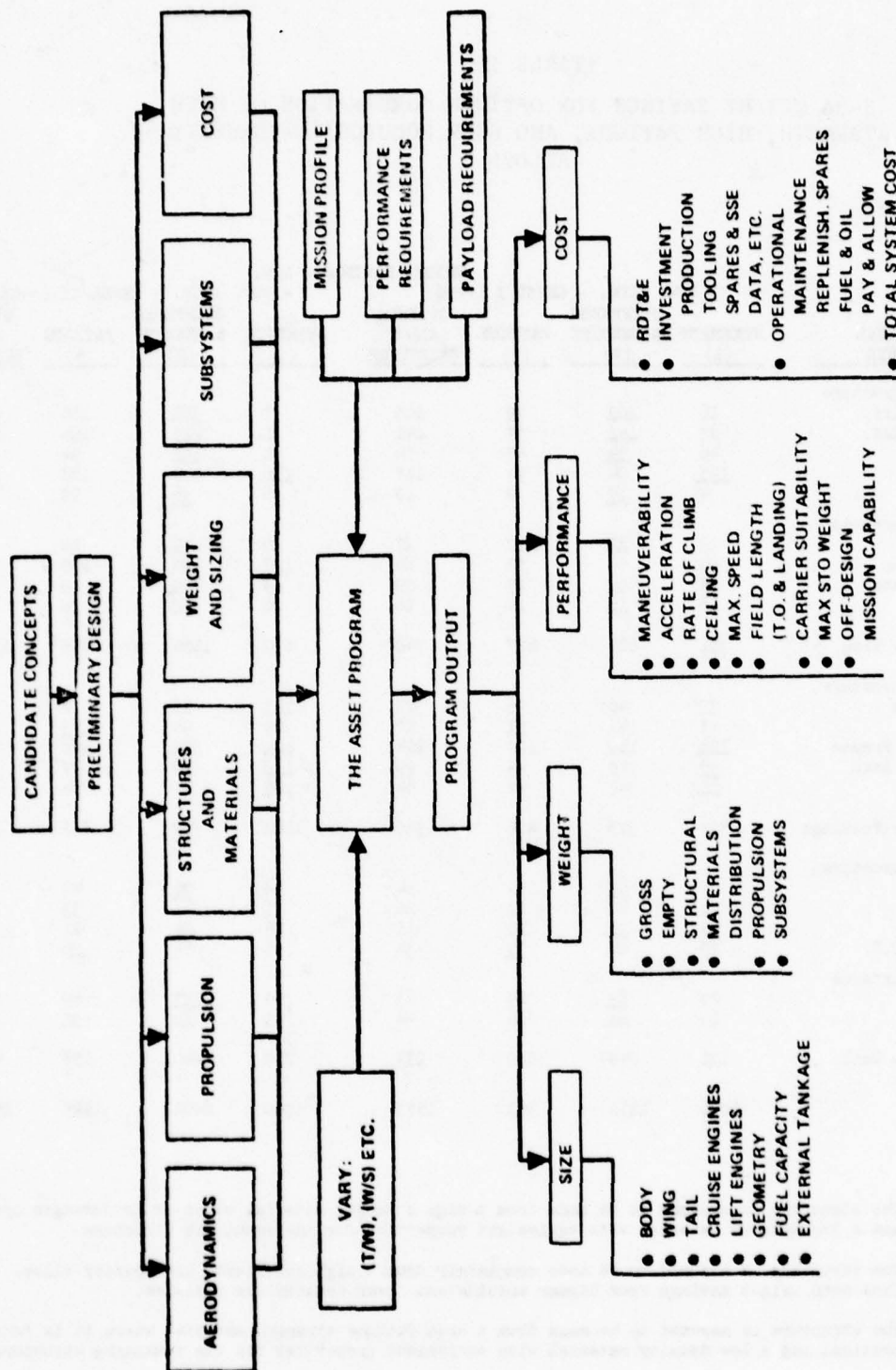
Figure 44  ASSET Program Synthesis Cycle

112
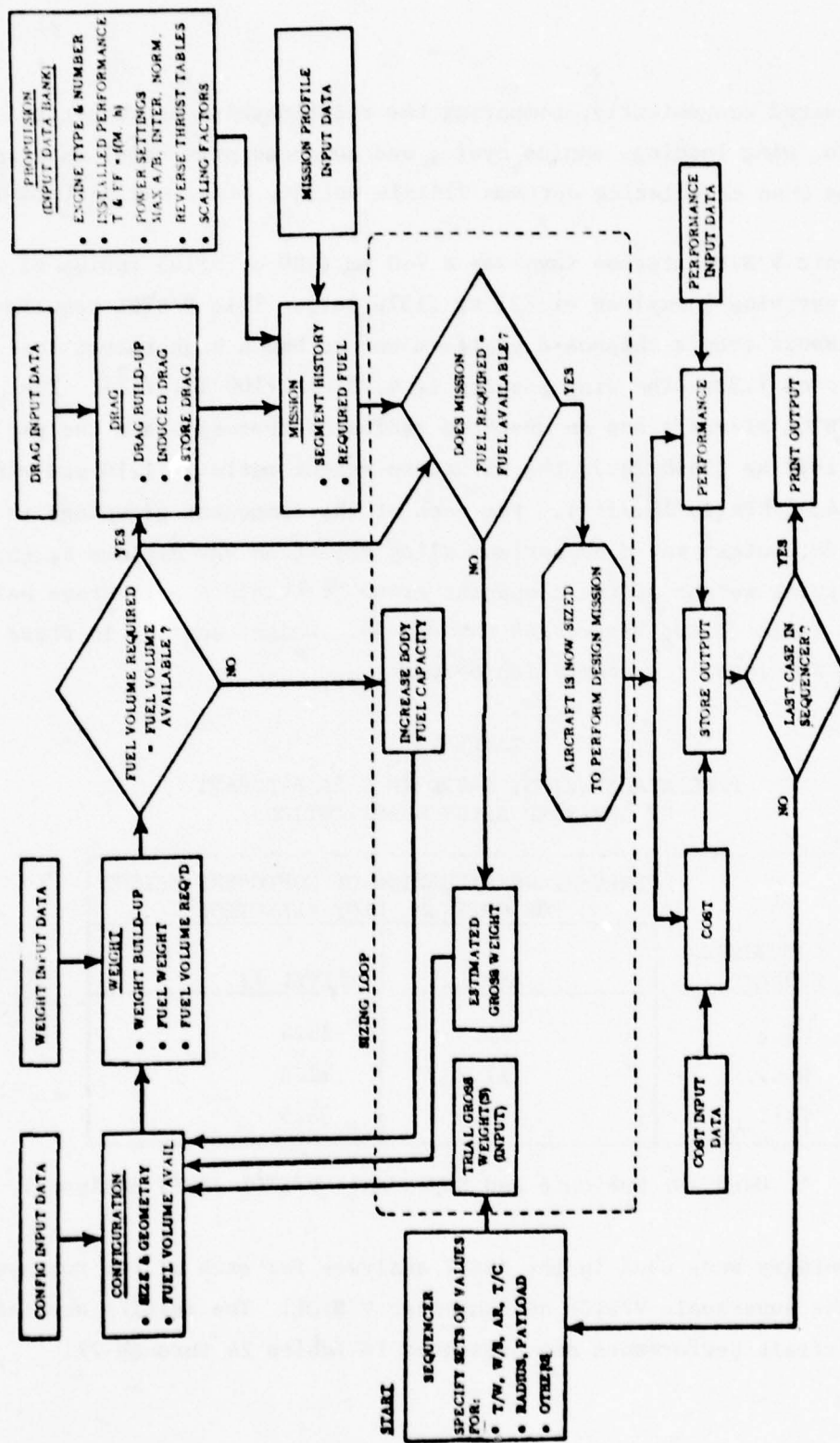
Figure 45  ASSET Program Schematic

113

can be evaluated conveniently, comparing the relationships of thrust-to-weight ratio, wing loading, engine cycle, and advanced structural material applications then calculating optimum vehicle weight, size, and performance.

The supersonic V/STOL mission involves a 740 km (400 n. mile) radius of operation, carrying a payload of 621 kg (1370 lb.). This V/STOL requires vertical takeoff from a shipboard platform and so has a high thrust-to-weight ratio of 1.33. The wing loading is 4.79 kPa (100 lb./ft$^2$). The subsonic V/STOL aircraft has an unstated radius of operation and the payload is larger, 1618 kg (3568 lb.); the thrust-to-weight ratio is 1.10 and wing loading is 4.31 kPa (90 lb./ft$^2$). For each of the component groupings in the S-3A aircraft, weight saved by optimum alloy selection was divided by the total structural weight of the component group to obtain a percentage weight saving, see Table 23 and Figures 46 through 50. Weight savings in these figures are for level I property improvement.

TABLE 23

PERCENTAGE WEIGHT SAVED IN S-3A AIRCRAFT
BY ADVANCED ALLOY SUBSTITUTION

| COMPONENT GROUP | PERCENTAGE REDUCTION OF COMPONENT WEIGHT FOR OPTIMUM ALLOY SELECTION* | |
|---|---|---|
| | LEVEL I | LEVEL II |
| Wing | 15.3 | 28.4 |
| Body | 11.2 | 22.3 |
| Tail | 19.6 | 36.5 |

* Used for Subsonic and Supersonic V/STOL ASSET Analyses.

These percentages were used in the ASSET analyses for each of the two new aircraft, the supersonic V/STOL and subsonic V/STOL. The results obtained in terms of aircraft performance are presented in Tables 24 through 27.

114
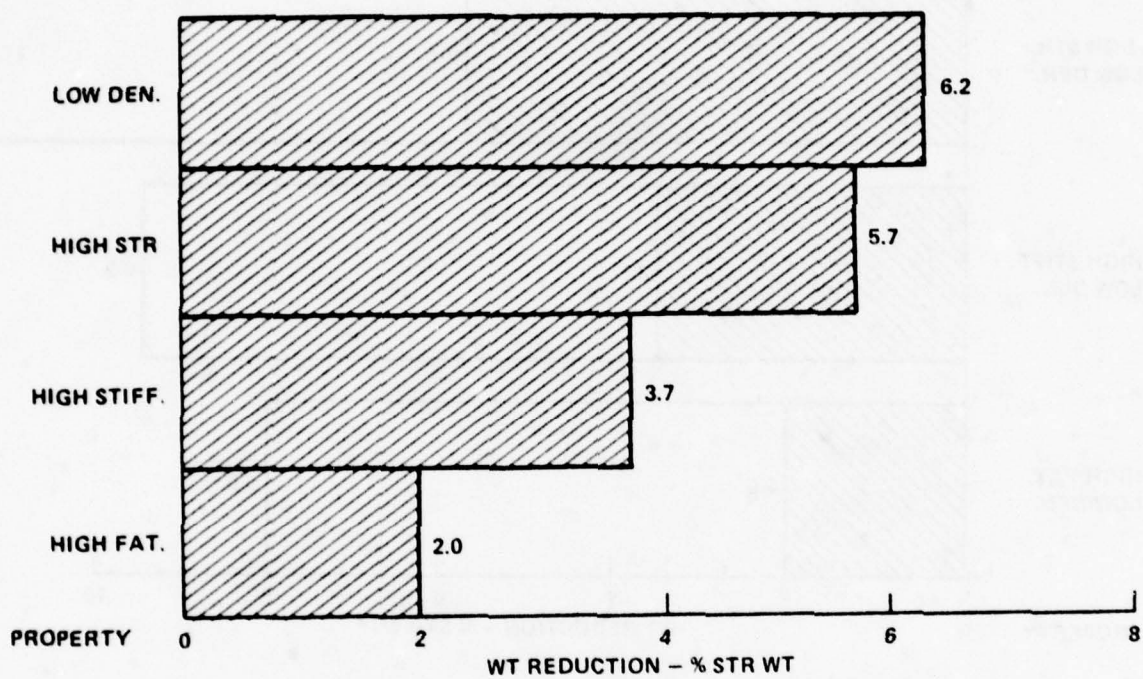
Figure 46    Weight Reduction Comparison in S-3A Aircraft
Resulting From Individual Property Improvement
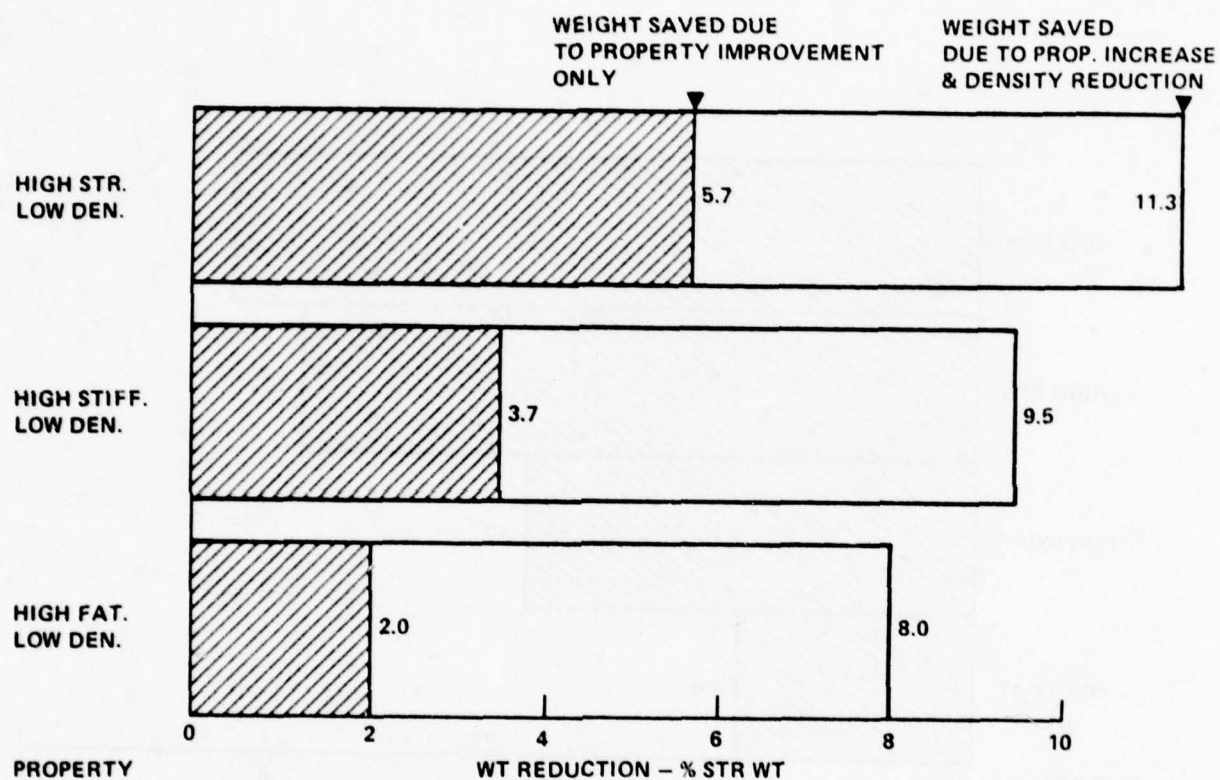
Figure 47    Weight Reduction Comparisons in S-3A Aircraft
Resulting From Individual Property Improvement
Combined With Reduction in Density

WT REDUCTION BY ALLOY

DISTRIBUTION OF WEIGHT
REDUCTION BY PROPERTY
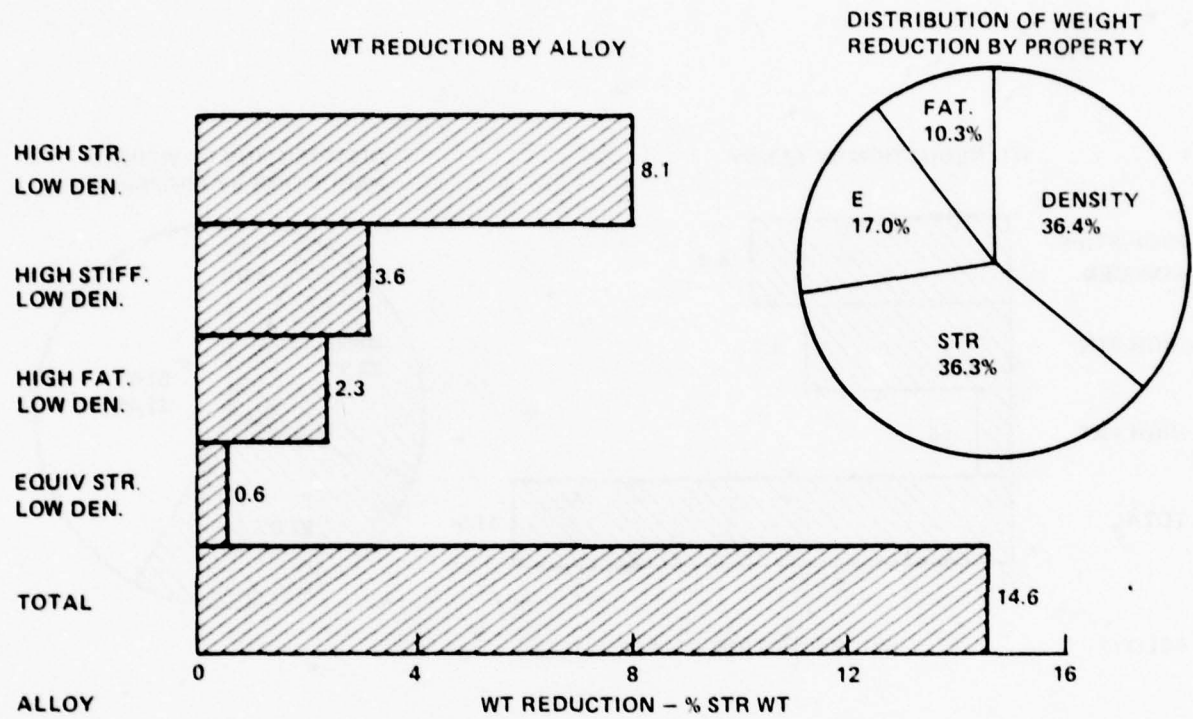


Figure 48  S-3A Aircraft Weight Reduction and Distribution
for Optimum Combination of Four Low Density
Advanced Aluminum Alloys - High Strength, High
Fatigue Resistance, High Modulus, and Equivalent
Strength

117

WT. REDUCTION BY ALLOY

DISTRIBUTION OF WEIGHT
REDUCTION BY PROPERTY

HIGH STIFF.
LOW DEN.        5.9

HIGH STR.        4.7

HIGH FAT.     0.8

TOTAL                          11.5

0        4        8        12

ALLOY        WT. REDUCTION — % STR  WT

FAT.
6.9%

DENSITY
23.9%

STR
41.4%

E
27.8%
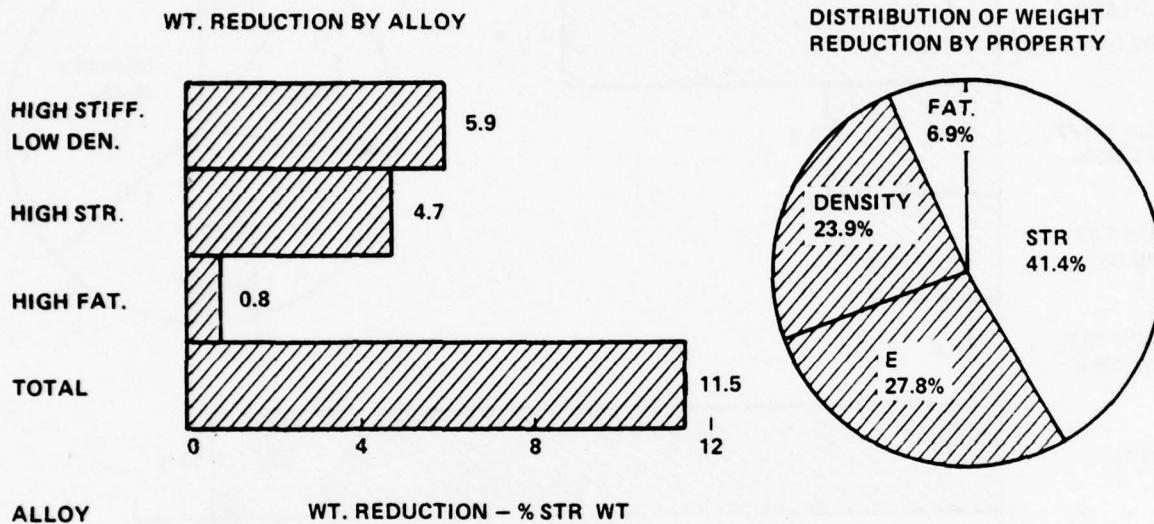
Figure 49   S-3A Aircraft Weight Reduction and Distribution
for Optimum Combination of Three Advanced
Aluminum Alloys - High Strength, High Modulus/
Low Density, and High Fatigue Resistance

118

| ALLOY DEVELOPMENT | | WEIGHT REDUCTION – % STRUCTURE WEIGHT |
|---|---|---|
| **NUMBER OF ALLOYS** | **TYPE OF ALLOY** | |
| BEST OF THREE | STR./DEN. STIFF./DEN. FAT./DEN. | 14.6 |
| BEST OF THREE | STR. STIFF./DEN FAT. | 11.4 |
| BEST OF THREE | STR. STIFF. FAT. | 9.3 |
| ONE | STR./DEN | 11.3 |
| | STIFF./DEN. | 9.5 |
| | FAT./DEN | 8.0 |
| ONE | DEN. | 6.2 |
| | STR. | 5.7 |
| | STIFF. | 3.7 |
| | FAT. | 2.0 |
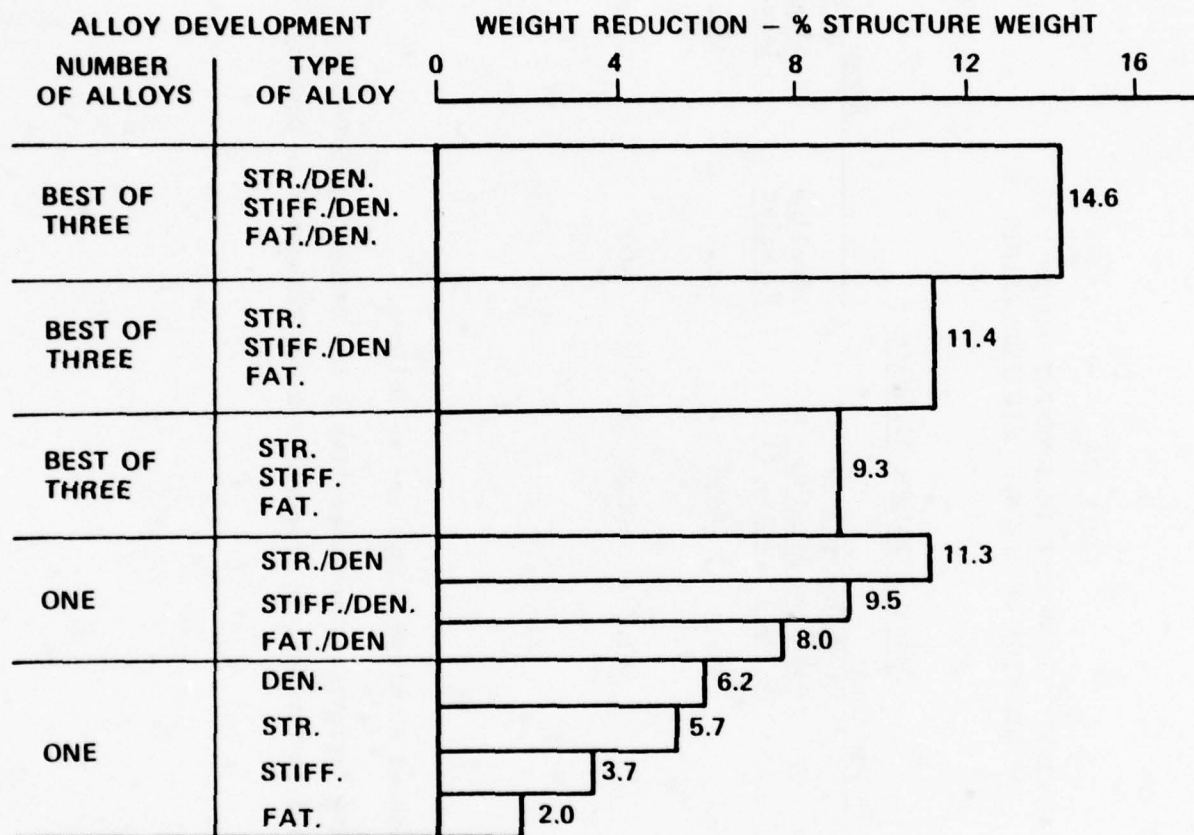
Figure 50 Optimum Payoff Comparisons for S-3A Aircraft in
Terms of Percent Weight Saved by Selected
Combinations of Advanced Aluminum Alloys

119

TABLE 24

V/STOL AIRCRAFT PERFORMANCE IMPROVEMENT OBTAINED BY
APPLICATION OF ADVANCED ALUMINUM ALLOYS

| | Pay Load | | | Range | | |
|---|---|---|---|---|---|---|
| | Constant Weight Aircraft | | | | | |
| | | % Change Due to Advanced Aluminum | | | % Change Due to Advanced Aluminum | |
| Aircraft | Baseline Pounds | Level I | Level II | Baseline N. Miles | Level I | Level II |
| Subsonic V/STOL | 3,568 | +35.2 | +66.8 | -- | -- | -- |
| Supersonic V/STOL | 1,370 | +47.7 | +90.9 | 400 | +24.7 | +48.0 |

NOTE: Improvements in Advanced Aluminum Alloys are as follows:

Level I - 20% Improvement in Properties & 10% Reduction in Density

Level II - 40% Improvement in Properties & 20% Reduction in Density

120

## TABLE 25

### EFFECT OF ADVANCED ALUMINUM ALLOYS ON WEIGHT, WING SPAN AND FUEL CONSUMPTION OF V/STOL AIRCRAFT

Constant Mission

| Aircraft | Gross Weight (GTOW) | | | Wing Span | | | Fuel Consumption per Flight | | |
|---|---|---|---|---|---|---|---|---|---|
| | Baseline Pounds | % Reduction Due to Adv. Alum. Level I | Level II | Baseline Feet | % Reduction Due to Adv. Alum. Level I | Level II | Baseline Pounds | % Reduction Due to Adv. Alum. Level I | Level II |
| Subsonic V/STOL | 47,530 | 8.4 | 14.8 | 61.66 | 4.2 | 10.1 | 11,372 | 8.1 | 14.4 |
| Supersonic V/STOL | 23,975 | 7.6 | 13.6 | 26.8 | 3.9 | 7.1 | 6,698 | 7.0 | 12.3 |

NOTE: Improvements in Advanced Aluminum Alloys are as follows:

Level I  - 20% Improvement in Properties & 10% Reduction in Density

Level II - 40% Improvement in Properties & 20% Reduction in Density

121

## TABLE 26

### WEIGHT SAVINGS FROM APPLICATION OF ADVANCED ALUMINUM ALLOYS TO V/STOL "A" SUBSONIC AIRCRAFT

| SECTION | BASE A/C CONVENTIONAL METHOD wt.# | ADVANCED ALUMINUM - LEVEL I | | | ADVANCED ALUMINUM - LEVEL II | | |
|---|---|---|---|---|---|---|---|
| | | INPUT % RED. | OUTPUT Wt.# | RED. | INPUT % RED. | OUTPUT Wt.# | % RED. |
| Wing | 4409 | 15.3 | 3403 | 22.8 | 28.4 | 2664 | 39.6 |
| Tail | 871 | 19.6 | 610 | 30.0 | 36.5 | 431 | 50.5 |
| Body | 3645 | 11.2 | 3175 | 12.9 | 22.3 | 2733 | 25.0 |
| Gear | 2652 | | 2559 | 3.5 | | 2483 | 6.4 |
| Engine Section | 2787 | | 2508 | 10.0 | | 2296 | 17.6 |
| TOTAL STR. | 14364 | (2)8.7 | 12255 | 14.7 | (2)16.6 | 10607 | 26.2 |
| Propulsion | 9492 | | 8609 | 9.3 | | 7939 | 16.4 |
| Sys. & Furn. | 7745 | | 7717 | .4 | | 7695 | .7 |
| MEW. | 31602 | | 28582 | 9.6 | | 26242 | 17.0 |
| Std.&Oper. Items | 987 | | 962 | 2.5 | | 941 | 4.7 |
| OEW | 32584 | | 29544 | 9.3 | | 27183 | 16.6 |
| Payload | 3568 | | 3568 | | | 3568 | |
| Fuel | 11372 | | 10454 | 8.1 | | 9739 | 14.4 |
| GTOW | 47530 | | 43565 | 8.3 | | 40490 | 14.8 |

NOTES: (1) Advanced Aluminum Alloys Consist of Two Levels of Improvement
Level I: 20% Improvement in Properties & 10% Reduction in Density
Level II: 40% Improvement in Properties & 20% Reduction in Density

(2) Not a Computer Input.

122

## TABLE 27

### WEIGHT SAVINGS FROM APPLICATION OF ADVANCED ALUMINUM ALLOYS TO V/STOL "B" SUPERSONIC AIRCRAFT

| SECTION | BASE A/C CONVENTIONAL METHOD wt.% | ADVANCED ALUMINUM - LEVEL I | | | ADVANCED ALUMINUM - LEVEL II | | |
|---|---|---|---|---|---|---|---|
| | | INPUT % RED. | OUTPUT Wt.# | RED. | INPUT % RED. | OUTPUT Wt.# | % RED. |
| Wing | 2099 | 15.3 | 1620 | 22.8 | 28.4 | 1270 | 39.5 |
| Tail | 411 | 19.6 | 290 | 29.4 | 36.5 | 205 | 50.1 |
| Body | 2243 | 11.2 | 1953 | 12.9 | 22.3 | 1690 | 24.7 |
| Gear | 1324 | | 1255 | 5.2 | | 1201 | 9.3 |
| Engine Section | 743 | | 687 | 7.5 | | 643 | 13.5 |
| TOTAL STR. | 6820 | (2)9.6 | 5805 | 14.7 | (2)18.3 | 5010 | 26.5 |
| Propulsion | 4263 | | 3974 | 6.8 | | 3750 | 12.0 |
| Sys. & Furn. | 3483 | | 3428 | 1.6 | | 3384 | 2.8 |
| MEW | 14566 | | 13207 | 9.3 | | 12142 | 16.6 |
| Std.&Oper. Items | 1302 | | 1296 | 0.5 | | 1292 | 0.8 |
| OEW | 15868 | | 14503 | 8.6 | | 13434 | 15.3 |
| Payload | 1370 | | 1370 | | | 1370 | |
| Fuel | 6698 | | 6232 | 7.0 | | 5877 | 12.3 |
| GTOW | 23936 | | 22105 | 7.7 | | 20681 | 13.6 |

NOTES:  (1)  Advanced Aluminum Alloys Consist of Two Levels of Improvement.
Level I:  20% Improvement in Properties & 10% Reduction in Density
Level II:  40% Improvement in Properties & 20% Reduction in Density

(2)  Not a Computer Input.

123

### 4.3.3 Advanced Transport Aircraft

The wide bodied advanced commercial transport has a range of 5556 km (3000 n. miles) with a 36,000 kg (80,000 lb) payload. The thrust-to-weight ratio is 0.261 and wing loading is 5.46 kPa (1144 lb/ft$^2$).

For property improvement Level 1, weight savings were calculated for structural elements in the wing, fuselage, and empennage. Table 28 summarizes the weight saved by individual property improvements and includes amount of structure changed in terms of weight percent and weight. Similarly, Table 29 summarizes the weight saved by optimum combination of three advanced aluminum alloys - high strength, high fatigue resistance and high modulus/low density. The methods employed to calculate these weight changes were the same as that described above for the S-3A aircraft.

The percent weight saved by advanced alloy application is summarized in Table 30. These data were input to the ASSET program to determine the optimum system weight reductions, Table 31. ASSET was also used to calculate performance improvements resulting from reduced component weight. The values for increased payload or range assuming a constant gross weight aircraft are presented in Table 32. Similarly, values for reduced gross weight, wing span, and fuel consumption for a constant mission, assuming a constant mission, are presented in Table 33.

Comparisons of weight savings by individual and combined property improvements are presented in Figures 51 through 55. On an individual property improvement basis, 10 percent lower density is found to be more effective in saving weight in the S-3A or wide-body transport than either 20 percent higher strength, modulus, or fatigue resistance, see Figures 46 and 51. In the S-3A airplane, strength and stiffness property improvement save more weight than fatigue property improvement. In the wide-body transport, strength, fatigue and modulus improvements are almost equally important in saving weight. This is the result of the high service life, and lower performance mission requirements, compared to the S-3A or V/STOL.

124

## TABLE 28

### WEIGHT SAVINGS IN ADVANCED WIDE-BODY TRANSPORT
### AIRCRAFT RESULTING FROM INDIVIDUAL PROPERTY IMPROVEMENTS

|  | ADVANCED ALUMINUM – LEVEL I (+20%) | | | | | |
|---|---|---|---|---|---|---|
|  | STRENGTH | | STIFFNESS | | FATIGUE | |
| STRUCTURAL ELEMENTS | % STRUCTURE CHANGED | WEIGHT-LBS. | % STRUCTURE CHANGED | WEIGHT-LBS. | % STRUCTURE CHANGED | WEIGHT-LBS. |
| **Primary Structure** | | | | | | |
| Upper Surface | 100 | 318 | 100 | 900 | - | - |
| Lower Surface | - | - | 100 | - | - | - |
| Cover | 100 | 102 | - | - | 100 | 1200 |
| Stiffeners | 100 | 54 | - | - | 100 | 300 |
| Spars | | | | | | |
| Cap | 100 | 114 | 47 | 20 | 53 | 40 |
| Web | 100 | 158 | 100 | 260 | - | - |
| Ribs | 25 | 100 | 100 | 330 | - | - |
| MLG | 100 | 20 | - | - | - | - |
| L.E. & T.E. | - | - | - | - | - | - |
| Cover & Stiff. etc. | - | - | - | - | - | - |
| Ribs | 100 | 150 | - | - | - | - |
| Joints & Fasteners | - | - | - | - | 100 | 100 |
| Control Surfaces; Secondary & Misc. | - | - | - | - | - | - |
| **Subtotal - Wing** | | 1016 | | 1510 | | 1640 |
| | | | | | | |
| **Primary Structure** | | | | | | |
| Covering | 100 | 300 | 100 | 250 | 100 | 1200 |
| Str. & Long. | 34 | 200 | - | - | - | - |
| Pres. - Blhd. | - | - | - | - | 100 | 40 |
| - Deck | 100 | 125 | - | - | 100 | 60 |
| Blhd. & Frames | 25 | 250 | 100 | 500 | - | - |
| Doors | - | - | - | - | 100 | 100 |
| Floor Supp. | 100 | 500 | - | - | - | - |
| Seat Tracks | 100 | 150 | - | - | - | - |
| Keelson | 60 | 150 | 100 | 100 | - | - |
| Other Str. | - | - | - | - | - | - |
| **Secondary Structure** | | | | | | |
| Frames & Doors | 60 | 300 | - | - | - | - |
| Other Str. | - | - | - | - | - | - |
| **Subtotal - Fuselage** | | 1975 | | 850 | | 1400 |

WING (row group label for Primary Structure wing section)

FUSELAGE (row group label for fuselage section)

TABLE 28 (Cont'd)

| | | ADVANCED ALUMINUM - LEVEL I (+20%) | | | | |
|---|---|---|---|---|---|---|
| | | STRENGTH | | STIFFNESS | | FATIGUE |
| STRUCTURAL ELEMENTS | % STRUCTURE CHANGED | WEIGHT- LBS. | % STRUCTURE CHANGED | WEIGHT- LBS. | % STRUCTURE CHANGED | WEIGHT- LBS. |
| **Stabilator** | | | | | | |
| Upper Cover | 100 | 60 | 100 | 50 | 100 | 100 |
| Lower Cover | 100 | 30 | 100 | 100 | - | - |
| Spars | 100 | 70 | 100 | 50 | - | - |
| Ribs | 100 | 25 | 100 | 70 | - | - |
| Pivot | - | - | - | - | 100 | 80 |
| L.E. | - | - | 100 | 40 | - | - |
| Other | - | - | - | - | - | - |
| **Fin** | | | | | | |
| Cover & Stiff. | 100 | 45 | 100 | 45 | - | - |
| Spars | 100 | 17 | 100 | 10 | - | - |
| Ribs | 100 | 5 | 100 | 10 | - | - |
| Other | - | - | - | - | - | - |
| Elevator | - | - | 49 | 55 | - | - |
| Rudder | - | - | 45 | 26 | - | - |
| Secondary | - | - | - | - | - | - |
| Subtotal - Emp. | | 252 | | 456 | | 180 |
| Total | | 3243 | | 2816 | | 3220 |

(Left margin label, rotated: EMPENNAGE)

# TABLE 29

WEIGHT SAVINGS IN ADVANCED WIDE-BODY TRANSPORT AIRCRAFT
RESULTING FROM OPTIMUM COMBINATION OF HIGH STRENGTH,
HIGH FATIGUE RESISTANCE, AND HIGH MODULUS/LOW DENSITY ALLOYS

| | STRUCTURAL ELEMENTS | ADVANCED ALUMINUM - LEVEL I (+20%) | | | OPTIMUM ALLOY SELECTION |
| --- | --- | --- | --- | --- | --- |
| | | STRENGTH (1) | STIFFNESS & DENSITY (2) | FATIGUE & TOUGHNESS (3) | |
| **WING** | **Primary Structures** | | | | |
| | Upper Surface | 318 | <u>1737</u> | 927 | 1737 |
| | Lower Surface | | | | |
| |   Cover | 102 | 862 | <u>1200</u> | 1200 |
| |   Stiffeners | 54 | <u>453</u> | 300 | 453 |
| | Spars | | | | |
| |   Cap | 114 | <u>132</u> | 94 | 132 |
| |   Web | 158 | <u>498</u> | 264 | 498 |
| | Ribs | 408 | <u>705</u> | 408 | 705 |
| |   M.L.G. | <u>20</u> | 19 | 19 | 20 |
| | L.E. & T.E. | | | | |
| |   Cover, Stiff., etc. | 206 | <u>206</u> | 206 | 206 |
| |   Ribs | 150 | <u>159</u> | 159 | 159 |
| | Joints, Fastener, Misc. | 191 | <u>191</u> | 121 | 191 |
| | Control Surfaces & Secondary Str. | 1009 | <u>1009</u> | 1009 | 1009 |
| | **Subtotal Wing** | 2730 | 5971 | 4707 | 6310 |
| **FUSELAGE** | **Primary Structure** | | | | |
| | Covering | <u>1216</u> | <u>1446</u> | 1200 | 1446 |
| | Str. & Long | <u>555</u> | 537 | 537 | 555 |
| | Press.-Bkhd. | 41 | <u>41</u> | 40 | 41 |
| |   -Deck | 125 | <u>125</u> | 60 | 125 |
| | Bkhd. & Frames | 932 | <u>1360</u> | 909 | 1360 |
| | Doors-Doublers | 96 | 96 | <u>100</u> | 100 |
| | Floors Supp. | <u>500</u> | 489 | 489 | 500 |
| | Seat Tracks | <u>150</u> | 142 | 142 | 150 |
| | Keelson | 247 | <u>332</u> | 242 | 332 |
| | Other Str. | 97 | <u>97</u> | 97 | 97 |
| | **Secondary** | | | | |
| | Frames & Doors | <u>500</u> | 499 | 499 | 500 |
| | Other Str. | 471 | <u>471</u> | 471 | 471 |
| | **Subtotal Fuselage** | 4930 | 5635 | 4786 | 5677 |

TABLE 29 (Cont'd)

| STRUCTURAL ELEMENTS | ADVANCED ALUMINUM - LEVEL I (+20%) | | | OPTIMUM ALLOY SELECTION |
| | STRENGTH (1) | STIFFNESS & DENSITY (2) | FATIGUE & TOUGHNESS (3) | |
|---|---|---|---|---|
| **Stabilator** | | | | |
| Upper Cover | 60 | _141_ | 100 | 141 |
| Lower Cover | 30 | _192_ | 102 | 192 |
| Spars | 70 | _113_ | 68 | 113 |
| Ribs | 25 | _139_ | 76 | 139 |
| Pivot | 71 | _71_ | _80_ | 80 |
| L.E. | 60 | _96_ | 60 | 96 |
| Other | 97 | _97_ | 97 | 97 |
| **Fin** | | | | |
| Cover & Stiff | 45 | _83_ | 42 | 83 |
| Spars | 17 | _27_ | 18 | 27 |
| Ribs | 5 | _25_ | 16 | 25 |
| Other | 32 | _32_ | 32 | 32 |
| Elevator | 77 | _113_ | 77 | 113 |
| Rudder | 40 | _59_ | 40 | 59 |
| Secondary | -- | -- | -- | -- |
| Subtotal Tail | 629 | 1188 | 808 | 1197 |
| Total | 8289 | 12894 | 10301 | 13184 |

(In left margin: TAIL)

NOTES:

(1)     The structure is assumed to be made from a high strength material where it is strength critical and a low density material with equivalent properties for the remaining structure.

(2)     The structure is assumed to be made completely from a high stiffness, low density alloy. Thus both weight savings from higher modulus and lower density are included.

(3)     The structure is assumed to be made from a high fatigue strength high toughness material where its fatigue & toughness are equally critical and a low density material with equivalent properties for the remaining structure.

# TABLE 30

## PERCENTAGE WEIGHT SAVED IN ADVANCED WIDE-BODY TRANSPORT AIRCRAFT BY ALLOY SUBSTITUTION

| COMPONENT GROUP | PERCENTAGE REDUCTION OF COMPONENT WEIGHT FOR OPTIMUM ALLOY SELECTION* | |
| --- | --- | --- |
| | LEVEL I | LEVEL II |
| Wing | 13.3 | 24.7 |
| Body | 11.2 | 22.3 |
| Tail | 13.2 | 24.6 |

*Used for ASSET Analyses.


# TABLE 31

## SUMMARY OF WEIGHT SAVINGS IN WIDE-BODY TRANSPORT AIRCRAFT BY APPLICATION OF ADVANCED ALUMINUM ALLOYS, ASSUMING CONSTANT PAYLOAD

| SECTION | BASE A/C CONVENTIONAL METHOD wt.# | ADVANCED ALUMINUM - LEVEL I | | | ADVANCED ALUMINUM - LEVEL II | | |
| --- | --- | --- | --- | --- | --- | --- | --- |
| | | INPUT % RED. | OUTPUT Wt.# | % RED. | INPUT % RED. | OUTPUT Wt.# | % RED. |
| Wing | 69077 | 13.3 | 54004 | 21.8 | 24.7 | 42875 | 37.9 |
| Tail | 7272 | 13.2 | 5540 | 23.8 | 24.6 | 4298 | 40.9 |
| Body | 61456 | 11.2 | 53477 | 13.0 | 22.3 | 45965 | 25.2 |
| Gear | 19602 | | 18345 | 6.4 | | 17316 | 6.4 |
| Engine Section | 8996 | | 8194 | 8.9 | | 7553 | 16.0 |
| TOTAL STR. | 166403 | (2)10.2 | 139560 | 16.1 | (2)19.6 | 118007 | 29.1 |
| Propulsion | 28577 | | 26314 | 7.9 | | 24499 | 14.3 |
| Sys. & Furn. | 62392 | | 61966 | .7 | | 61617 | 1.2 |
| MEW | 257370 | | 227839 | 11.5 | | 204124 | 20.7 |
| Std.&Oper. Items | 18340 | | 18320 | .1 | | 18304 | .2 |
| OEW | 275710 | | 246159 | 10.7 | | 222428 | 19.3 |
| Payload | 80000 | | 80000 | | | 80000 | |
| Fuel | 98266 | | 91714 | 6.7 | | 86356 | 12.1 |
| GTOW | 453976 | | 417873 | 8.0 | | 388785 | 14.4 |

NOTES: (1) Advanced Aluminum Alloys Consist of Two Levels of Improvement.
LEVEL I:  20% Improvement in Properties & 10% Reduction in Density
LEVEL II: 40% Improvement in Properties & 20% Reduction in Density

(2) Not a Computer Input.

TABLE 32

ADVANCED TRANSPORT PERFORMANCE IMPROVEMENT OBTAINED
BY APPLICATION OF ADVANCED ALUMINUM ALLOYS

PAYLOAD OR RANGE FOR CONSTANT WEIGHT AIRCRAFT

| | Payload | | | Range | |
|---|---|---|---|---|---|
| Baseline Pounds | % Change Due to Advanced Aluminum | | Baseline N. Miles | % Change Due to Advanced Aluminum | |
| | Level I | Level II | | Level I | Level II |
| 80,000 | +21.3 | +40.7 | 3,000 | +23.7 | +46.2 |

NOTE: Improvements in Advanced Aluminum Alloys are as follows:

Level I  - 20% Improvement in Properties and 10% Reduction in Density

Level II - 40% Improvement in Properties and 20% Reduction in Density

130

## TABLE 33

### EFFECT OF ADVANCED ALUMINUM ALLOYS ON WEIGHT, WING SPAN AND FUEL CONSUMPTION OF ADVANCED TRANSPORT AIRCRAFT

#### CONSTANT MISSION

| Gross Weight (GTOW) | | | Wing Span | | | Fuel Consumption | | |
|---|---|---|---|---|---|---|---|---|
| Baseline Pounds | Due to Adv. Alum. Level I | Level II | Baseline Feet | Due to Adv. Alum. Level I | Level II | Baseline Pounds | Due to Adv. Alum. Level I | Level II |
| 453,976 | 6.7 | 12.1 | 199.5 | 4.1 | 7.5 | 98,266 | 6.7 | 12.1 |

NOTE: Improvements in Advanced Aluminum Alloys are as follows:

Level I   - 20% Improvement in Properties and 10% Reduction in Density

Level II  - 40% Improvement in Properties and 20% Reduction in Density

Figure 51   Weight Reduction Comparisons in Wide-Body Transport
Aircraft Resulting From Individual Property
Improvement

132

WEIGHT SAVED DUE
TO PROPERTY IMPROVEMENT
ONLY

WEIGHT SAVED
DUE TO PROP. INCREASE
& DENSITY REDUCTION

HIGH STR.
LOW DEN.

2.4

9.7

HIGH FAT. & K
LOW DEN.

2.4

9.6

HIGH STIFF.
LOW DEN.

2.1

9.4

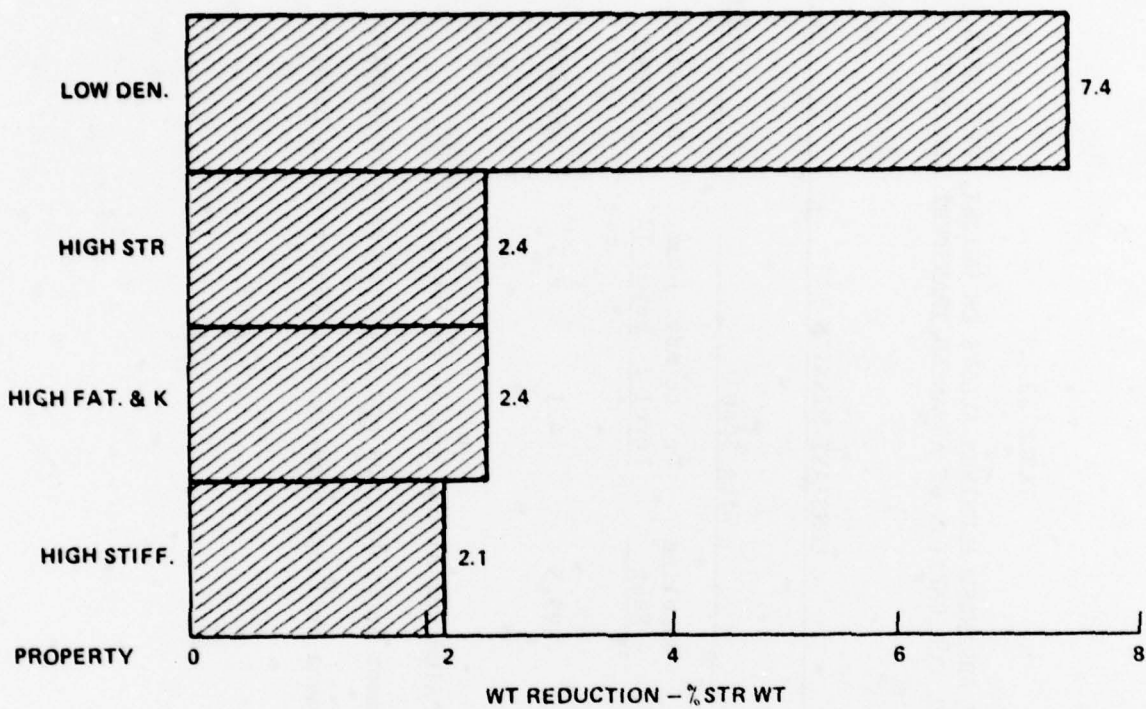2        4        6        8        10

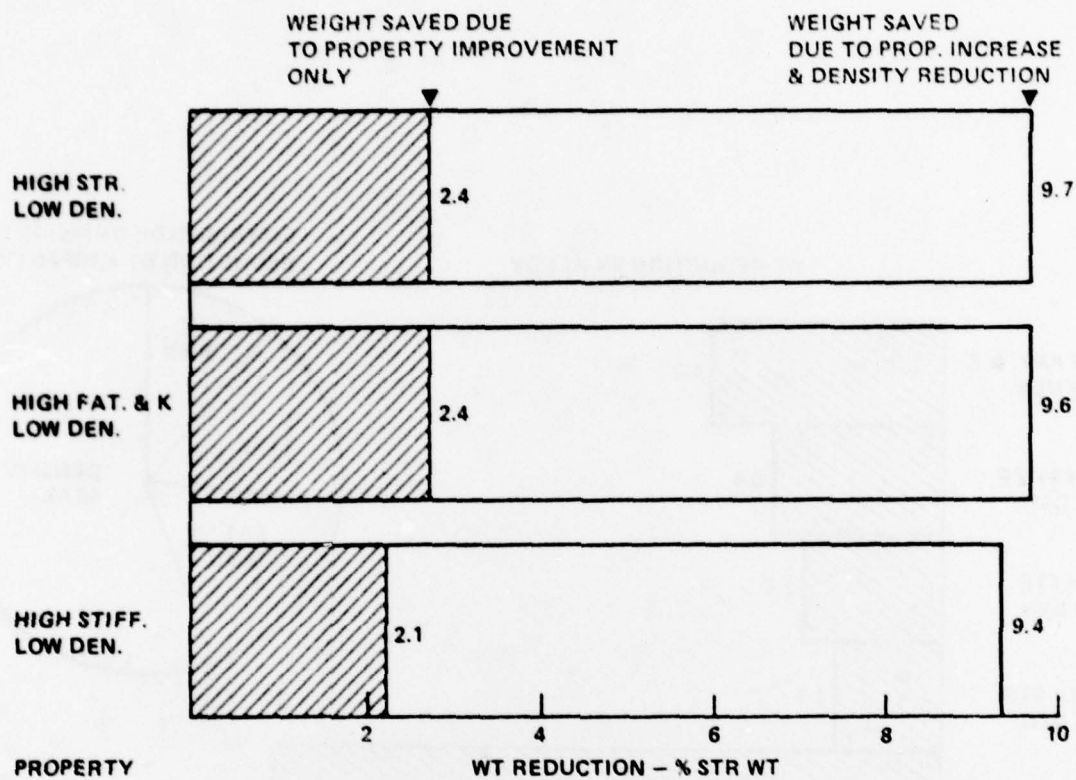PROPERTY

WT REDUCTION – % STR WT

Figure 52   Weight Reduction Comparison in Wide-Body Transport
Aircraft Resulting From Individual Property
Improvements Combined With Reduction in Density

WT REDUCTION BY ALLOY

DISTRIBUTION OF WEIGHT
REDUCTION BY PROPERTY

HIGH FAT. & K
LOW DEN.          4.2

HIGH STIFF.
LOW DEN.          3.6

HIGH STR.
LOW DEN.          2.5

EQUIV STR.
LOW DEN.          1.9

TOTAL             12.2

ALLOY

WT REDUCTION – % STR WT

4      8      12

STR
10.8%

E
14.0%

FAT.
18.8%

DENSITY
56.4%

Figure 53   Wide-Body Transport Aircraft Weight Reduction and
Distribution for Optimum Combination of Four Low
Density Advanced Aluminum Alloys - High Strength,
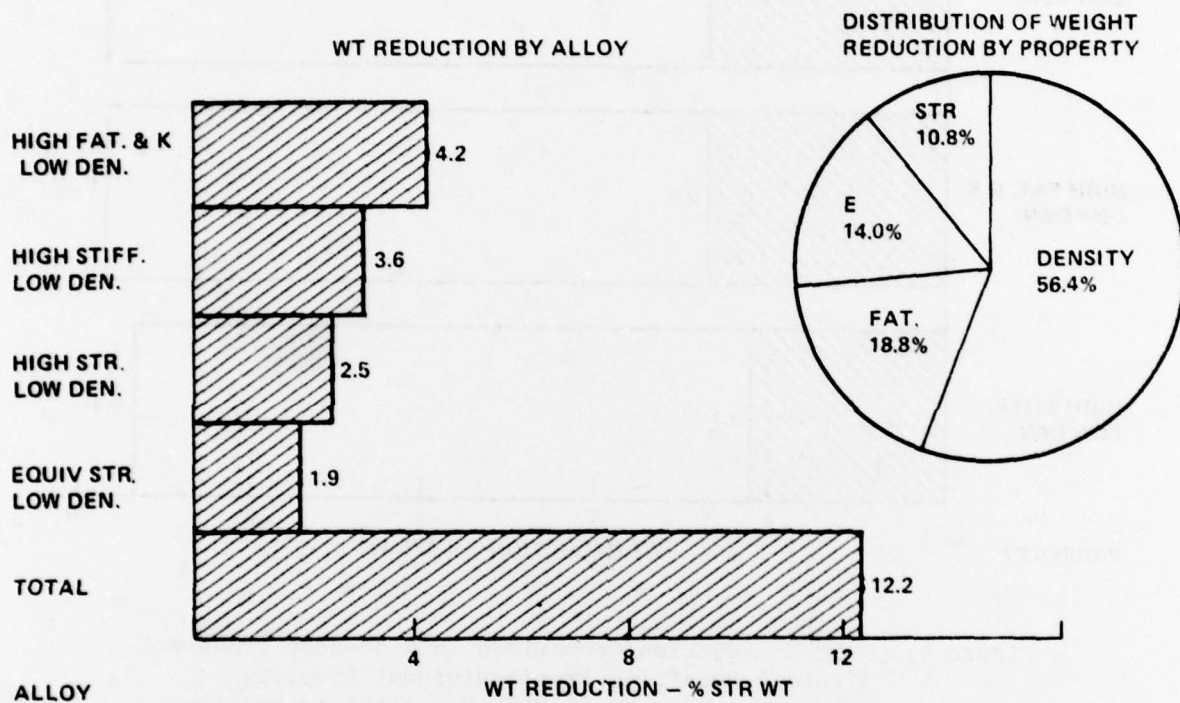High Fatigue Resistance, High Modulus, and
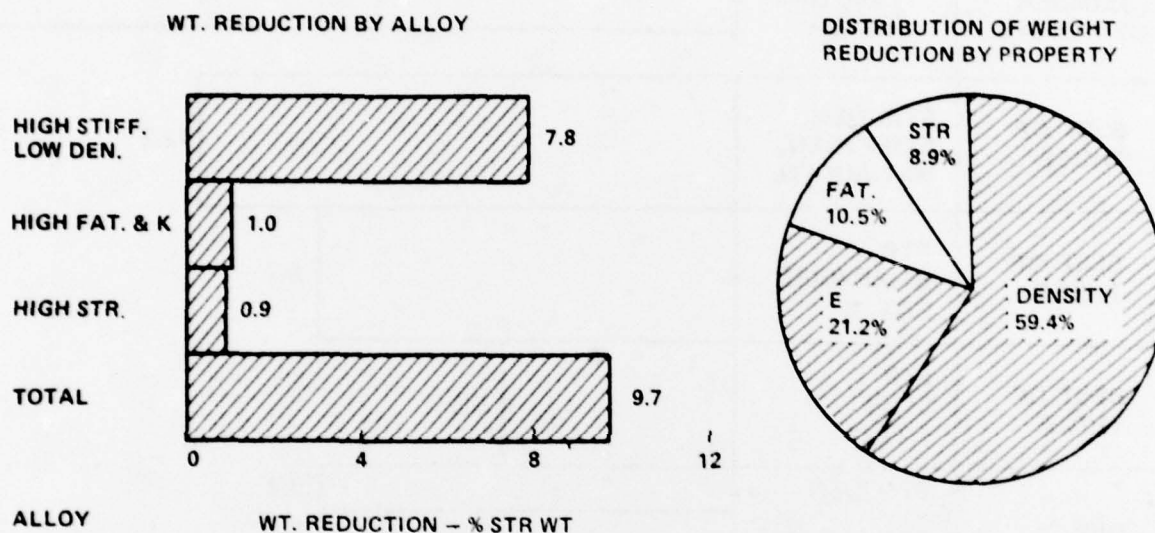Equivalent Strength

134

Figure 54   Wide-Body Transport Aircraft Weight Reduction and
Distribution for Optimum Combination of Three
Advanced Aluminum Alloys - High Strength, High
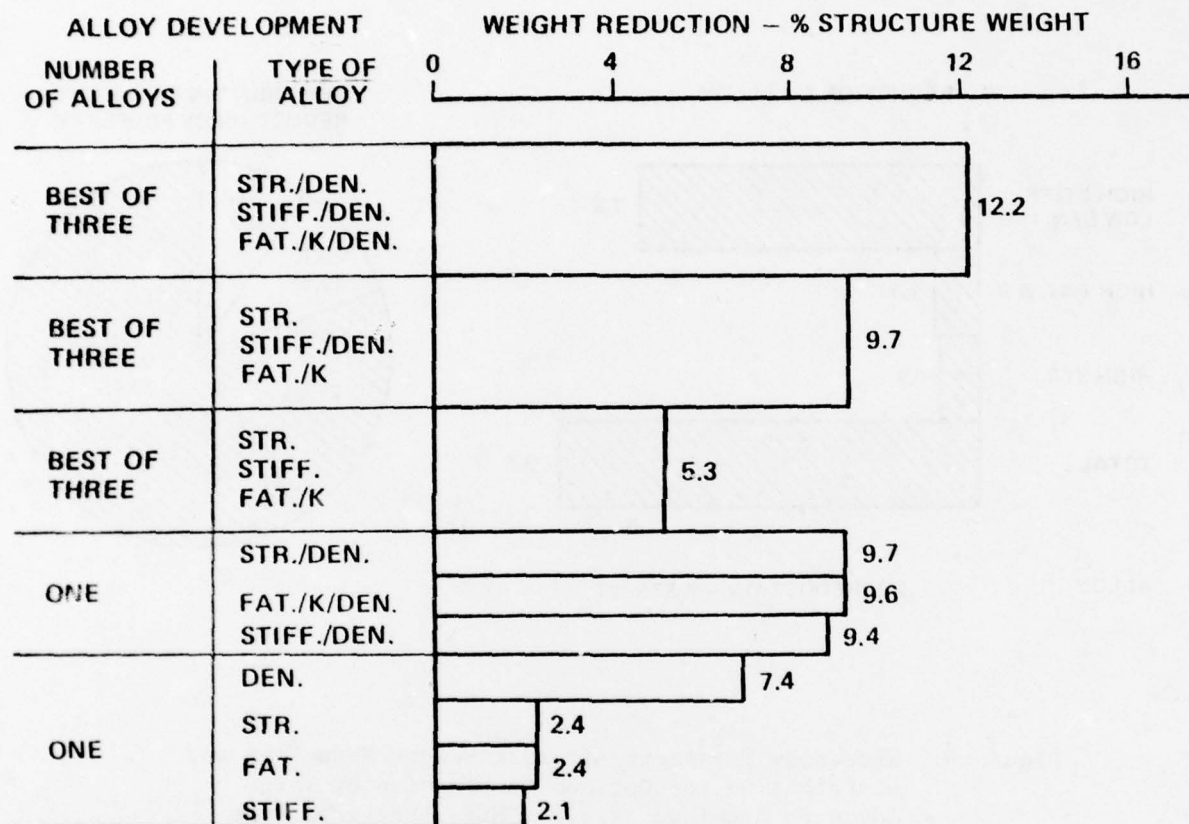Modulus/Low Density, and High Fatigue Resistance

Figure 55   Optimum Payoff Comparisons for Wide-Body Transport
in Terms of Percent Weight Saved by Selected
Combinations of Advanced Aluminum Alloys

When strength, modulus, and fatigue improvements are combined with low density, Figures 47 and 52, the S-3A benefits most from the combined strength and density improvement. However, increased modulus coupled with decreased density is 84 percent as effective as the strength/density improvement. In the wide-body transport, the weight savings is almost identical for all three combinations of strength, modulus, and fatigue resistance with density.

When optimum combinations of property improvements are considered, Figures 48 and 53, then the majority of weight savings comes from strength/density improvement in the S-3A and fatigue/density improvement in the wide-body transport. Combining optimum properties of low density alloys results in higher weight savings than if a mix of alloys were not considered.

Because preliminary alloy development approaches have already identified promising alloy systems combining increased modulus and decreased density, (Section 2, this report), the weight savings comparisons shown in Figures 49 and 54 are most pertinent to relatively short term development goals. In the S-3A aircraft, 11.5 percent of structural weight is saved by replacing presently used aluminum alloys with an optimum combination of high strength, high fatigue resistance, and high modulus/low density alloys (Level I property set). This is only 21 percent less savings than if the improved alloys were also low density, compare Figures 48 and 49. The same compromise obtains for weight savings in the wide-body transport, about 20 percent less. These results are important from the standpoint of alloy development goals, because it is apparent that if a high modulus, low density alloy is successfully developed, it is not necessary to also develop low density alloys having high strength and fatigue resistance in order to achieve significant weight savings in advanced aircraft systems.

4.3.4 Conclusions

Advanced aluminum alloys having 20 percent higher strength, fatigue resistance, and modulus, with 10 percent lower density contribute significant improvements in aircraft performance, both for the V/STOL and advanced wide-body transport. For a constant weight aircraft, the advanced alloys save sufficient weight

to increase payload by 35, 48 and 21 percent for the subsonic V/STOL, super-
sonic V/STOL and Advanced Transport, respectively. Of these, the improvement
is probably most important for the subsonic V/STOL. This is presently in
advanced concept design consideration for fleet development in the next few
years, with major redesign windows probably to occur in about 1985. Al-
though not described here, the weight savings indicated can also be trans-
lated into significant range increase, if payload is held constant. The
specific range values are not included herein because they are classified
information.

For the subsonic V/STOL, application of the above set of improved alloys
would also result in significant changes for a constant mission configuration.
The gross weight would be reduced by 8.4 percent (1810 kg), wing span reduced
by 4.2 percent (0.8 m), and fuel consumption reduced by 8.1 percent (418 kg).
For a large fleet of aircraft, these improvements would result in significant
savings in fuel, increased mission capability (range or payload) or reduced
shipboard launch platform size. Additionally, weight savings by substitution
of advanced aluminum alloys instead of advanced composites is attractive to
airframe manufactures because of the extensive experience and fabrication
facilities for aluminum alloys that could be used for low-cost manufacturing.

## Section 5
## CONCLUSIONS

Aluminum alloys produced from rapidly solidified powders of conventional composition may or may not have significantly improved properties compared to conventional ingot metallurgy products.  However, alloys of non-conventional compositions can be produced from rapidly solidified powders which have significantly better properties.  One example is the improved elevated temperature mechanical properties of an aluminum alloy containing 8 weight percent iron. Another example is the high modulus/low density of aluminum alloys containing lithium, although the effect of solidification rate on properties has yet to be fully characterized.

Experimental aluminum alloys containing 20 weight percent Mg or 2 weight percent Ca have a dispersed submicroscopic phase which is thermally stable to above 700 K, thus indicating possible usefulness for high temperature applications.

An experimental  aluminum alloy containing 2 weight percent Ca exhibits a 12 percent  higher room temperature elastic modulus than 7075 and other commercial structural aluminum alloys.  Ca additions may therefore contribute to the development of high modulus/high strength alloys.

The tradeoff studies performed indicate significant weight savings would obtain in a variety of aerospace structural applications by application of new aluminum alloys exhibiting 15 percent or more increased elastic modulus coupled with 11 percent or more decreased density.  Strength-critical aerospace components would also significantly benefit in weight savings by application of alloys combining a 20 percent or more increase in strength with 10 percent or more decrease in density.

139

## Section 6
## RECOMMENDATIONS

It is recommended that the development of advanced aluminum alloys from rapidly solidified powders be undertaken which meet specific property goals, along with development of a metallurgical basis suitable for further scale-up and application to new weapons systems. Rapidly solidified powders will produce a fine grain size with control of size and distribution of intermetallics, and, where appropriate, extend the solid solubility of alloying elements beyond that practical by conventional ingot metallurgy. A primary property goal that would provide a major payoff in the performance of selected new aerospace structures is the development of an alloy with specific stiffness (elastic modulus-to-density ratio) increase of at least 30 percent compared to Al 7075-T76 and without significant loss in strength, toughness, fatigue behavior, or stress corrosion resistance. An alternative property goal would be to identify an aluminum alloy that has a specific strength increase of at least 20 percent combined with an increase in specific modulus of 15 to 20 percent, compared to Al 7075-T76, without significant loss in toughness, fatigue behavior, or stress corrosion resistance. An appropriate plan should include both fundamental alloy and fundamental process studies, alloy production scale-up and evaluation phases, and a component design evaluation phase that utilizes scaled-up alloy properties.

## Section 7

## REFERENCES

1.  Proceedings of the Second International Conference on Rapidly Quenched Metals, Eds. N. J. Grant and B. C. Giessen, MIT Press, Cambridge, Mass., 1976, Section I

2.  Proceedings of the Second International Conference on Rapidly Quenched Metals, Eds. N. J. Grant and B. C. Giessen, Mater. Sci. Eng., 23, 1976, Section II

3.  H. Jones, Splat Cooling and Metastable Phases, Rep. Prog. Phys., 36, 1973, 1425

4.  P. Predecki, A. W. Mullendore and N. J. Grant, A Study of the Splat Cooling Technique, Trans. AIME, 233, 1965, 1581

5.  H. Warlimont, W. Zingg and P. Furrer, Structure of Splat-Cooled Al-Cr Alloys, Proc. Second Int. Conf. on Rapidly Quenched Metals, II, 1975, 101

6.  P. Furrer and H. Warlimont, Crystalline and Amorphous Structures of Rapidly Solidified Al-Cr Alloys, Mater. Sci. Eng., 28, 1977, 127

7.  A. Fontaine, Clustering Effects in Splat-Cooled Al-Transition Metal Alloys, Proc. Second Int. Conf. on Rapidly Quenched Metals, I, 1975, 162

8.  D. B. Williams and J. W. Edington, High Resolution Microanalysis and Microstructural Characteristics of Splat Quenched Al-Cu Alloys, Proc. Second Int. Conf. on Rapidly Quenched Metals, I, 1975, 135

9.  D. B. Williams and J. W. Edington, Microstructural Characteristics of Splat Quenched Al-Cu Alloys, J. Mater. Sci., 12, 1977, 126

10. H. A. Davies and J. B. Hull, Some Aspects of Splat-Quenching in an Inert Atmosphere and of the Formation of Non-Crystalline Phases in Al-17.3 at % Cu, Ge and Te., J. Mater. Sci., 9, 1974, 707

11. K. D. Krishnanand and R. W. Cahn, Properties of Plasma-Sprayed Al-Cu Alloys, Proc. Second Int. Conf. on Rapidly Quenched Metals, I, 1975, 67

12. H. Jones, Observations on a Structural Transition in Aluminum Alloys
Hardened by Rapid Solidification, Mater. Sci. Eng., 5, 1969, 1

13. M. H. Jacobs, A. G. Doggett and M. J. Stowell, The Microstructure of
Al-8 wt.% Fe-Based Alloys Prepared by Rapid Quenching From the Liquid
State, J. Mater. Sci., 9, 1974, 1631

14. W. Gruhl, B. Grzemba, G. Ibe and W. Hiller, Hardening From the Molten
State of Aluminum Semiproducts using the Electron Beam, Aluminum, 53,
1977, 177

15. S. K. Bose and R. Kumar, Rapid Solidification of Al-Mg-Si Alloys From
the Liquid State, Proc. Second Int. Conf. on Rapidly Quenched Metals I,
1975, 169

16. H. Warlimont and P. Kunzman, Effects of Rapid Solidification in Arc
Sprayed Al Alloys, Proc. Second Int. Conf. on Rapidly Quenched Metals,
I, 1975, 197

17. T. Ikeda and S. Nishi, Kinetics of the Precipitation Process in a
Supersaturated Al-3% Mn Solid Solution Solidified Rapidly, J. Jpn.
Inst. Metals, 40, 1976, 571

18. S. P. Bhat, T. R. Ramachandran and A. K. Jena, Splat Cooling of Al-Mn
Alloys, J. Mater. Sci., 9, 1974, 1759

19. K. Chattopadhyay, P. Ramachandrarao, S. Lele, and T. R. Anantharaman,
Crystal Structure of a Metastable Al-Ni Phase Obtained by Splat Cooling,
Proc. Second Int. Conf. on Rapidly Quenched Metals, I, 1975, 157

20. E. Nes and H. Billdal, Non-Equilibrium Solidification of Hyperperitectic
Al-Zr Alloys, Acta. Met., 24, 1977, 1031

21. W. Dahl, W. Gruhl, W. Burchard, G. Ibe and C. Dumitrescu, Precipitation
Processes in Al-Zr Casting Alloys, Z. Metallkd., 68, 1977, 188

22. N. Ryum, Precipitation in an Al-1.78 wt.% Hf Alloy After Rapid
Solidification, J. Mater. Sci., 10, 1975, 2075

23. M. Lebo and N. J. Grant, Structure and Properties of a Splat Cooled
2024 Al Alloy, Met. Trans., 5, 1974, 1547

24. J. P. H. A. Durand, R. M. Pelloux and N. J. Grant, Properties of Splat
Quenched 7075 Al Type Alloys, Proc. Second Int. Conf. on Rapidly
Quenched Metals, II, 1975, 247

25. C. E. Mobley, A. H. Clauer and B. A. Wilcox, Microstructures and Tensile Properties of 7075 Al Compacted From Melt-Spun Ribbon, J. Inst. Metals, 100, 1972, 142

26. G. Faninger, D. Merz and H. Winter, Investigation of the Corrosion Behavior of Splat-Cooled Al-Fe Alloys With Small Additions of Mg, Mn and Cr, Proc. Second Int. Conf. on Rapidly Quenched Metals, I, 1975, 483

27. G. Thursfield and M. J. Stowell, Mechanical Properties of Al-8 wt.% Fe-Based Alloys Prepared by Rapid Quenching from the Liquid State, J. Mater. Sci., 9, 1974, 1644

28. R. J. Towner, Metal Prog., 73, 1958, 70

29. W. Rostoker, R. Dudek, C. Freda and R. Russell, Fast Freezing as a Method for Aluminum Alloy Development, Final Report, Contract F 33615-70-C-1525, AFML-TR-73-36, March 1973

30. T. Sheppard, Production of Extruded Material From Metal Powders, Proc. 15th Int. Mach. Tool Des. and Res. Conf., Birmingham, England, Sept. 18-20, 1974, 659

31. Symposium on Advances in the Physical Metallurgy of Al Alloys, Met. Trans., 6A, 1975, 624

32. J. T. Staley, Aluminum Alloy and Process Developments for Aerospace, Metals Eng. Quart., 16, 1976, 52

33. E. A. Starke, Jr., Aluminum Alloys of the 70's: Scientific Solutions to Engineering Problems. An Invited Review, Mater. Sci. Eng., 29, 1977, 99

34. N. Dudzinski, J. R. Murray, B. W. Mott and B. Chalmers, J. Inst. Metals, 74, 1947-1948, 291

35. Aluminum Vol. 1. Properties, Physical Metallurgy and Phase Diagrams Ed. K. V. Van Horn, ASM, 1967, 167

36. G. T. Hahn and A. R. Rosenfield, Metallurgical Factors Affecting Fracture Toughness of Al Alloys, Met. Trans., 6A, 1975, 653

37. D. E. Piper, W. E. Quist and W. E. Anderson, Application of Fracture Toughness Parameters to Structural Metals, Vol. 31, Metallurgical Society Conference, 1966, 227

38. J. R. Low, Jr., R. H. Van Stone and R. H. Merchant, NASA Tech. Report No. 2, Research Grant NGR 38-087-003, Carnegie-Mellon Univ., 1972

39. D. S. Thompson and S. A. Levy, AFML-TR-70-171, Wright-Patterson AFB, Ohio, 1970

40. D. S. Thompson, Metallurgical Factors Affecting High Strength Aluminum Alloy Production, Met. Trans., 6A, 1975, 671

41. E. Nes, The Influence of Microstructure on Localized Shear Failure in Al-Zn-Mg Alloys, Z. Metallkd, 69, 1978, 35

42. P. G. Boswell and G. A. Chadwick, The Grain Size of Splat-Quenched Alloys, Scripta. Met., 11, 1977, 459

43. R. C. Bates and W. G. Clark, Jr., Fractography and Fracture Mechanics, Trans. Quart. ASM, 62(2), 1969, 380

44. M. O. Spiedel, Stress Corrosion Cracking of Al Alloys, Met. Trans., 6A, 1975, 631

45. M. E. Fine, Precipitation Hardening of Al Alloys, Met. Trans., 6A, 1975, 625

46. T. H. Sanders and E. S. Balmuth, Al-Li Alloys: Low Density and High Stiffness, Metal Prog., 113(3), 1978, 32

47. D. Webster, Unpublished LMSC Independent Research Work, 1977

48. K. K. Sankaran, Structure and Properties of Splat Quenched 2024-type Al Alloys Containing Li, Ph.D. Thesis, MIT, Cambridge, Mass., 1978

49. B. Noble and G. E. Thompson, Precipitation Characteristics of Al-Li Alloys, Met. Sci. J., 5, 1971, 114

50. D. B. Williams and J. W. Edington, Met. Sci. J., 9, 1975, 529

51. H. K. Hardy, Trace-Element Effects in Some Precipitation-Hardening Al Alloys, J. Inst. Metals, 84, 1955-56, 429

52. J. M. Silcock, The Structural Aging Characteristics of Al-Cu-Li Alloys, J. Inst. Metals, 88, 1959-60, 357

53. B. Noble, I. R. McLaughlin and G. Thompson, Solute Atom Clustering Processes in Al-Cu-Li Alloys, Acta. Met., 18, 1970, 339

54. T. H. Sanders, Jr., Final Report, Naval Air Development Center Contract No. N6 2269-74-C-438 for Naval Air Systems Command, June 1976

55. G. E. Thompson and B. Noble, Precipitation Characteristics of Al-Li Alloys Containing Mg, J. Inst. Metals, 101, 1973, 111

56. T. H. Sanders, Jr., Factors Influencing Fracture Toughness and Other Properties of Al-Li Alloys, Semi-Annual Report on Naval Air Development Center Contract N6 2269-76-C-0271, March 1977

57. I. N. Fridlyander, O. A. Romanova and Z. N. Archakova, Russ. Met. Fuels, 4, 1962, 52

58. I. N. Fridlyander, S. M. Abartsumyan, N. V. Shiryaeva and R. M. Gabidullin, New Light Alloys of Al with Li and Mg, Met. Sci. and Heat Treatment, 3, 1968, 211

59. J. W. Evancho, Development of an Al-Mg-Li Alloy, Final Report, Naval Air Development Center Contract No. N6 2269-73-C-0219, June 1974

60. J. P. Lyle and W. S. Cebulak, Powder Metallurgy Approach for Control of Microstructure and Properties in High Strength Al Alloys, Met. Trans., 6A, 1975, 685

61. W. L. Otto, Metallurgical Factors Controlling Structure in High Strength Al P/M Products, Final Report, Contract No. F33615-74-C-5077, AFML-TR-76-60, May 1976

62. W. Koster and K. Rosenthal, Z. Metallkd., 32, 1940, 163

63. John R. Low, Jr. et al, "Rapid Inexpensive Tests for Determining Fracture Toughness," Publication NMAB-328, National Materials Advisory Board, National Academy of Sciences, Washington, D. C., 1976

64. G. M. Orner and C. E. Hartbower, "Sheet Fracture Toughness Evaluated by Charpy Impact and Slow Bend," Welding J., Res. Supplement, 40, 1961, 405

65. T. M. F. Ronald, J. A. Hall and C. M. Pierce, "Usefulness of Precracked Charpy Specimens for Fracture Toughness Screening Tests of Titanium Alloys," Met. Trans., 3, 1972, 813

66. D. B. Rezin, "Preliminary Design and Analysis Studies of an Advanced Metal Matrix Structural Component," Lockheed Missiles and Space Co. Report No. N60921-76-C-0211-3, to Naval Surface Weapons Center, Contract No. N60921-76-C-0211, 1 March 1977